An Analysis of Future Trends in Extreme Precipitation Events Over Several Canadian Locations

by

Daniel Betancourt

A Thesis submitted to the Faculty of Graduate Studies of

The University of Manitoba

in partial fulfilment of the requirements of the degree of

MASTER OF SCIENCE

Department of Environment and Geography

University of Manitoba

Winnipeg

ACKNOWLEDGMENTS

I would like to thank my supervisor Dr. Ronald Stewart for giving me the opportunity to further my academic career and pursue graduate studies. I would like to thank my mother and the rest of my family for their support during the process of completing my Master's and writing of my thesis. I would also like to thank the members of my committee, John Hanesiak and Bob Kochtubajda, who along with Dr. Stewart provided valuable wisdom and advice during the entire process. The assistance of George Liu was much appreciated in supplying scripts and logistical support necessary for the downloading and manipulation of data utilized in this study.

ABSTRACT

Trends in precipitation and extreme occurrence were analyzed for five locations across Canada using the Canadian Regional Climate Model. Results from the model's base simulation were compared to those from a future scenario of increased atmospheric CO_2. The climatology of nearby weather stations was used to assess the model's ability to simulate the present and future climate. Other parameters such as 850 and 500 hPa geopotential associated with the most extreme events were analyzed to infer changes in the mechanisms causing such events. The model underestimates annual precipitation along with extreme occurrence and intensity. A wetter, but more variable climate is projected for most locations. Frequency and intensity of extreme events increases at most locations. Simulated extreme events over western locations were found to be associated with cold lows, while eastern events were linked with moisture transport at 850 hPa. Western events were reproduced accurately, whereas eastern ones were not.

TABLE OF CONTENTS

Acknowledgements..i

Abstract……………………………………………………………………………..ii

List of Tables……………………………………………………………………….v

List of Figures……………………………………………………………………..vii

Chapter 1: Introduction…………………………………………………………1

1.1 Impacts...1

1.2 Physical Insights...3

1.3 Mechanisms..4

1.4 Model Studies...7

1.5 Observational Results...13

1.6 Vulnerability and Risk..15

Chapter 2: Objectives……………………………………………………………17

Chapter 3: Methodology………………………………………………………..19

3.1 Background on Corrected Data and Model Used in Study….21

3.2 Review of Climatology...21

3.3 Validation..22

3.4 Trends...22

3.5 Characteristics...23

Chapter 4: Results……………………………………………………………….25

4.1 Analysis of Local Climatology..25

4.2 Validation..27

4.3 Comparison of Model Simulations and Projections.............46

4.4 Assessment of Characteristics...58

Chapter 5: Discussion……………………………………………………………….82

5.1 Review of Climatology...82

5.2 Site-specific Points..83

5.3 Statistical Distribution and Extremes................................85

5.4 Comparison of Annual Precipitation..................................87

5.5 Monthly Distribution of Extreme Events............................87

5.6 Context of Results Within Previous Findings......................90

5.7 Characteristics and Phenomena Associated With Extreme Events...91

5.8 Validation of Characteristics...92

5.9 Future Characteristics..92

Chapter 6: Summary and Conclusions……………………………………….94

References…………………………………………………………………………….97

LIST OF TABLES

Table 3.1: Datasets and time periods used in this study..20

Table 4.1: Comparison of average annual frequency and contribution to total accumulation for daily precipitation classes in the 1961-1990 climatology and the 1961-1990 model simulation at Cold Lake..28

Table 4.2: Comparison of average annual frequency and contribution to total accumulation for daily precipitation classes in the 1961-1990 climatology and the 1961-1990 model simulation at Assiniboia...32

Table 4.3: Comparison of average annual frequency and contribution to total accumulation for daily precipitation classes in the 1961-1990 climatology and the 1961-1990 model simulation at High Prairie..36

Table 4.4: Comparison of average annual frequency and contribution to total accumulation for daily precipitation classes in the 1961-1990 climatology and the 1961-1990 model simulation at Guelph..40

Table 4.5: Comparison of average annual frequency and contribution to total accumulation for daily precipitation classes in the 1961-1990 climatology and the 1961-1990 model simulation at Muskoka..45

Table 4.6: Comparison of average annual frequency and contribution to total accumulation for classes in daily precipitation between the 1961-1990 model simulation and the 2041-2070 model projection at Cold Lake...49

Table 4.7: Comparison of average annual frequency and contribution to total accumulation for classes in daily precipitation between the 1961-1990 model simulation and the 2041-2070 model projection at Assiniboia...51

Table 4.8: Comparison of average annual frequency and contribution to total accumulation for classes in daily precipitation between the 1961-1990 model simulation and the 2041-2070 model projection at High Prairie..53

Table 4.9: Comparison of average annual frequency and contribution to total accumulation for classes in daily precipitation between the 1961-1990 model simulation and the 2041-2070 model projection at Guelph..55

Table 4.10: Comparison of average annual frequency and contribution to total accumulation for classes in daily precipitation between the 1961-1990 model simulation and the 2041-2070 model projection at Muskoka...57

Table 4.11: Top 10 precipitation events for the 1961-1990 model simulation and the 2041-2070 model projection at all locations…………………………………………………………...59

LIST OF FIGURES

Figure 4.1: Average monthly precipitation over the annual cycle for the climatology at all locations using all available data..26

Figure 4.2: Monthly occurrence of 99^{th} percentile daily precipitation events for the climatology at all locations using all available data..26

Figure 4.3: Comparison of extreme daily precipitation (90^{th}, 99^{th}, and 99.9^{th} percentile) for the observed 1961-1990 climatology and the 1961-1990 model simulation at Cold Lake...28

Figure 4.4: Comparison of the 1961-1990 climatology with the 1961-1990 model simulation over the annual cycle for Cold Lake...29

Figure 4.5: Monthly frequency of 90^{th}, 99^{th}, and 99.9^{th} percentile events for the 1961-1990 climatology, the 1961-1990 model simulation and the 2041-2070 model projection at Cold Lake..30

Figure 4.6: Cumulative annual precipitation for wettest months, average, and driest months and monthly average precipitation for the 1961-1990 climatology, the 1961-1990 model simulation and the 2041-2070 model projection at Cold Lake...31

Figure 4.7: Comparison of extreme daily precipitation (90^{th}, 99^{th}, and 99.9^{th} percentile) for the observed 1961-1990 climatology and the 1961-1990 model simulation at Assiniboia...32

Figure 4.8: Comparison of the 1961-1990 climatology with the 1961-1990 model simulation over the annual cycle for Assiniboia...33

Figure 4.9: Monthly frequency of 90^{th}, 99^{th}, and 99.9^{th} percentile events for the 1961-1990 climatology, the 1961-1990 model simulation and the 2041-2070 model projection at Assiniboia..34

Figure 4.10: Cumulative annual precipitation for wettest months, average, and driest months and monthly average precipitation for the 1961-1990 climatology, the 1961-1990 model simulation and the 2041-2070 model projection at Assiniboia...35

Figure 4.11: Comparison of extreme daily precipitation (90^{th},99^{th}, and 99.9^{th} percentile) for the observed 1961-1990 climatology and the 1961-1990 model simulation at High Prairie...36

Figure 4.12: Comparison of the 1961-1990 climatology with the 1961-1990 model simulation over the annual cycle for High Prairie......37

Figure 4.13: Monthly frequency of 90^{th}, 99^{th}, and 99.9^{th} percentile events for the 1961-1990 climatology, the 1961-1990 model simulation and the 2041-2070 model projection at High Prairie......38

Figure 4.14: Cumulative annual precipitation for wettest months, average, and driest months and monthly average precipitation for the 1961-1990 climatology, the 1961-1990 model simulation and the 2041-2070 model projection at High Prairie......39

Figure 4.15: Comparison of extreme daily precipitation (90^{th},99^{th}, and 99.9^{th} percentile) for the observed 1961-1990 climatology and the 1961-1990 model simulation at Guelph......41

Figure 4.16: Comparison of the 1961-1990 climatology with the 1961-1990 model simulation over the annual cycle for Guelph......41

Figure 4.17: Monthly frequency of 90^{th}, 99^{th}, and 99.9^{th} percentile events for the 1961-1990 climatology, the 1961-1990 model simulation and the 2041-2070 model projection at Guelph......42

Figure 4.18: Cumulative annual precipitation for wettest months, average, and driest months and monthly average precipitation for the 1961-1990 climatology, the 1961-1990 model simulation and the 2041-2070 model projection at Guelph......43

Figure 4.19: Comparison of extreme daily precipitation (90^{th},99^{th}, and 99.9^{th} percentile) for the observed 1961-1990 climatology and the 1961-1990 model simulation at Muskoka......45

Figure 4.20: Comparison of the 1961-1990 climatology with the 1961-1990 model simulation over the annual cycle for Muskoka......46

Figure 4.21: Monthly frequency of 90^{th}, 99^{th}, and 99.9^{th} percentile events for the 1961-1990 climatology, the 1961-1990 model simulation and the 2041-2070 model projection at Muskoka......47

Figure 4.22: Cumulative annual precipitation for wettest months, average, and driest months and monthly average precipitation for the 1961-1990 climatology, the 1961-1990 model simulation and the 2041-2070 model projection at Muskoka......48

Figure 4.23: Comparison of extreme daily precipitation (90th, 99th, and 99.9th percentile) for the 1961-1990 model simulation and the 2041-2070 model projection at Cold Lake....49

Figure 4.24: Comparison of the 1961-1990 model simulation and the 2041-2070 model projection over the annual cycle at Cold Lake....50

Figure 4.25: Comparison of extreme daily precipitation (90th, 99th, and 99.9th percentile) for the 1961-1990 model simulation and the 2041-2070 model projection at Assiniboia....51

Figure 4.26: Comparison of the 1961-1990 model simulation and the 2041-2070 model projection over the annual cycle at Assiniboia....52

Figure 4.27: Comparison of extreme daily precipitation (90th, 99th, and 99.9th percentile) for the 1961-1990 model simulation and the 2041-2070 model projection at High Prairie....53

Figure 4.28: Comparison of the 1961-1990 model simulation and the 2041-2070 model projection over the annual cycle at High Prairie....54

Figure 4.29: Comparison of extreme daily precipitation (90th, 99th, and 99.9th percentile) for the 1961-1990 model simulation and the 2041-2070 model projection at Guelph....55

Figure 4.30: Comparison of the 1961-1990 model simulation and the 2041-2070 model projection over the annual cycle at Guelph....56

Figure 4.31: Comparison of extreme daily precipitation (90th, 99th, and 99.9th percentile) for the 1961-1990 model simulation and the 2041-2070 model projection at Muskoka....57

Figure 4.32: Comparison of the 1961-1990 model simulation and the 2041-2070 model projection over the annual cycle at Muskoka....58

Figure 4.33: Comparison of 500 hPa geopotential height, 500 hPa vector wind, 850 geopotential height, and 850 hPa vector wind composites for top 3 daily precipitation events at Cold Lake....62

Figure 4.34: Comparison of 500 hPa geopotential height, 500 hPa vector wind, 850 geopotential height, and 850 hPa vector wind composites for top 3 daily precipitation events at Assiniboia....66

Figure 4.35: Comparison of 500 hPa geopotential height, 500 hPa vector wind, 850 geopotential height, and 850 hPa vector wind composites for top 3 daily precipitation events at High Prairie..70

Figure 4.36: Comparison of 500 hPa geopotential height, 500 hPa vector wind, 850 geopotential height, and 850 hPa vector wind composites for top 3 daily precipitation events at Guelph..74

Figure 4.37: Comparison of 500 hPa geopotential height, 500 hPa vector wind, 850 geopotential height, and 850 hPa vector wind composites for top 3 daily precipitation events at Muskoka...78

Figure 5.1: Difference in the percent contribution from daily precipitation classes to total accumulation between the 1961-1990 climatology and the 1961-1990 model simulation at all locations……………………………………………………………………………….86

Figure 5.2: Difference in the percent contribution from daily precipitation classes to total accumulation between the 1961-1990 model simulation and the 2041-2070 model projection at all locations……………………………………………………………………….88

Figure 5.3: Julian day number of the top 3 daily precipitation events for the 1961-1990 climatology, the 1961-1990 model simulation and the 2041-2070 model projection at all locations……………………………………………………………………………….90

CHAPTER 1: INTRODUCTION

Extreme precipitation events have a profound impact on our society. Such occurrences are closely associated with flash flooding and significant property damage. Extreme rainfalls often overwhelm drainage systems and can lead to contamination of drinking supplies. Curriero et al. (2001) found a statistical association between extreme precipitation events and outbreaks of waterborne disease. In 2000 heavy precipitation led to the contamination of ground wells at Walkerton, Ontario leading to an outbreak of E coli (Hrudey et al. 2003). This and other effects have the greatest impact among the most vulnerable elements of our society. Poorer and smaller communities have less capacity to cope with such events and their infrastructures have a lower threshold of stress regarding maximum precipitation. Therefore it is very important to assess whether physical changes to our climate system - brought on by global warming – will lead to an increased risk of extreme precipitation.

1.1 IMPACTS

1.1.1 Flash Floods

Extreme precipitation events often lead to flash flooding (rapid water level response in a small basin) given that certain hydrological conditions such as soil saturation, terrain and land slope etc are met (Doswell et al. 1996). French et al. (1983) found flooding to be the deadliest weather related hazard in the United States. More recently however, the National Weather Service has ranked flooding the second leading cause of weather related deaths in the United

States behind extreme heat (http://www.nws.noaa.gov/os/hazstats.shtml). Ashley and Ashley (2007) found that it was specifically flash floods which were associated with the most fatalities. With an increase in extreme precipitation, urbanization, and land use practices leading to rapid channeling of runoff it can be expected that the risk of injury or death from flash flooding will become even more significant.

1.1.2 Health-related Issues

During periods of intense precipitation, local drainage systems may become overwhelmed and contamination of water supplies with sewage may occur (Patz et al. 2000). Curriero et al. (2001) established a statistically significant relationship between extreme precipitation events and outbreaks of waterborne illness in the United States. Fifty-one percent of all outbreaks of waterborne disease in the United States were found to have been preceded by precipitation events equal to or greater than the 90th percentile. Cases linked to surface water contamination were associated with events recorded in the same months while a lag was associated with incidents involving groundwater contamination. In Canada, the significant rains in the spring of 2000 led to the contamination of drinking supplies with E coli bacteria at Walkerton, Ontario (Hrudey et al. 2003). Extreme precipitation events in regions of poor drainage can also lead to high concentrations of mosquito development which are vectors for parasitic diseases like malaria (Patz et al. 2000). Climate change therefore has the potential to significantly impact the occurrence of such outbreaks.

1.1.3 Agricultural Damages

Extreme precipitation events have the capability of inflicting great agricultural losses due to inundation and fostering conditions favorable to the development of fungal and other plant diseases. In a study of climate extremes affecting California agriculture between 1993 and 2007, Lobell et al. (2009) found that excess precipitation was the leading cause of agricultural damages and insurance payments. A shift to larger, less frequent rainfall events has significant implications on soil moisture dynamics (Knapp et al. 2008). In particular mesic regions (those with an even or adequate moisture supply) would experience an increase in periods outside the optimal soil moisture ranges of plants. There would be more time outside of the stress thresholds of soil moisture due both to drought and waterlogged conditions. Rosenzweig et al. (2002) used the crop model CERES to simulate increased agricultural damages to maize due to saturated root zones. The authors projected an increase in damages of nearly double current values given a 30 percent increase in extreme precipitation events (greater than 25 mm, 50 mm, and 75 mm) by 2030.

1.2 PHYSICAL INSIGHTS

The basis for anticipated increases in extreme precipitation is the expected rise in temperature brought on by higher concentrations of atmospheric carbon dioxide (Trenberth 1999). Specifically, due its radiative properties, an increase in terrestrial radiation reflected back down to the earth will lead to increases in air and ocean temperatures. There is an established relationship between temperature and the saturated water vapor pressure over water known as the Clausius – Clapeyron relation (Christensen and Christensen 2002). Vapor pressure is the force exerted by molecules of a particular substance suspended in the air and increases as the concentration of that substance becomes greater. At a particular temperature, there is a balance between the rate of evaporation and condensation from a water surface resulting in a specific saturated water vapor pressure. As the temperature increases the rate of evaporation shifts upwards and leads to a greater water vapor pressure.

In fact, an empirical relationship between increases in water temperature and precipitable water (total or vertically integrated moisture content of the whole atmospheric column over a given point) has been worked out using satellite estimates of atmospheric water content (Gordon et al. 1992). As a consequence more moisture becomes available to the entire spatial scale of meteorological systems from micro to synoptic (Trenberth 1999). Along with anticipated northward shifts in the jet stream and storm tracks, and alteration of pressure patterns (Meehl et al. 2005), increased moisture advection will set the stage for extreme precipitation events in new regions.

1.3 MECHANISMS

To understand future changes in extreme precipitation occurrence, a further review of the mechanisms driving such events is necessary. This is particularly true since the characteristics related to extreme events may change for certain regions in the future. Ultimately the amount of precipitation that occurs during a fixed time interval is determined by the intensity at which it is falling. Extreme rates of precipitation are associated with rapidly ascending air. This upwards acceleration causes air to cool adiabatically, until it reaches the lifted condensation level (LCL). It follows that the faster the air is lifted and the more moisture present the greater the rate of precipitation. In more quantitative terms, the rate of precipitation is proportional to the product of vertical velocity and mixing ratio (Doswell et al. 1996).

The advection of moisture may either be vertical or horizontal. Horizontal advection is represented by the transport of moisture from the oceans – in North America the main sources are the Pacific Ocean and the Gulf of Mexico. Vertical advection comes in the form of evaporation and transpiration from the ground surface up through the atmospheric column. Some studies such as Raddatz (2005) have found that in wet years, the contribution from the combined effects of evaporation and transpiration (evapotranspiration) was higher than in dry years. Therefore, high soil moisture can be seen as a precursor to extremes in precipitation and a positive feed-back loop between initial moisture conditions and increased precipitation exists.

There are several atmospheric processes which are responsible for upwards lift. Large scale ascent is produced from geostrophic forcing consisting of two components – positive vorticity advection and warm air advection ahead of upper atmospheric disturbances. In particular isentropic up-glide, whereby air ascends along constant density surfaces (represented by potential and equivalent potential isentropes), has been linked with intense precipitation. Shear vorticity effects caused by the entrance and exit regions of upper level wind maxima are also important. Frontogenetic forcing associated with thermal direct circulations across temperature gradients also contributes to lift in the atmosphere. However, the above dynamic mechanisms are usually not sufficient to sustain a high enough rate of upwards motion to generate the upwards moisture flux needed for intense precipitation (Doswell et al. 1996). Extreme rates of precipitation are associated with rapidly ascending air associated with thermodynamically unstable air or forced topographic lifting.

Many North American studies have shown that large precipitation events are linked with instability. Raddatz and Hanesiak (2008) found that 79% of all significant warm season precipitation events involved convective processes on the Canadian Prairies. Similarly, Heideman and Fritsch (1988) estimated that 80% of significant rain events from June 1982 to August 1983 in the United States were attributable to convection. Meanwhile, Raddatz and Khandekar (1979) found that prolonged upslope flows associated with occluded lows across the Canadian Prairies have lead to very high precipitation totals. In many cases, both mechanisms may occur simultaneously. Szeto et al. (2011) noted a bimodal spatial pattern in the maximum precipitation associated with a catastrophic rain event affecting the Northern Plains and Canadian Prairies during June 2002. One maximum was associated with stratiform precipitation and orographic lift along the foothills and mountains of Alberta while a convective complex led to an eastern centre of high rainfall further east in Manitoba.

The tendency of an air parcel to accelerate in the direction of its initial displacement represents its instability. It is important to note that instability need not be surface based – instability may be rooted at a higher level above nocturnal or frontal inversions and insolated from the thermal effects of the surface (Colman 1990a). Even if the atmosphere is gravitationally stable (surface based or elevated), inertial or symmetric instability may be present (Coleman 1990b) resulting in what is known as slant-wise convection.

Intense convection can organize itself into many forms on different spatial scales. Maddox et al. (1979) developed a climatology for extreme precipitation events associated with flash flooding. At one end of the spectrum were synoptically induced events and on the other end were events induced thru meso-scale processes such as convergence from outflow boundaries. The synoptic type events were found to be more common during the winter seasons while those tied to more meso-scale processes peaked in the warmer season. Schumacher and Johnson (2005) found that only 28% of extreme rain events in the United States east of the Rocky Mountains were associated with synoptic forcing whereas Raddatz and Hanesiak (2008) determined that less than 30% of significant precipitation events on the Canadian Prairies were not driven by synoptic processes. In a follow-up, Schumacher and Johnson (2006) showed that synoptic type events were most common outside the summer season. Synthesizing an explanation for the above results, as the core of westerly air flow and associated disturbances migrates northwards, mesoscale mechanisms become dominant in southerly latitudes during summer. The Canadian Prairies represent a high enough latitude zone that synoptic forcing remains common place even in summer.

1.4 MODEL STUDIES

1.4.1 Global Circulation Model Studies

The above physical assumptions are confirmed in multiple simulations showing increases in extreme precipitation across many regions under a scenario of increased atmospheric carbon dioxide. Early studies had a global focus relying on Global Circulation Models. Many showed higher precipitation averages for several areas driven by increased frequency of higher magnitude precipitation events (Houghton et al. 1992). Noda and Tokiaoka (1989) found an increase in convective precipitation using the MRI global circulation model from the Japanese Meteorological Research Institute with a doubling of carbon dioxide levels in the atmosphere. It is convection that is responsible for the most intense precipitation rates because it is associated with rapidly ascending air (Doswell et al. 1996). Gordon et al. (1992), using the CSIRO global circulation model reinforced the previous findings as they also discovered an increase in intense, convective precipitation and a reduction in stratiform rains particularly over the lower latitudes. Hennessy et al. (1997) using CSIRO9, which is a later version of the above model, along with the Hadley Centre for Climate Prediction and Research global circulation model UKHI also found an increase in convective precipitation over lower and mid latitudes and more extreme precipitation at high latitudes even though it was non convective in nature. Zwiers and Kharin (1998) used a Canadian Global Climate Model (CGCM2) developed by the Canadian Centre for Climate Modeling and Analysis (CCCma) to show an increase in extreme precipitation across virtually the entire globe with particular emphasis over Northwest India related to possible changes in the South Asian monsoon. This echoes the findings of Palmer and Raisanen (2002); namely that the probability of extreme precipitation totals (as defined by amounts greater than two standard deviations from the mean) would increase over the monsoon regions of South Asia and wintertime Europe when data from several global climate models run under doubled atmospheric carbon dioxide concentrations were examined. Kimoto et al. (2005) when analyzing data from the Model for Interdisciplinary

Research on Climate (MIROC) GCM showed that regionally, the frequency of daily precipitation exceeding 30 mm increases over Japan in a future scenario of midrange carbon dioxide induced warming.

1.4.2 Downscaling and Regional Circulation Models

Global models however are characterized by coarse spatial resolutions which can make accurately simulating intense, convective precipitation very difficult. Such occurrences often affect regions considerable smaller than the area of each grid cell. Consequently extreme events are not reproduced effectively as the average conditions within the course parameters of the grid cell are generated. To address such limitations, downscaling procedures have been developed for application on Global Circulation Model generated data to improve accuracy and to better model convective precipitation. The downscaling processes can be either statistical or dynamic. The use of higher resolution, dynamic Regional Climate Models nested within (and driven by global scale models) has been used in several studies to examine the impacts of global warming on extreme precipitation occurrence. Many of these simulations have focused on Europe and the United Kingdom.

Christensen and Christensen (2002) using the high resolution regional climate model HIRAM4 from the Danish Meteorological Institute (driven by an ocean atmosphere coupled global climate model known as ECHAM4/OPYC), found an increase in precipitation events exceeding the 95th percentile for many regions of Europe under conditions of greater atmospheric carbon dioxide concentrations. In a follow up, Christensen and Christensen (2004) used two global circulation models with different boundary conditions (ECHAM4/OPYC and HadAM3H from the Hadley Centre) to drive the same, higher resolution Regional Climate Model (HIRAM4). Reinforcing the previous study they found statistically significant increases in 95th percentile precipitation for many regions of Europe and an increase (although not statistically significant due to small sample size) for 99th percentile precipitation. The findings are also in line with the earlier study of Jones and Reid (2001) using the global HadCM2 and a regional model from the Hadley Centre, to show both an increase in the frequency of days with extreme precipitation (exceeding the threshold for various return periods) and increases in the amount of precipitation associated with each of those particular return periods. Huntingford et al. (2003) also using global and regional model from the Hadley centre found the return interval for specific 30 day precipitation totals capable of triggering floods diminished from 20 to as little as 2 or 3 years in some instances.

1.4.3 Model Ensembles

Although the use of regional models allows for better resolution and modeling of the complicated processes behind precipitation and especially convective precipitation, the downscaling process incurs a large amount of uncertainty. In order to improve confidence in the simulations and to provide a measure of uncertainty in their results (Beniston 2007), several studies using multiple models have been conducted recently taking advantage of Model Inter-comparison Projects (MIPs). One such study was the aforementioned Palmer and Raisanen (2002) analysis utilizing 19 global models from the Second Coupled Model Inter-comparison

Project (CMIP2). More recently projects have been developed incorporating suites of high resolution climate models into ensembles such as PRUDENCE (Prediction of Regional scenarios and Uncertainties for Defining European Climate change risks and Effects) in Europe (Christensen and Christensen 2007) and NARCCAP (North American Regional Climate Change Assessment Program: http://www.narccap.ucar.edu/about/acknowledgements.html) for North America. Beniston (2007), using PRUDENCE found an increase in the 1 day and 5 day precipitation totals associated with a 5 year return interval for almost all of Europe north of 45 degrees latitude under a scenario of increased carbon dioxide emissions. Fowler et al. (2007) also used PRUDENCE to demonstrate increases in the values of 10 day precipitation events with one in 5 year and one in 25 year occurrences by 10 to 20 % over the UK under a midrange increase in atmospheric carbon dioxide (IPCC SRES A2). The above study incorporated 6 regional climate models with equal weight given to all. Fowler and Ekstrom (2009) reanalyzed trends in extreme precipitation by making use of seven additional models for a total of 13 in their ensemble, and weighted output from each model according to their performance in validation. They reported increases in precipitation extremes of between 5 to 30% with particular emphasis on winter. Gutowski et al. (2008) utilized an ensemble set from NARCCAP to demonstrate that the threshold values for extreme precipitation associated with winter-time, synoptic scale systems will increase in the future along with saturated water vapor levels over the upper Midwest region.

1.4.4 Statistical Perspective

Several studies have also focused on a probabilistic or statistical approach as opposed to a deterministic one to assess future trends in extreme precipitation. Using a statistical model based on observational reports of precipitation for a number of North American stations, Groisman et al. (1999) demonstrated that with a constant shape parameter for the distribution, a 5 % increase in mean precipitation would lead to a 20 % increase in the occurrence of precipitation events greater than 25 mm at high latitudes and 50 mm for middle and low latitudes. Conversely Voss et al. (2002), showed that a stretching of the probability density functions in data from a general circulation model leads to more extreme precipitation episodes with increased carbon dioxide emissions. This reaffirmed the conclusions of Katz and Brown (1992) that changes in variability are the most important driver of increased extreme occurrences.

1.4.5 Recent Studies

Recently, studies focused over Canada using a Canadian Regional Climate Model have been carried out. The findings tend to support the consensus of most previous model studies. Specifically, extremes in precipitation and moisture regimes will become more exaggerated in the future climate with increases in the magnitude of extreme rainfall events over most regions (Mladjic 2011) and at the same time, longer and more frequent droughts (PaiMazumder 2010).

As well, there have recently been studies utilizing so-called extended models which have higher resolution at the level of the stratosphere to better model processes associated with that level of the atmosphere. Scaife (2011) found that increased wind shear through the upper troposhere and stratosphere over the midlatitudes led to a southwards shift in the preferred storm track during the winter season. This introduces some uncertainty into previous assumptions of how the jet stream and storm tracks will respond to increased atmospheric carbon dioxide concentrations.

1.5 OBERVATIONAL RESULTS

In light of all the projections and simulations - whether derived from global or regional models, dynamic or statistical - researchers began analyzing whether actual observations were in fact validating what was being predicted. Among the first of such studies carried out was by Iwashima and Yamamoto (1993), who studied historical trends in extreme precipitation at 55 stations in Japan and 14 stations in the United States. They reported an upwards trend in the percentage of extreme precipitation events (top 3 recorded for each stations) occurring in bi-decadal periods for Japan and decadal periods for the United States through the twentieth century. The work of Iwashima and Yamamoto (1993) spurred on further studies of the United States using a larger sample of recording stations.

Karl et al. (1995) showed that the area of the United States having experienced an above normal percentage of its precipitation from events greater than 50.8 mm has increased from 9 to 11 % in the period from 1921 to 1985. However as Kunkel et al. (1999) pointed out , many arid regions of North America do not experience daily precipitation totals of 50 mm or greater. In their next study, Karl and Knight (1998) altered the criteria for assessing extreme precipitation to the total contribution of precipitation from events greater than or equal to the 90^{th} percentile, and found that it is increasing for most regions of the United States. Kunkel et al. (1999) reaffirmed these findings when examining precipitation observations from 1931 to 1996 - detecting an upwards trend in 7 day extreme precipitation totals associated with a 1 year return interval.

Zhang et al. (2000) studied adjacent regions of southern Canada and found that generally the climate is becoming wetter; reflected by 5 to 30 % increases in precipitation. The authors also detected an increase in areas experiencing greater than or equal to 64^{th} percentile precipitation events. Zhang et al. (2001) using a more stringent criteria for extreme events, namely the 90^{th} percentile for daily precipitation, discovered an increase in heavy rain events during spring over eastern Canada that agrees with the findings of the American studies. However Akinremi et al. (1999) did not find any increase in precipitation intensity over the Canadian Prairies, although low to moderate events were found to be contributing to increases in overall precipitation. These findings are also consistent with the studies of Karl and Knight (1998) and Kunkel et al. (1999) which depicted regions of no increase or decrease over North Dakota and Montana.

Osborn et al. (2000) used a similar method to Karl and Knight (1998) to show a positive trend in occurrence of extreme precipitation during the winter season for the United Kingdom. Moberg et al. (2006) found a similar pattern of winter time increases in 90^{th}, 95^{th}, and 98^{th} percentile events across all of Europe in their analysis of data spanning the twentieth century.

Similar results were reported in studies focused over southern Europe where Brunetti et al. (2001) found an increase in the intensity of daily precipitation in the period spanning 1951 to 1996 over Italy, and Alpert et al. (2002), in their study of the broader Mediterranean region, discovered a fourfold increase in the contribution from torrential (greater than 128 mm) daily rainfall at Italy and an increased frequency of extreme events (greater than 64 mm) over Spain. For India, Roy and Balling (2004) analyzed 903 time series of extreme precipitation indices and found an upwards trends for 61% of the cases. Zhai et al. (2005) found an increase in 95th percentile daily rainfall events in China for the Southern and Southeastern coastal areas and in western regions.

A particular spatial pattern of increased extreme precipitation in the Northern Hemisphere is revealed when examining the above studies - validating what the array of models and simulations have been projecting. Although it is apparent that not all regions are experiencing an increase, many other locations are in response to changing synoptic patterns as carbon emissions into the atmosphere continue to rise.

1.6 VULNERABILITY AND OVERALL RISK

Compounding the physical changes in our climate that increase the probability of extreme precipitation events, certain social and economic activities are making populations more susceptible to the effects of such occurrences. As a consequence our total risk, which is a function of both physical exposure and social vulnerability, will become even greater. For example, the concentration of people in low lying areas increases vulnerability to the most obvious manifestations of extreme precipitation, namely flooding (Few 2003). Urbanization itself encourages a more rapid run-off of intense precipitation and flash flooding due to paving of ground surfaces with impermeable substances such as concrete. Pelling (1997) noted that a 50 % increase in the coverage of impervious surfaces in Georgetown, Guyana during the period from 1963 to 1993, led to more frequent flooding. Nirupama and Simonovic (2007) linked the significant urbanization that had taken place along the Upper Thames River watershed to an increased risk of flooding for the city of London, Ontario. The destruction of wetlands and the straightening of drainage channels in order to increase agricultural production reduce the landscapes ability to absorb large amounts of precipitation. The clearing of vegetation along slopes and hillsides increases the risk for slope failure and mudslides when extreme precipitation occurs. This was illustrated by the devastation wrought from Hurricane Mitch in Central America in 1998 (Comfort et al. 1999). Given the combination of physical and social changes relating to extreme precipitation events and their consequences, it is important to ask what the future impacts of such trends will be.

CHAPTER 2: OBJECTIVES

Given the intriguing pattern seen in the observational trends in extreme precipitation events, and the fact that there have only been a few model simulations specific to Canada, the overall objective of this study is to examine the characteristics and mechanisms of extreme precipitation events in the past and future climate. Specifically the purpose of this study is:

i) To analyze historical observations at five selected locations across Canada to understand current regional differences in annual and monthly precipitation and frequency of extreme events.

ii) To determine whether the magnitude and occurrence of extreme events in the future - as projected by the Canadian Regional Climate Model version 4.2.0 - increases compared with the historical records and base period simulation for the same locations.

iii) To assess the model's ability to simulate the past and present climate by comparing data from the base period simulation with the historical observations for the five locations.

iv) To examine the synoptic characteristics of simulated extreme events in the present and future and note any changes in the mechanisms responsible for them.

v) To study the synoptic characteristics of observed extreme events using The National Centers for Environmental Prediction reanalysis data, and to assess the model's accuracy in simulating the mechanisms behind them.

CHAPTER 3: METHODOLOGY

Five locations were chosen for this study – three western and two eastern representing different climate regions across Canada. The selections were based on input from the Canadian Water Network and represent small or aboriginal communities which are more vulnerable to increased extreme events. The five locations are situated near:

i) Frog Lake, AB (near Cold Lake)

ii) Atikameg, AB (near High Prairie)

iii) Assiniboia, SK

iv) Guelph, ON

v) MacTier, ON (near Muskoka)

For the purposes of clarity and simplicity the Frog Lake, Atikameg, and Mactier locations will be referred to as Cold Lake, High Prairie, and Muskoka respectively for the rest of this study. Three precipitation datasets were examined and analyzed for each site. The first consisted of corrected precipitation observations acquired for the nearest available Environment Canada weather station. The second and third sets are model output from the CRCM 4.2 (Canadian Regional Climate Model version 4.2). They consist of a base period simulation spanning 1961 to 1990 and future scenario of mid range CO_2 increases (IPCC SRES A2) from 2041 to 2070. The precipitation observations were acquired from Environment Canada whereas the model data was downloaded via the Data Access Integration (DAI) website and the relevant grid points for each location were subsequently extracted.

A statistical analysis was carried out on all three datasets to characterize their mean annual and monthly precipitation totals and their respective 90th, 99th and 99th percentiles. Furthermore, the frequency and contribution of various precipitation classes was established. The precipitation bins were as follows:

i) 0 mm – no precipitation

ii) 0.1 to 5 mm

iii) 5 to 10 mm

iv) 10 to 25 mm

v) 25 to 50 mm

vi) 50 to 100 mm

vii) 100 to 200 mm

The monthly occurrence and frequency of days with 90th, 99th and 99.9th percentiles was established. Lastly the cumulative totals of the wettest and driest months were calculated. The various datasets have been summarized in the table below for the sake of clarity (Table 3.1).

Table 3.1: Datasets and Time Periods Used in This Study.

Dataset	Time Period
Corrected precipitation observations (a)	1900 - 2007
Corrected precipitation observations (b)	1961-1990
NCEP Reanalysis	1961 - 1990
CRCM base period simulation of precipitation intensity (adj)	1961 – 1990
CRCM future projection of precipitation intensity (adk)	2041 -2070

3.1 Background on Corrected Data and Model Used in Study

The Environment Canada data utilized in this study belong to a rehabilitated time series of precipitation records for Canadian recording stations. Mekis and Hoggs (1999) developed a protocol for adjusting precipitation records to correct for various biases which different precipitation gauges display with respect factors such as wind, evaporation, and overspill. Instances of trace precipitation are flagged in the datasets; correction procedures have been outlined and can be applied to estimate values for the trace amounts of precipitation. In this particular study, trace amounts of precipitation were treated as zero.

As mentioned previously, the model used in this investigation is the latest version of the CRCM (version 4.2). It was driven by the fourth member of the Canadian Global Climate Model with which it shares much of its physical parameterization (Sushama et al. 2010). The model incorporates the latest Canada Land Surface Scheme (CLASS 2.7) and the Bechtold–Kain–Fritsch convection parameterization (Sushama et al. 2010). Horizontal resolution is 45 x 45 km with 29 vertical levels.

3.2 Review of Climatology

An analysis of the observed climatologies (including comparison of annual and monthly precipitation averages, extreme percentile values, and monthly distribution of extreme occurrence) was undertaken. The selected locations from across the country represent vastly different climates and precipitation regimes. In order to understand the effects of global warming on overall precipitation and extreme occurrence, one must first understand the existing diversity in climate patterns present across various regions of the country. It is the above local variations through which the effects of global warming will be modulated. A basic analysis was conducted for the entire time period of data available for each station - which varies from location to location (Corrected precipitation observations (a) from Table 3.1). However for the purposes of validating the model base period simulation (see below), a more thorough analysis was conducted specific to the 1961 to 1990 timeframe (corrected precipitation observations (b) from Table 3.1).

3.3 Validation

The analyzed datasets for the historical observations and the model base period simulation were compared to assess the model ability to replicate overall climate and extreme occurrences. Data for the grid points, corresponding to each of the locations, was extracted from a time-series of netCDF files using the Grid Analysis and Display System and written to a text file. Surrounding grid points were not utilized. The text file (one for each location) was then imported to excel where macros were developed to perform various statistical manipulations and calculate averages. Specifically, annual and monthly precipitation averages, 90^{th}, 99^{th}, and 99.9^{th} percentile values, and monthly distributions of extreme events were calculated. These were then compared for the two datasets.

3.4 Trends

The analyzed datasets for the base period simulation and the future scenario (2041-2070) were compared in order to examine trends in overall precipitation and occurrence of extreme precipitation events. Data for the relevant grid points was extracted from a time-series of netCDF files using the Grid Analysis and Display System (GrADS) and written to a text file. This file was then imported to Excel where macros were developed to perform various statistical manipulations and calculate averages. Specifically, annual and monthly precipitation averages, 90^{th}, 99^{th}, and 99.9^{th} percentile values, and monthly distributions of extreme events were calculated. Those specific values and any trends through the annual cycle were then compared for the two datasets.

3.4 Characteristics

Additional model data was acquired through the data access integration site for meteorological variables such as 850 and 500 hPa geopotential and winds for the model's entire North American domain. Data for both the base period and future scenario was downloaded. This was to examine the large scale characteristics associated with extreme events by identifying the top 3 precipitation events for all five locations and examining the above parameters. GrADS was used to view and manipulate the data. Additionally, a composite of various parameters was generated based on the top 3 events, and an anomaly was developed against the 30 year mean for the variable in question. The analyses for the base period and future simulation were compared to assess any changes in the mechanisms behind extreme precipitation events. Additionally the top ten precipitation events for both time periods were identified, listed and viewed on GrADS to get a more general sense of the characteristics for that group of events.

In order to validate the model simulations, composites of the same parameters (for all of North America) were generated for the observed top 3 precipitation events at each location using the National Oceanic and Atmospheric Administration's (NOAA) Physical Sciences Division online plotting tool (available at http://www.esrl.noaa.gov/psd/data/histdata/). The National Centers for Environmental Prediction reanalysis data used for the plots are available starting from January 1948. The top three events in the 1961 – 1990 climatology for each site were using to create the composites. The plots were compared with those generated from the simulated (1961-1990) model dataset to assess how accurately the model reproduced the synoptic characteristics associated with extreme events.

CHAPTER 4: RESULTS

A number of critical results are described in this chapter. These results are arranged in a progressive order from climatology through to the characteristics of extreme events.

4.1 Analysis of Local Climatologies

A review of the observed precipitation data from nearby surface weather observing stations reveal a clear contrast between western and eastern sites. The Prairie stations have considerably lower annual precipitation totals and display a warm seasonal maximum in monthly precipitation whereas the Ontario sites show a more even seasonal distribution of precipitation and even a cold season maximum in the case of Muskoka (Figure 4.1). The peaks in monthly precipitation occur in June, July, and August for Assiniboia, High Prairie, and Cold Lake respectively and in November for Muskoka. In terms of extreme occurrence however, there is a tendency even for the eastern locations to display a warm season maximum particularly in the case of 99th percentile events (Figure 4.2). Both eastern and western sites show a peak in average monthly occurrence in the June to September timeframe, although the maxima for the Ontario locations are not as pronounced and in the latter part of summer.

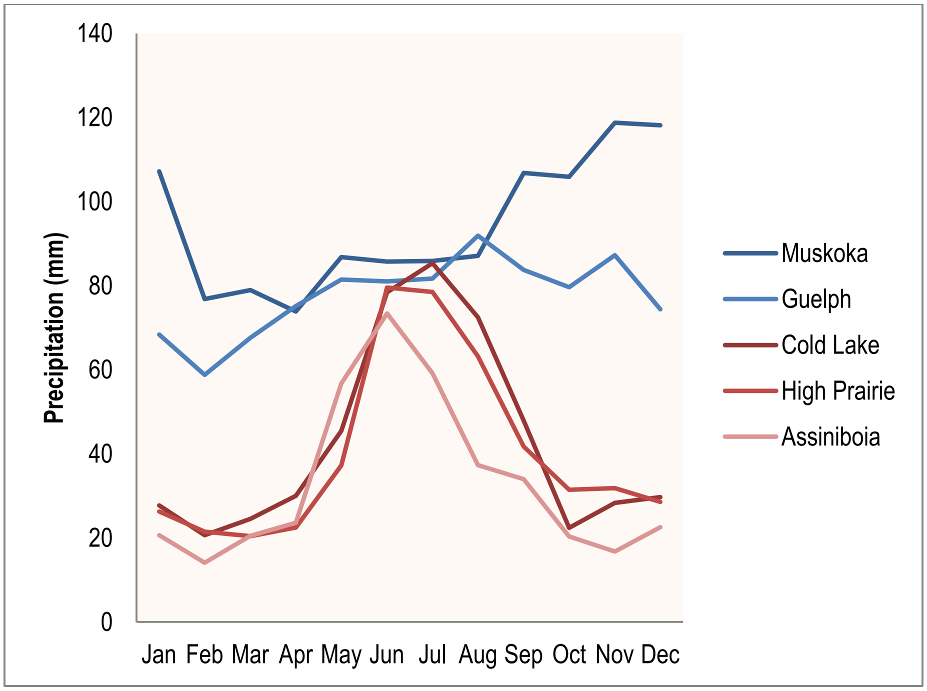

Fig 4.1: Average monthly precipitation over the annual cycle for the climatology at all locations using all available data.

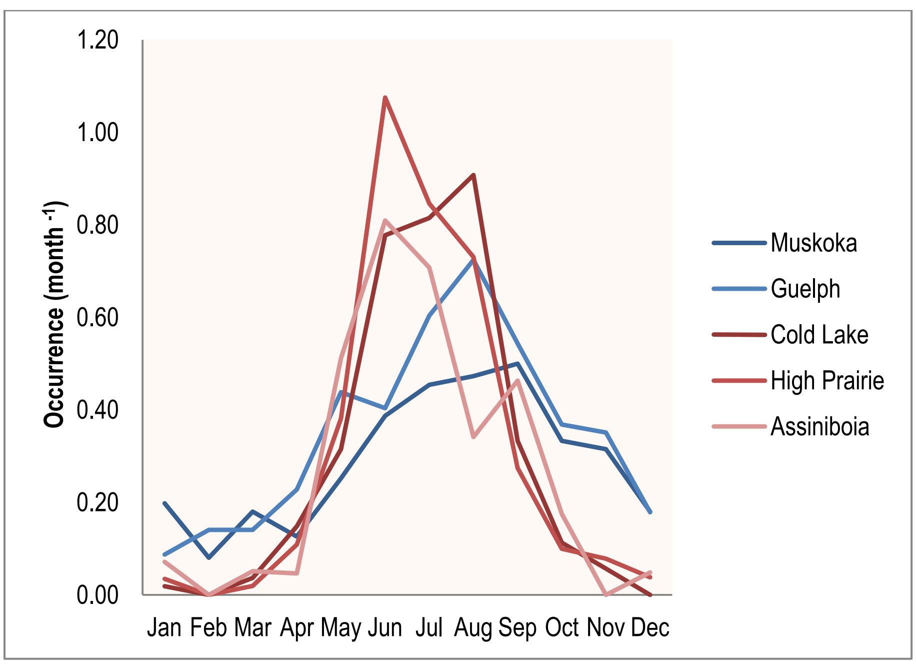

Fig 4.2: Monthly occurrence of 99th percentile daily precipitation events for the climatology at all locations using all available data. Units are the average number of occurrences per month.

4.2 Validation

Comparisons between the observed climatologies and data from the model base period simulation are outlined below for each location in terms of overall precipitation, extreme frequency and occurrence, including a monthly breakdown.

4.2.1 Cold Lake

The model overestimates frequency and contribution of small precipitation events (less than 5 mm) and underestimates number of days without precipitation (Table 4.1). The model underestimates the value for the 90th, 99th, and 99.9th percentile (Fig 4.3). The model also underestimates all other precipitation classes (both in terms of frequency and contribution to overall precipitation), including ones in the 25-50 mm and 50-100 mm which are above the 99.9th percentile for the observed climatology. The base period simulation underestimates annual precipitation with averages underestimated for every month except October (Figure 4.4). An early and exaggerated peak in monthly occurrence of 90th and 99th percentile events is observed (Figure 4.5). The model cumulative total for wettest months is lower than what is actually observed and conversely the cumulative total for driest months is higher suggesting the model cannot adequately reproduce the full extent of precipitation variability (see Figure 4.6).

Table 4.1: Comparison of average annual frequency and contribution to total accumulation for daily precipitation classes in the (a) 1961-1990 climatology and the (b) 1961-1990 model simulation at Cold Lake.

Precipitation (mm)	Annual Occurrence	Contribution (%)	Precipitation (mm)	Annual Occurrence	Contribution (%)
0	147.4	0.0%	0	109.9	0.0%
0.1 - 5	191.5	36.6%	0.1 - 5	240.7	65.7%
5 -10	16.0	22.2%	5 - 10	11.9	20.5%
10 - 25	9.4	27.6%	10 -25	3.2	11.1%
25 - 50	1.7	10.8%	25 -50	0.3	2.3%
50 - 100	0.2	2.8%	50 - 100	0.0	0.4%
100 - 200	0.0	0.0%	100 - 200	0.0	0.0%

(a) (b)

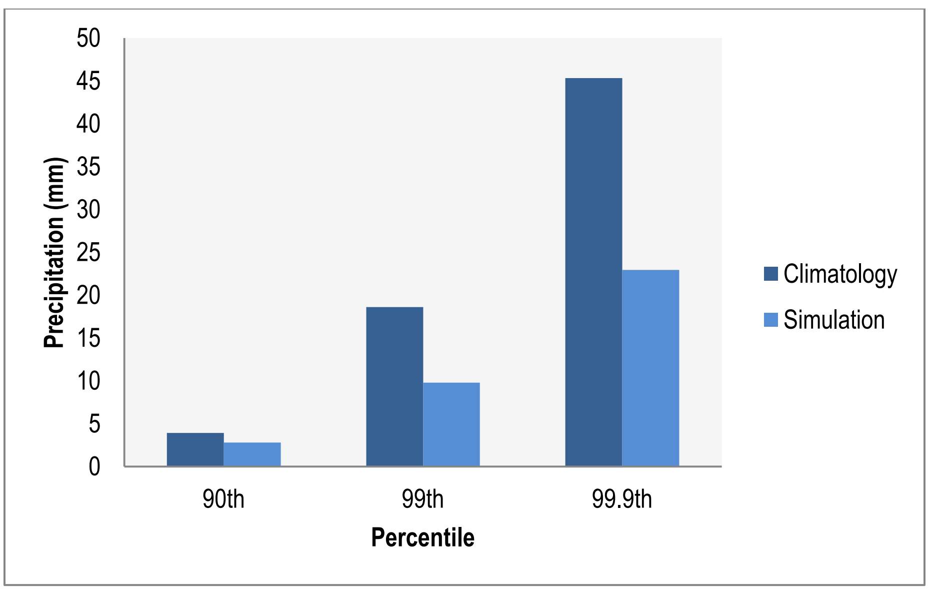

Figure 4.3: Comparison of extreme daily precipitation (90th,99th, and 99.9th percentile) for the observed 1961-1990 climatology and the 1961-1990 model simulation at Cold Lake.

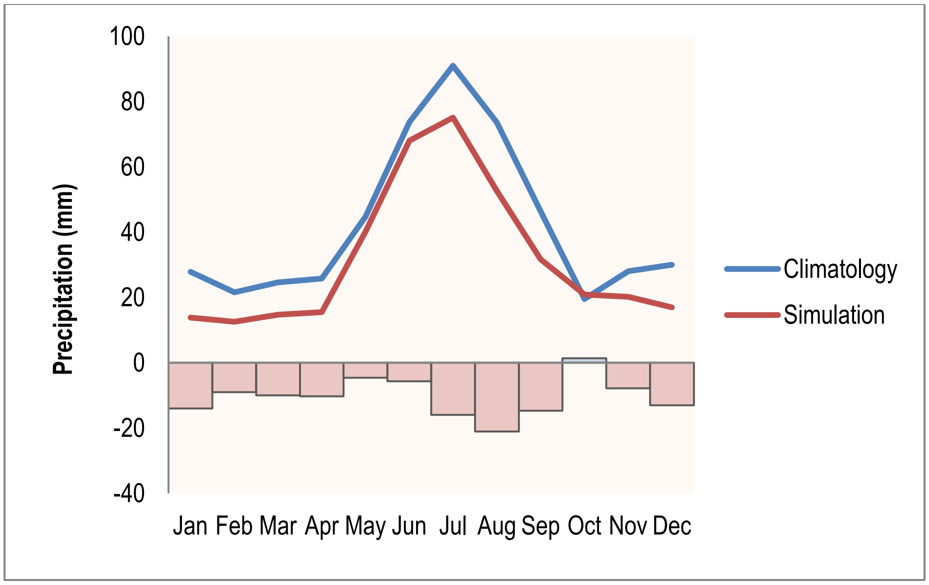

Figure 4.4: Comparison of the 1961-1990 climatology with the 1961-1990 model simulation over the annual cycle for Cold Lake. Red and blue bars represent model under and overestimation.

4.2.2 Assiniboia

Model largely underestimates the number of days without precipitation and greatly overestimates frequency and contribution of small precipitation events (Table 4.2). All other precipitation event classes are underestimated both in terms of frequency and contribution to overall precipitation - especially the 10 to 25 and 50 to 100 mm event classes. The value for the 90th percentile is slightly overestimated while those of the 99th and 99.9th percentile are underestimated by a large amount (Figure 4.7). The base period simulation slightly overestimates annual precipitation. Warm season precipitation from April to August is overestimated while winter precipitation is underestimated from December through March (Figure 4.8). The model displays an exaggerated summer peak in the monthly frequency of 90th, 99th, and 99.9th percentile events (Figure 4.9). The model cumulative total for wettest month is lower than observed and conversely the cumulative total for driest

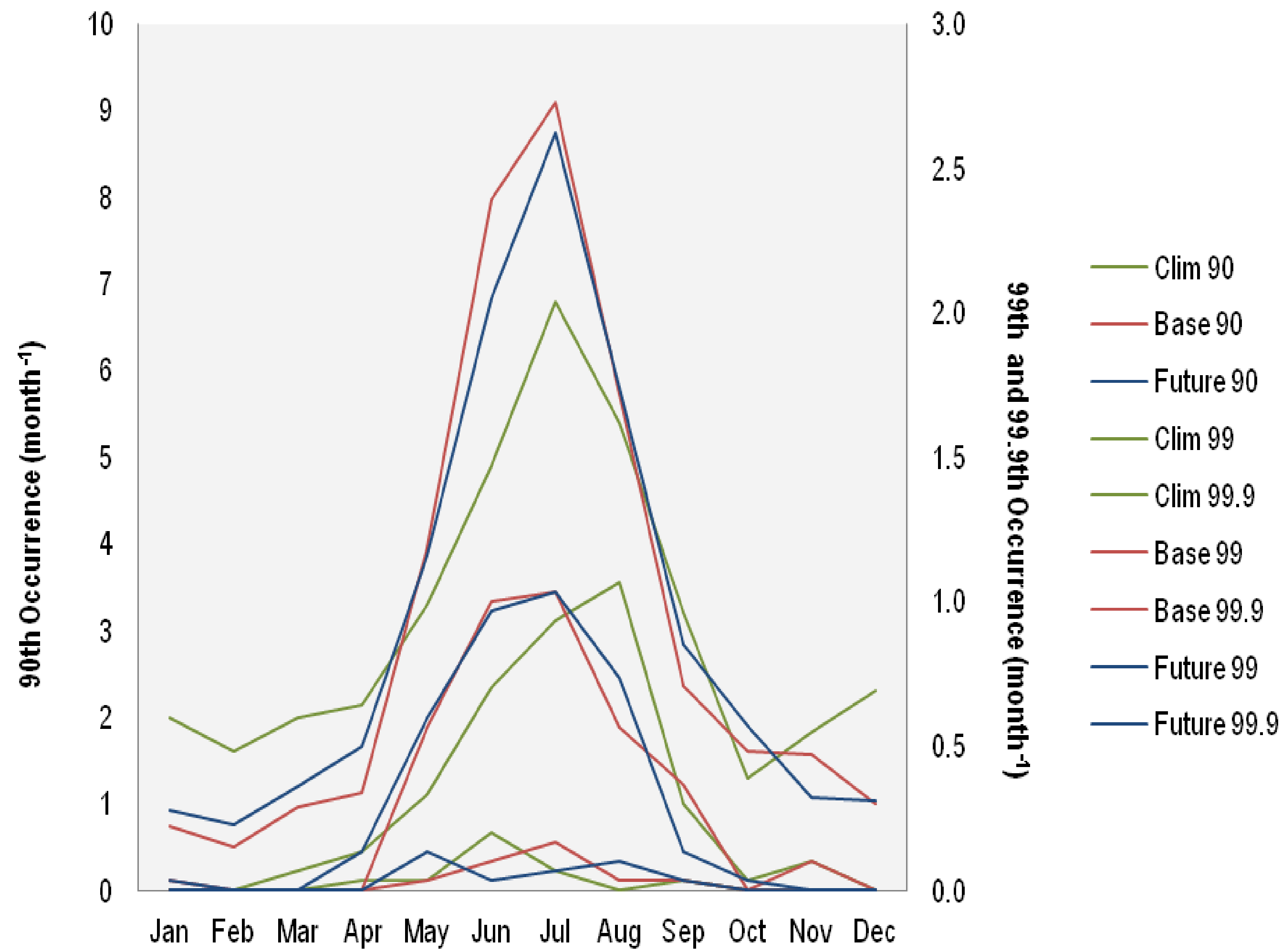

Figure 4.5: Monthly frequency of 90th, 99th, and 99.9th percentile events for the 1961-1990 climatology, the 1961-1990 model simulation and the 2041-2070 model projection at Cold Lake. The units are the average number of events per month.

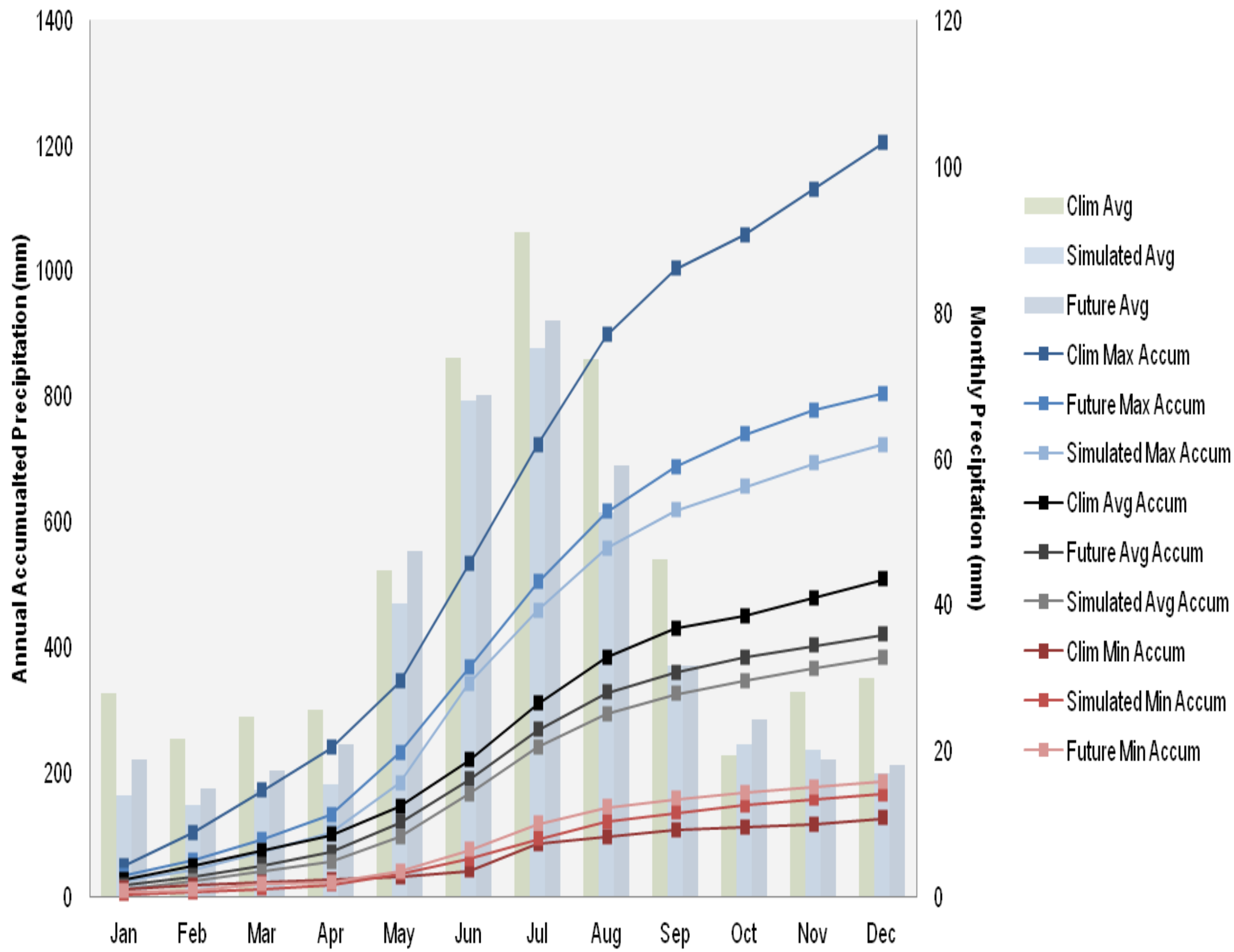

Figure 4.6: Cumulative annual precipitation for wettest months, average, and driest months and monthly average precipitation for the 1961-1990 climatology, the 1961-1990 model simulation and the 2041-2070 model projection at Cold Lake.

months is higher suggesting the model cannot adequately reproduce the full extent of precipitation variability (Figure 4.10).

Table 4.2: Comparison of average annual frequency and contribution to total accumulation for daily precipitation classes in the (a) 1961-1990 climatology and the (b) 1961-1990 model simulation at Assiniboia.

Precipitation (mm)	Annual Occurrence	Contribution (%)	Precipitation (mm)	Annual Occurrence	Contribution (%)
0	257.5	0.0%	0	128.3	0.0%
0.1 - 5	84.9	28.5%	0.1 - 5	219.1	57.9%
5 - 10	13.9	24.7%	5 - 10	13.9	23.6%
10 - 25	8.4	31.8%	10 - 25	4.4	16.0%
25 - 50	1.7	15.0%	25 - 50	0.3	2.5%
50 - 100	0.0	0.0%	50 - 100	0.0	0.0%
100 - 200	0.0	0.0%	100 - 200	0.0	0.0%

(a) (b)

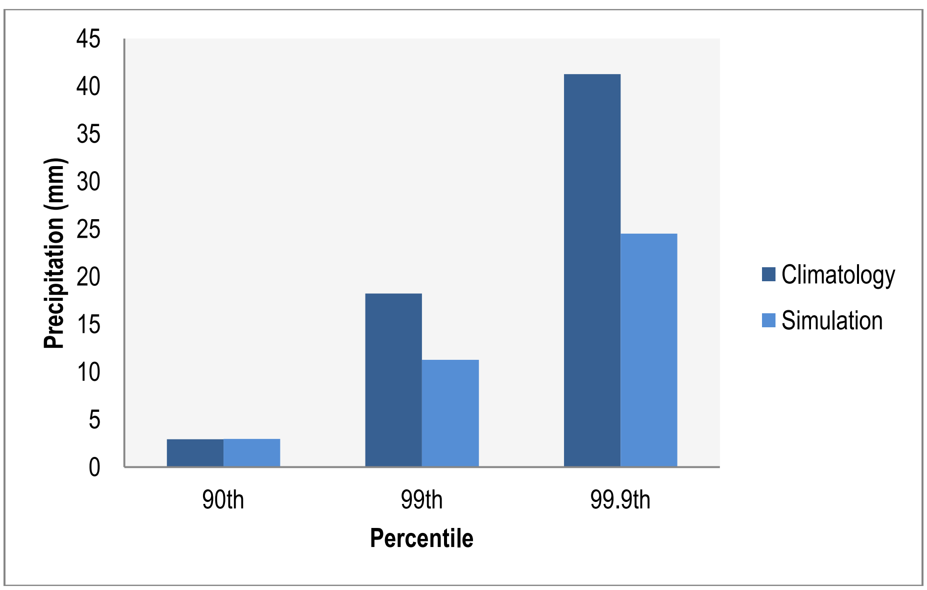

Figure 4.7: Comparison of extreme daily precipitation (90th,99th, and 99.9th percentile) for the observed 1961-1990 climatology and the 1961-1990 model simulation at Assiniboia.

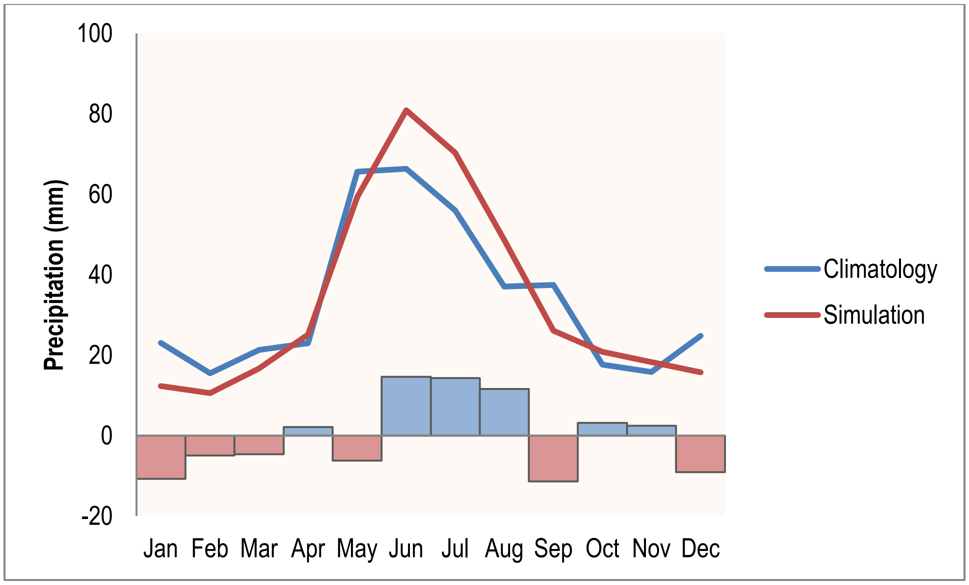

Figure 4.8: Comparison of the 1961-1990 climatology with the 1961-1990 model simulation over the annual cycle for Assiniboia

4.2.3 High Prairie

Model underestimates the number of days without precipitation and greatly overestimates frequency and contribution of small precipitation events (Table 4.3). All other precipitation event classes are underestimated both in terms of frequency and contribution to overall precipitation - including ones in the 25-50 mm and 50-100 mm which are above the 99.9th percentile for the observed climatology. The model slightly underestimates the value of the 90th percentile and greatly for the 99th and 99.9th percentile (Figure 4.11). Base period simulation slightly overestimates annual precipitation compared to actual observations. There is a somewhat exaggerated and delayed peak in monthly precipitation (Figure 4.12). A similar pattern is observed for the monthly peak in frequency of extreme occurrences, particularly 90th and 99th percentile events (Figure 4.13). The model cumulative total for wettest month is lower than what is actually observed and conversely the cumulative total for

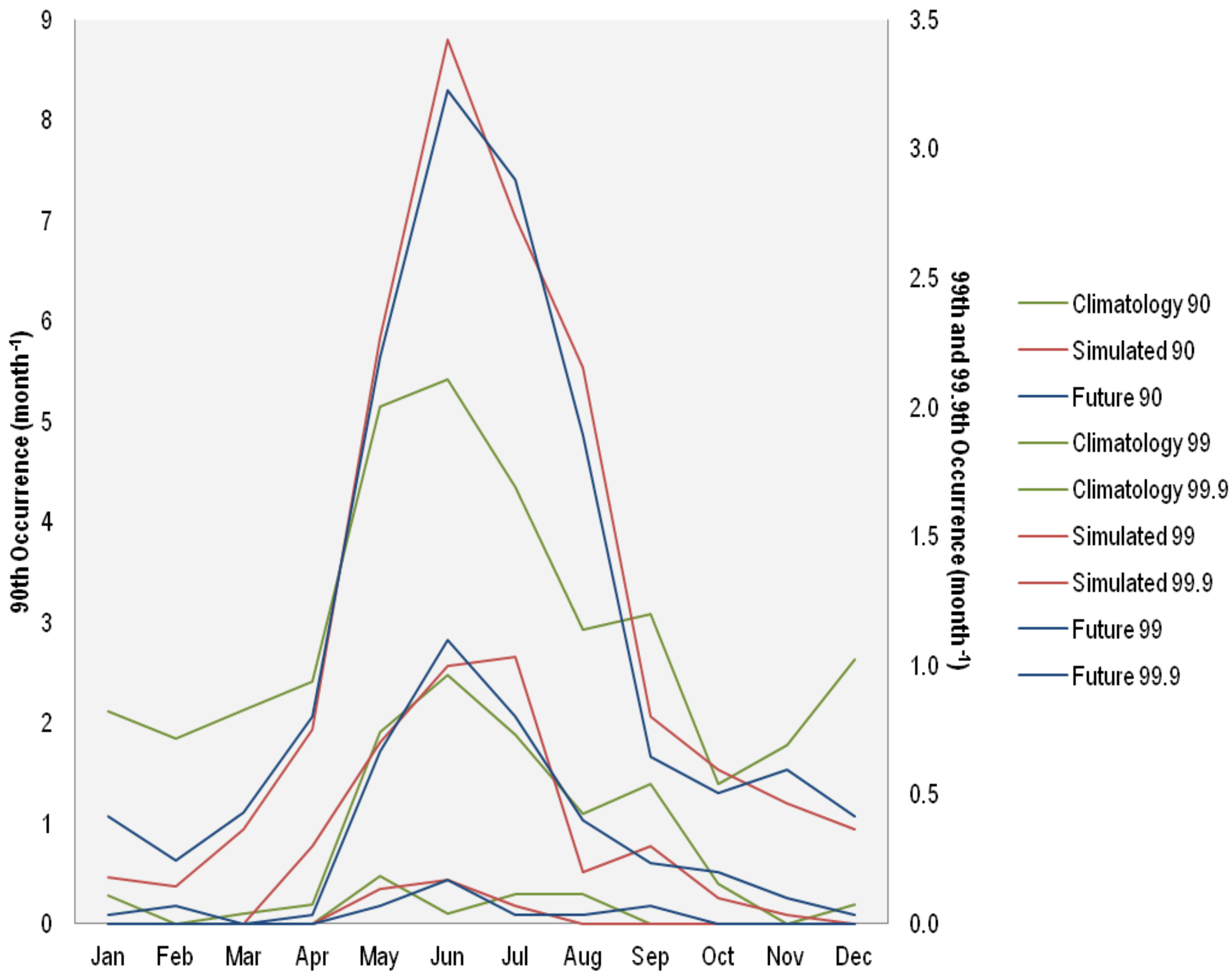

Figure 4.9: Monthly frequency of 90th, 99th, and 99.9th percentile events for the 1961-1990 climatology, the 1961-1990 model simulation and the 2041-2070 model projection at Assiniboia. The units are the average number of events per month.

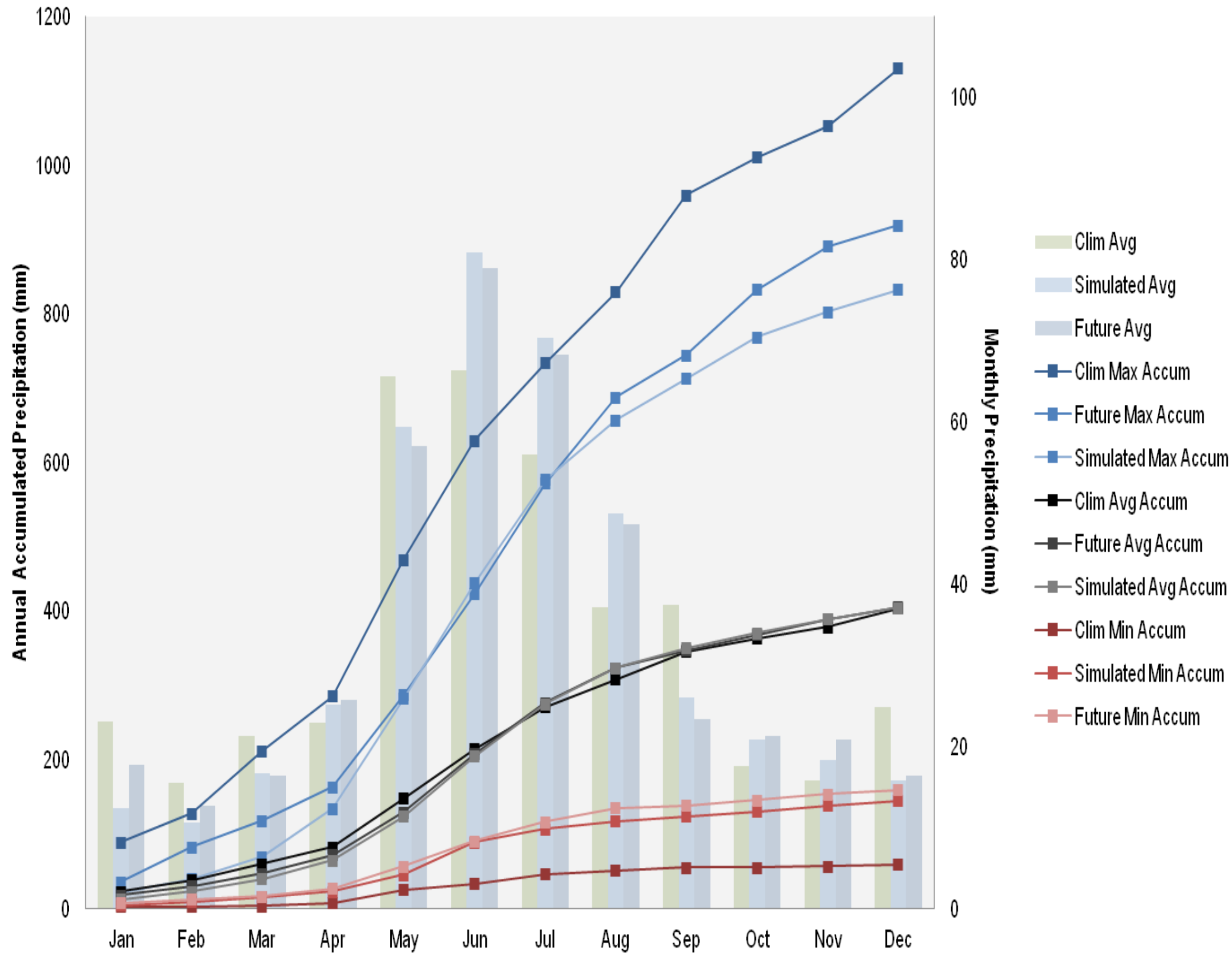

Figure 4.10: Cumulative annual precipitation for wettest months, average, and driest months and monthly average precipitation for the 1961-1990 climatology, the 1961-1990 model simulation and the 2041-2070 model projection at Assiniboia.

driest months is higher suggesting the model cannot adequately reproduce the full extent of precipitation variability Figure (4.14).

Table 4.3: Comparison of average annual frequency and contribution to total accumulation for daily precipitation classes in the (a) 1961-1990 climatology and the (b) 1961-1990 model simulation at High Prairie.

Precipitation (mm)	Annual Occurrence	Contribution (%)	Precipitation (mm)	Annual Occurrence	Contribution (%)
0	239.4	0.0%	0	93.5	0.0%
0.1 - 5	89.1	30.1%	0.1 - 5	250.3	64.1%
5 - 10	16.7	24.2%	5 - 10	18.2	24.3%
10 - 25	10.1	31.7%	10 - 25	3.8	10.5%
25 - 50	1.7	11.7%	25 -50	0.2	1.1%
50 - 100	0.1	1.0%	50 - 100	0.0	0.0%
100 - 200	0.0	1.3%	100 - 200	0.0	0.0%

(a) (b)

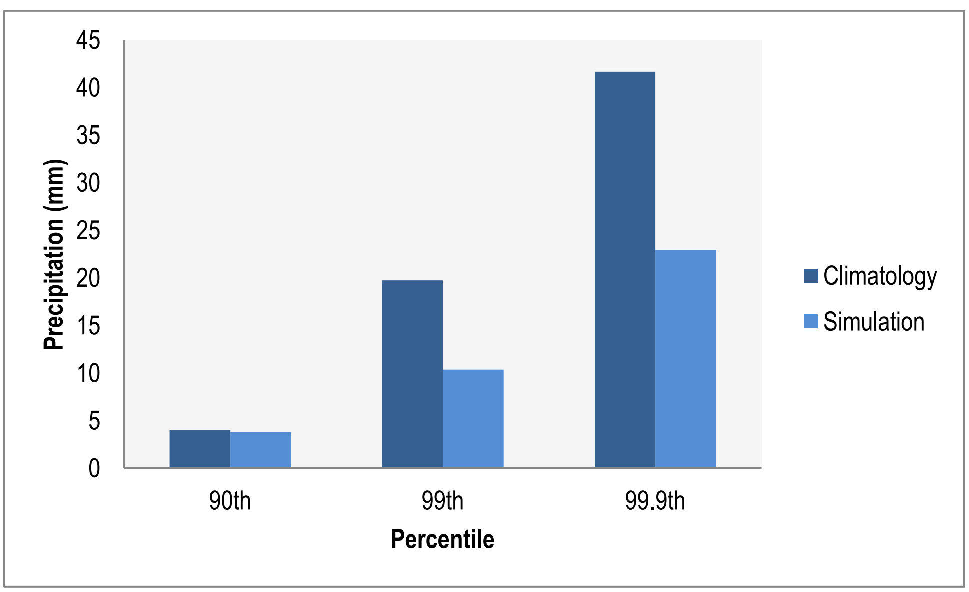

Figure 4.11: Comparison of extreme daily precipitation (90^{th},99^{th}, and 99.9^{th} percentile) for the observed 1961-1990 climatology and the 1961-1990 model simulation at High Prairie.

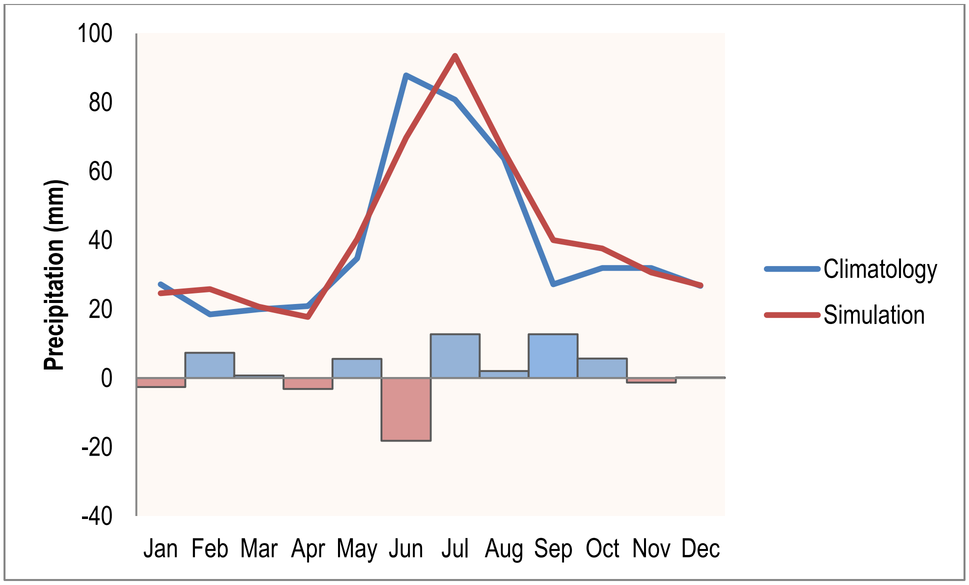

Figure 4.12: Comparison of the 1961-1990 climatology with the 1961-1990 model simulation over the annual cycle for High Prairie.

4.2.4 Guelph

By looking at Table 4.4, we can see the model underestimates the number of days without precipitation and overestimates small (but not as much as for the western locations) including frequency of events in the 5 to 10 mm class (also unlike the western sites). All other precipitation event classes are underestimated both in terms of frequency and contribution to overall precipitation especially the 25 to 50 mm class. The values for the 90th, 99th, and 99.9th percentiles are all underestimated - particularly the 99th and 99.9th (Figure 4.15). The base period simulation underestimates annual precipitation, with all monthly averages being lower than observed with the exception of May and June (Figure 4.16). The model displays a bi-modal peak in the occurrence of 99th and 99.9th percentile events centered on May and November/December respectively while the observed climatology shows a peak for all extreme percentiles in August (Figure 4.17). The simulated monthly frequencies

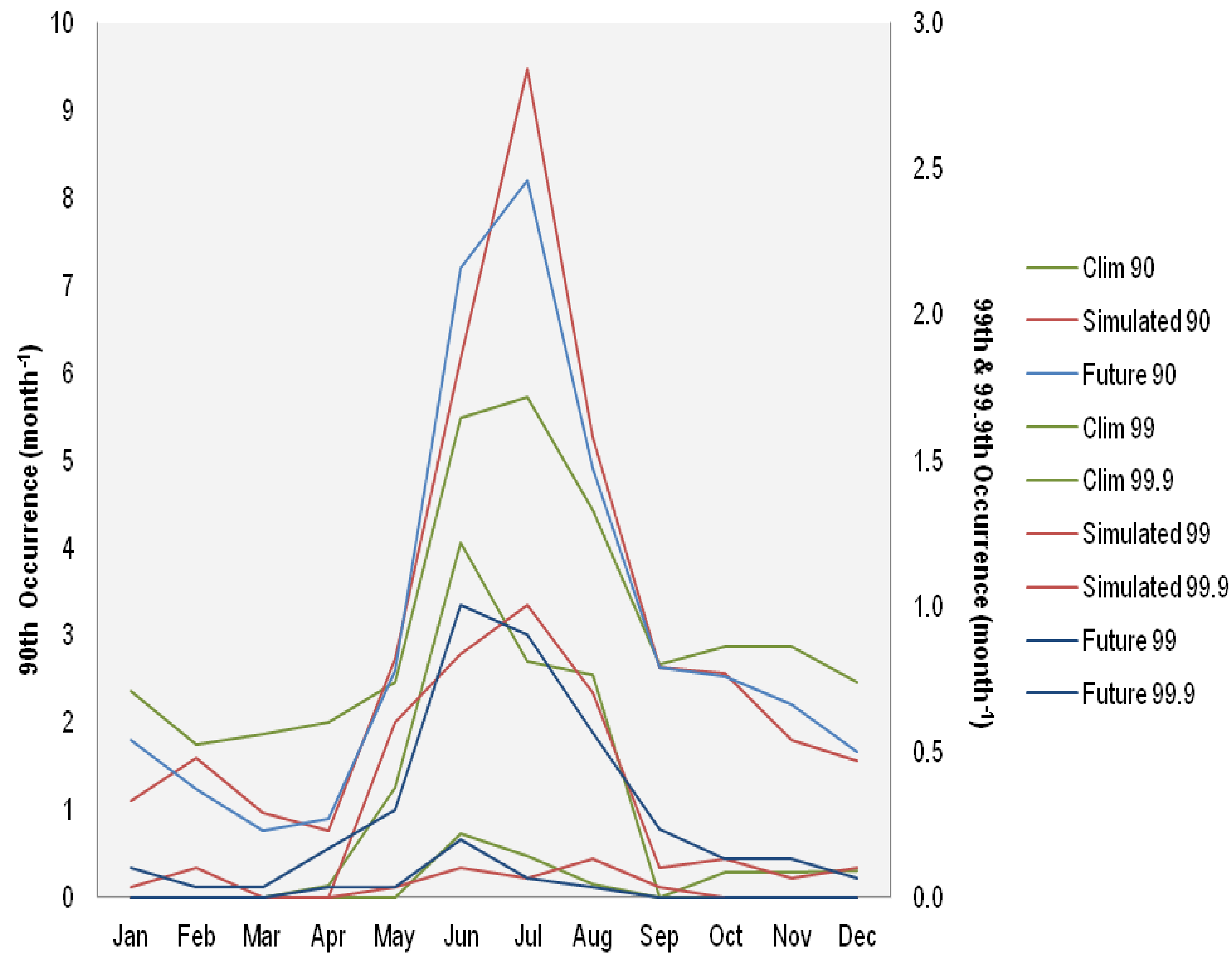

Figure 4.13: Monthly frequency of 90th, 99th, and 99.9th percentile events for the 1961-1990 climatology, the 1961-1990 model simulation and the 2041-2070 model projection at High Prairie. The units are the average number of events per month.

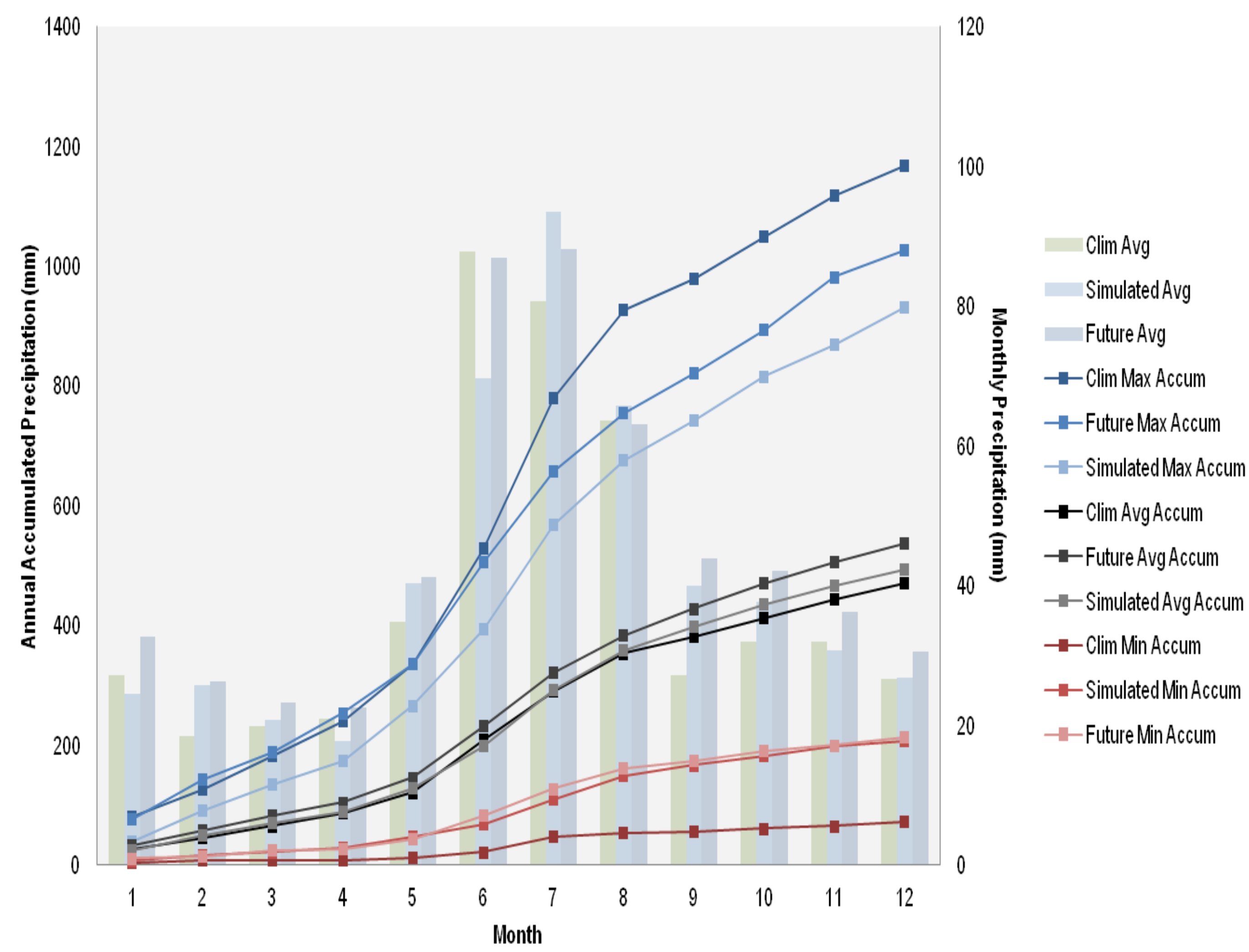

Figure 4.14: Cumulative annual precipitation for wettest months, average, and driest months and monthly average precipitation for the 1961-1990 climatology, the 1961-1990 model simulation and the 2041-2070 model projection at High Prairie.

for the 90th percentile do not show a late fall/early winter peak but do show an exaggerated May maximum as with 99th and 99.9th percentile events. The model cumulative total for wettest month is lower than what is actually observed and conversely the cumulative total for driest months is higher suggesting the model cannot adequately reproduce the full extent of precipitation variability (Figure 4.18).

Table 4.4: Comparison of average annual frequency and contribution to total accumulation for daily precipitation classes in the (a) 1961-1990 climatology and the (b) 1961-1990 model simulation at Guelph.

Precipitation (mm)	Annual Occurrence	Contribution (%)	Precipitation (mm)	Annual Occurrence	Contribution (%)
0	192.2	0.0%	0	79.0	0.0%
0.1 - 5	115.9	20.0%	0.1 - 5	234.7	35.6%
5 - 10	28.8	22.2%	5 - 10	30.9	24.9%
10 - 25	22.3	36.1%	10 - 25	19.5	32.8%
25 - 50	5.5	18.9%	25 - 50	1.9	6.7%
50 - 100	0.4	2.8%	50 - 100	0.0	0.0%
100 - 200	0.0	0.0%	100 - 200	0.0	0.0%

(a) (b)

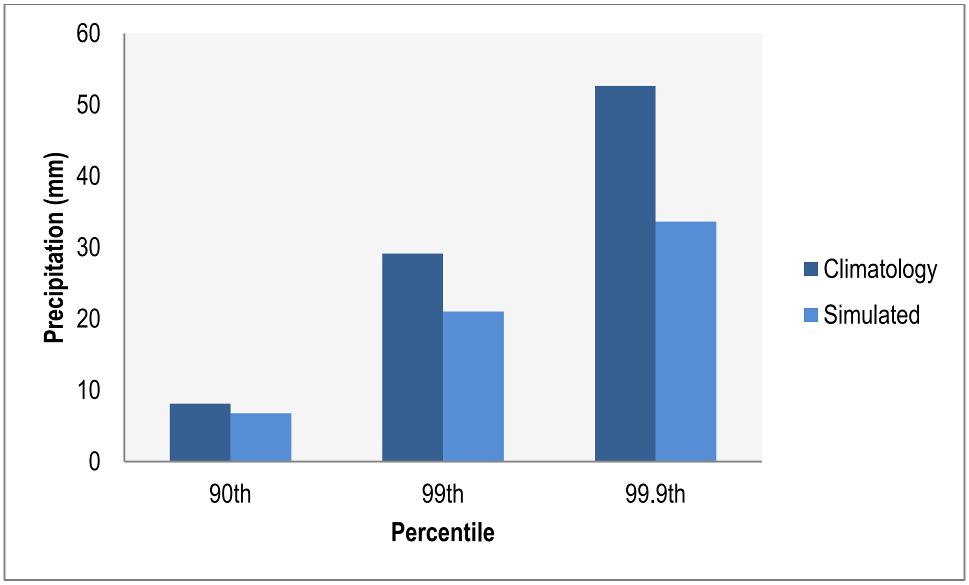

Figure 4.15: Comparison of extreme daily precipitation (90th,99th, and 99.9th percentile) for the observed 1961-1990 climatology and the 1961-1990 model simulation at Guelph.

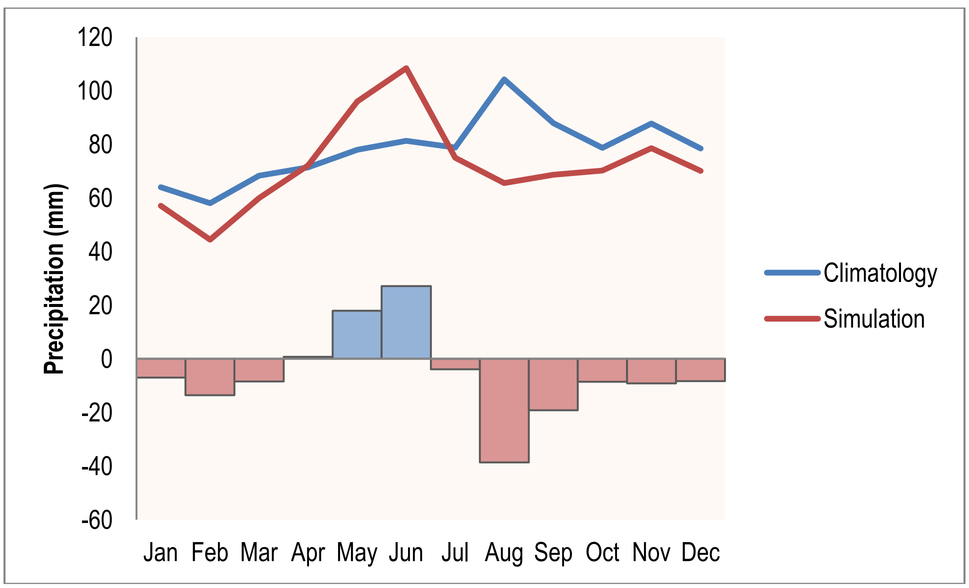

Figure 4.16: Comparison of the 1961-1990 climatology with the 1961-1990 model simulation over the annual cycle for Guelph.

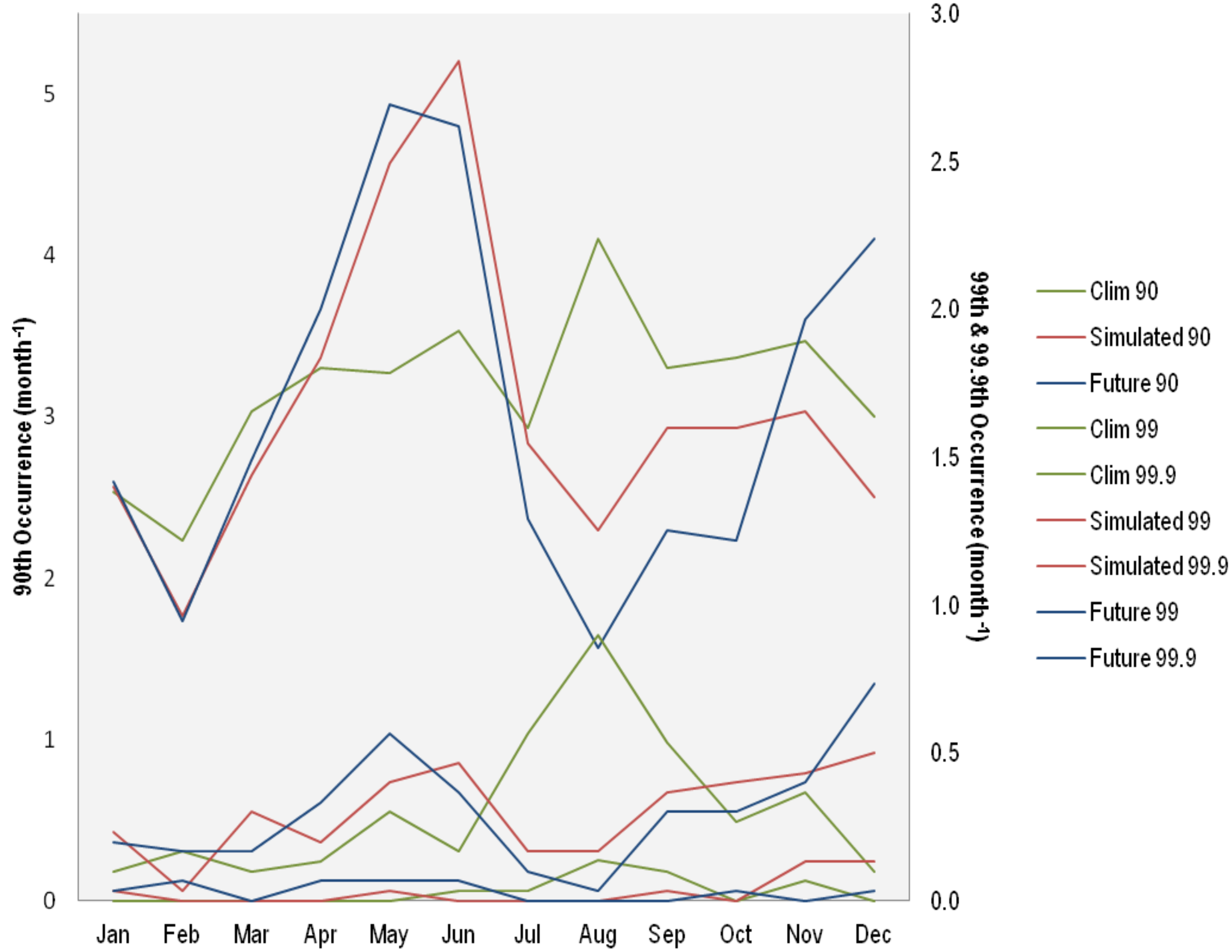

Figure 4.17: Monthly frequency of 90th, 99th, and 99.9th percentile events for the 1961-1990 climatology, the 1961-1990 model simulation and the 2041-2070 model projection at Guelph. The units are the average number of events per month.

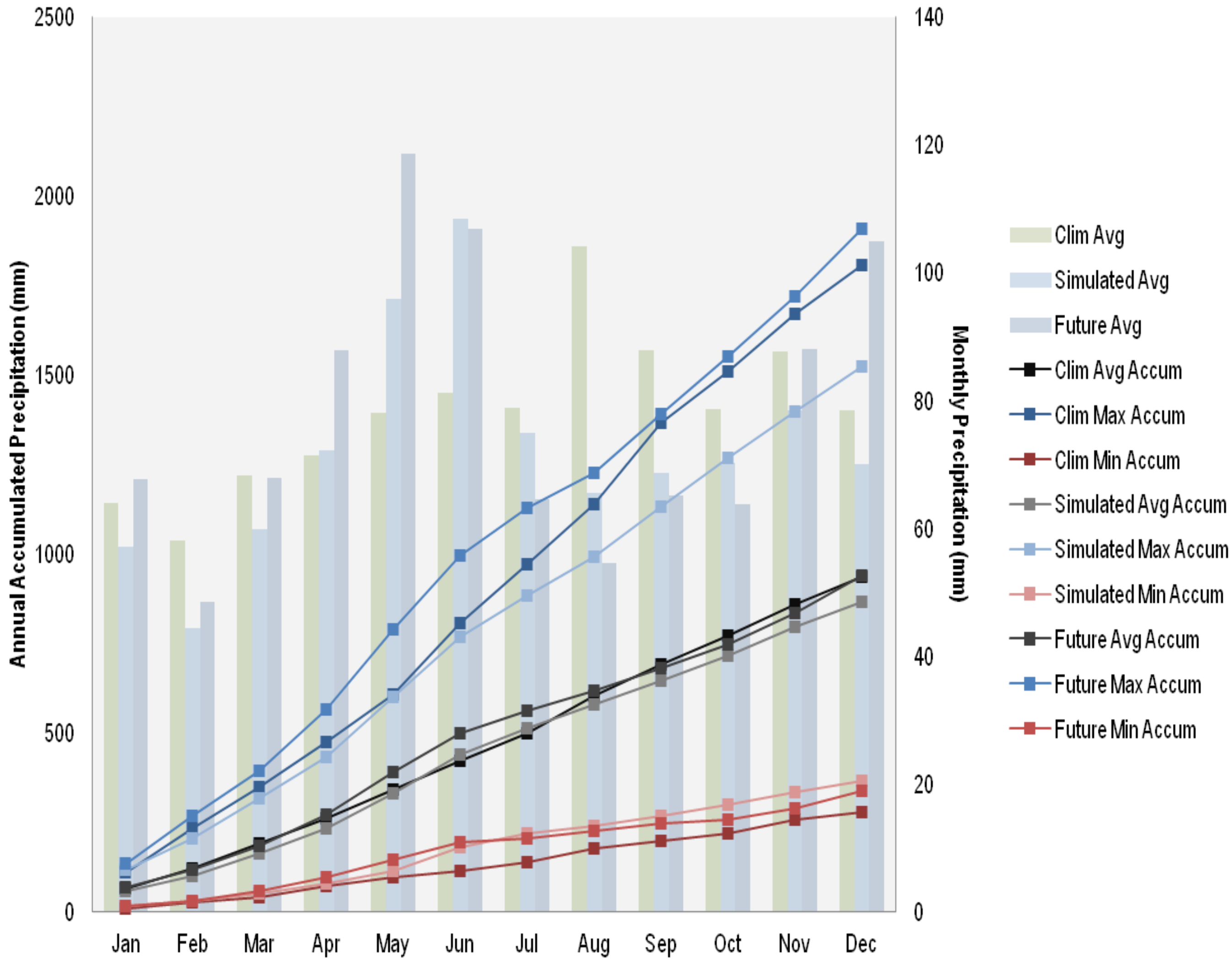

Figure 4.18: Cumulative annual precipitation for wettest months, average, and driest months and monthly average precipitation for the 1961-1990 climatology, the 1961-1990 model simulation and the 2041-2070 model projection at Guelph.

4.2.5 Muskoka

From Table 4.5, it is observed that the model underestimates the number of days without precipitation and overestimates small (but not as much as for the western locations) including frequency of events in the 5 to 10 mm class (also unlike the western sites). All other precipitation event classes are underestimated both in terms of frequency and contribution to overall precipitation - especially the 25 to 50 mm class. The values for the 90th, 99th, and 99.9th percentile of daily precipitation are all underestimated (Figure 4.19). The base period simulation underestimates annual precipitation, with all monthly averages being lower than observed with the exception of May and June (Figure 4. 20). There is a multimodal pattern seen in the monthly frequencies of extreme events as for Guelph with the first simulated peak is centered on June (Figure 4.21). The second peak is simulated as occurring in September with the 99th and 99.9th percentile events having a third peak in December. The actual monthly distribution of extreme events is rather complex with a generally more even curve. 90th percentile events peak in December, 99th percentile events peak in September, and 99.9th events peak in September as well with a secondary maxima at December and June. The model cumulative total for wettest month is lower than what is actually observed and conversely the cumulative total for driest months is higher suggesting the model cannot adequately reproduce the full extent of precipitation variability (Figure 4.22).

Table 4.5: Comparison of average annual frequency and contribution to total accumulation for daily precipitation classes in the (a) 1961-1990 climatology and the (b) 1961-1990 model simulation at Muskoka.

Precipitation (mm)	Annual Occurrence	Contribution (%)	Precipitation (mm)	Annual Occurrence	Contribution (%)
0	175.8	0	0	84.3	0.0%
0.1 - 5	112.9	17.0%	0.1 - 5	225.0	32.4%
5 - 10	38.8	23.7%	5 - 10	32.4	24.3%
10 - 25	33.1	42.9%	10 - 25	21.9	34.6%
25 - 50	5.2	13.8%	25 - 50	2.4	8.2%
50 - 100	0.5	2.6%	50 - 100	0.1	0.4%
100 - 200	0.0	0.0%	100 - 200	0.0	0.0%

(a) (b)

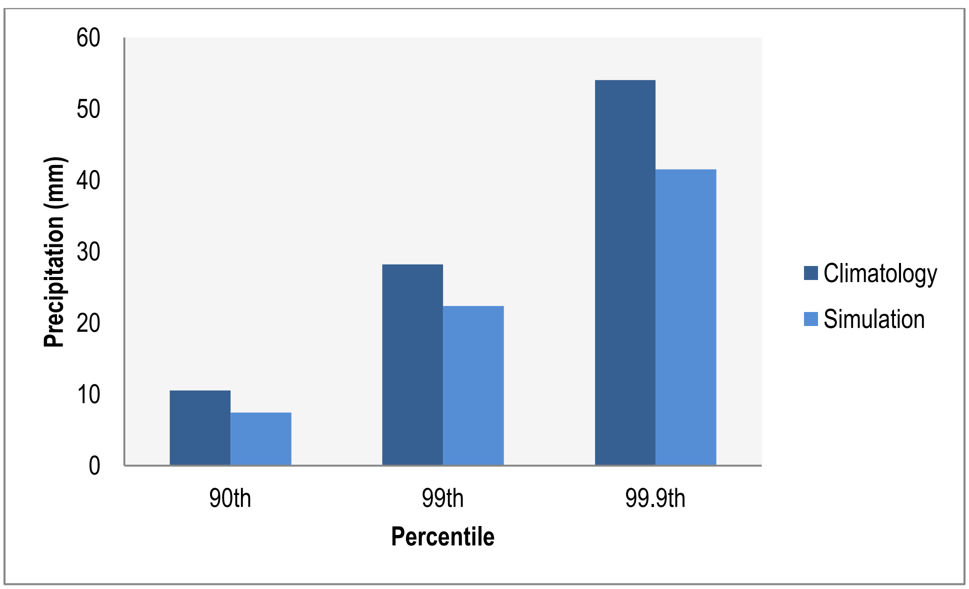

Figure 4.19: Comparison of extreme daily precipitation (90th,99th, and 99.9th percentile) for the observed 1961-1990 climatology and the 1961-1990 model simulation at Muskoka.

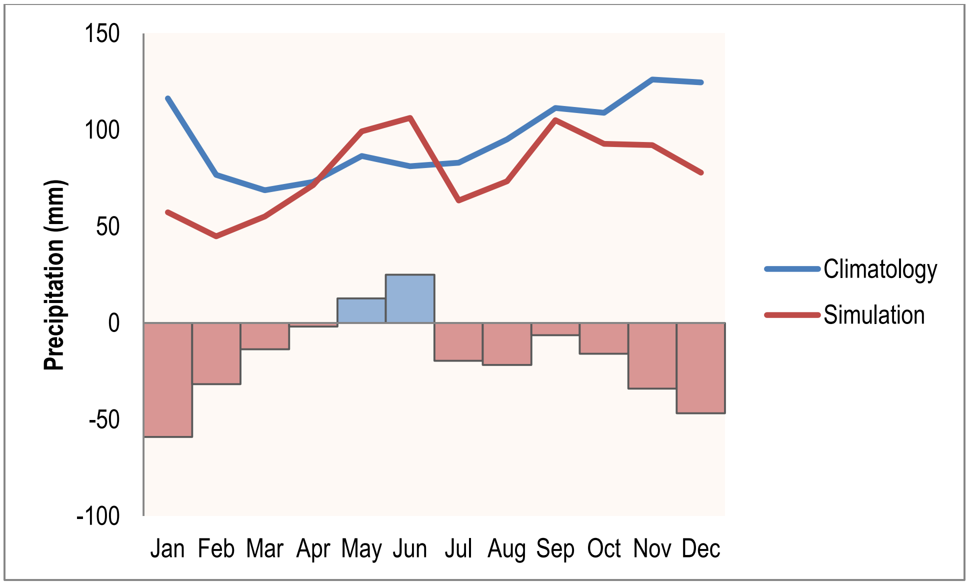

Figure 4.20: Comparison of the 1961-1990 climatology with the 1961-1990 model simulation over the annual cycle for Muskoka.

4.3 Comparison of Model Simulations and Projections

A comparison of the data between the base period simulation and the future scenario are outlined below for each location in terms of overall precipitation, extreme frequency and occurrence, including a monthly breakdown.

4.3.1 Cold Lake

Model projects a decrease in the frequency and contribution from small precipitation events (less than 5 mm) with an increase in the contribution of the 5-10 mm, 10-25 mm and 25-50 mm event classes (Table 4.6). The values for the 90th, 99th, and 99.9th percentile all increase in the future scenario (Figure 4.23). Annual precipitation is depicted as increasing by nearly 40 mm - distributed across almost all months Figure (4.24). Little change is seen in the

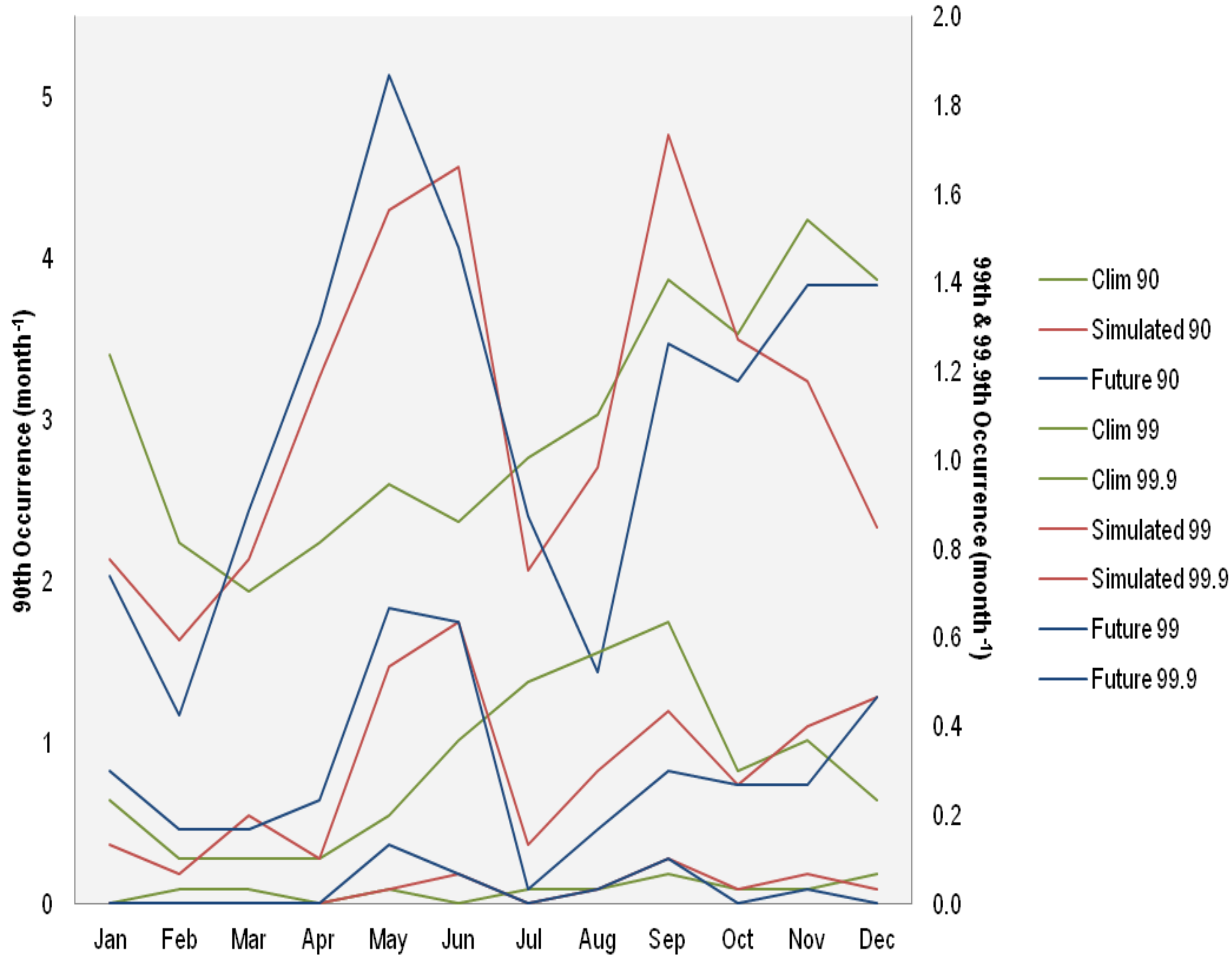

Figure 4.21: Monthly frequency of 90th, 99th, and 99.9th percentile events for the 1961-1990 climatology, the 1961-1990 model simulation and the 2041-2070 model projection at Muskoka. The units are the average number of events per month.

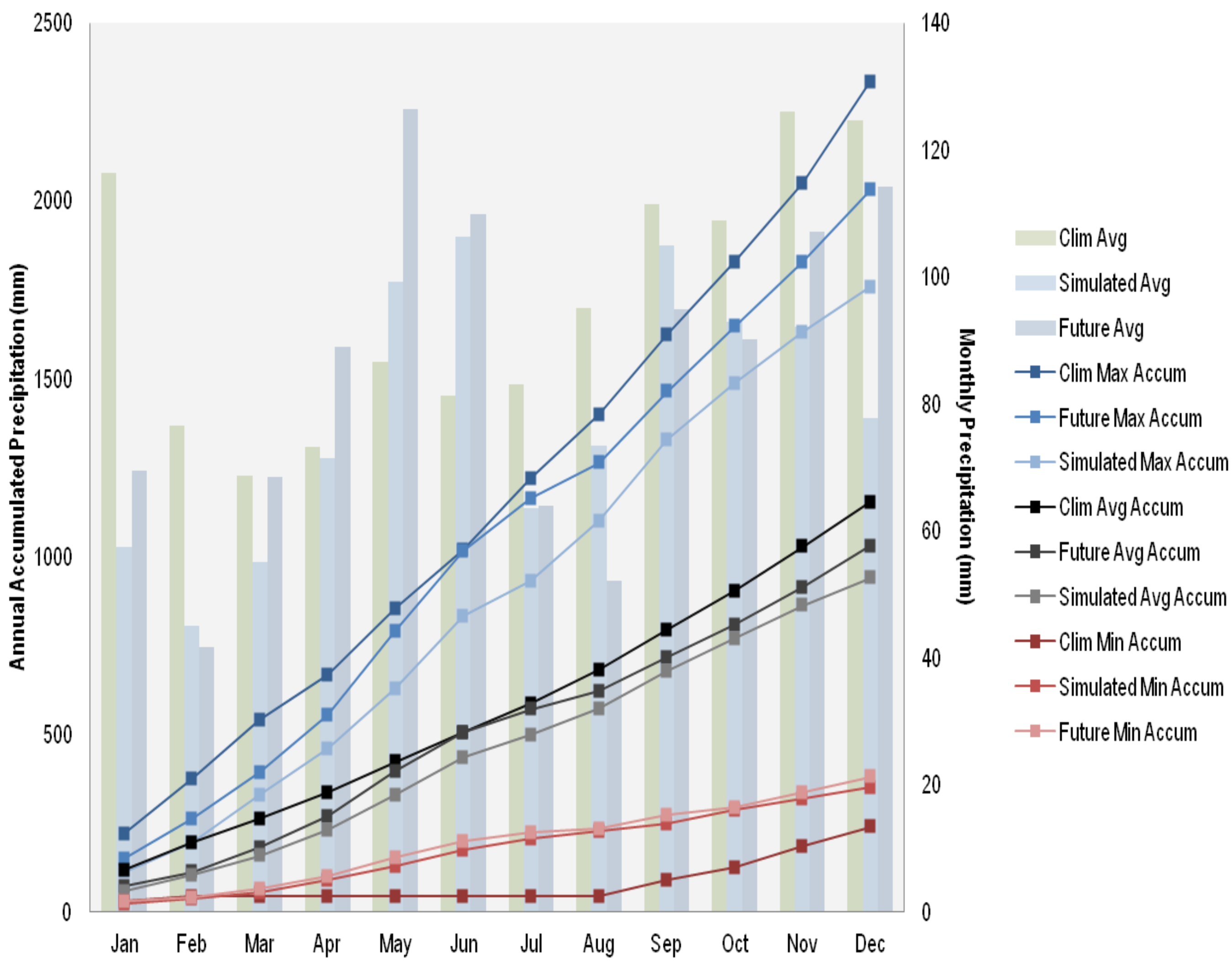

Figure 4.22: Cumulative annual precipitation for wettest months, average, and driest months and monthly average precipitation for the 1961-1990 climatology, the 1961-1990 model simulation and the 2041-2070 model projection at Muskoka.

monthly distributions of extreme precipitation events (Figure 4.5). The accumulated total of wettest months is greater in the future scenario than in the base period (Figure 4.6).

Table 4.6: Comparison of average annual frequency and contribution to total accumulation for classes in daily precipitation between the (a) 1961-1990 model simulation and the (b) 2041-2070 model projection at Cold Lake.

Precipitation (mm)	Annual Occurrence	Contribution (%)	Precipitation (mm)	Annual Occurrence	Contribution (%)
0	109.9	0.0%	0	108.4	0.0%
0.1 - 5	240.7	65.7%	0.1 - 5	240.1	62.5%
5 - 10	11.9	20.5%	5 - 10	13.0	21.0%
10 - 25	3.2	11.1%	10 - 25	4.2	13.9%
25 - 50	0.3	2.3%	25 - 50	0.4	2.6%
50 - 100	0.0	0.4%	50 - 100	0.0	0.0%
100 - 200	0.0	0.0%	100 - 200	0.0	0.0%

(a) (b)

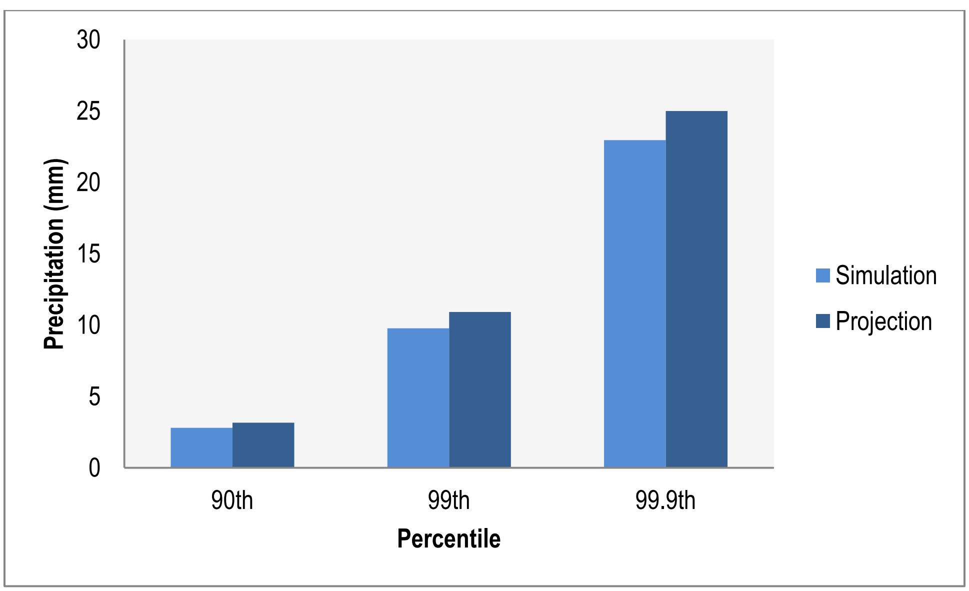

Figure 4.23: Comparison of extreme daily precipitation (90^{th}, 99^{th}, and 99.9th percentile) for the 1961-1990 model simulation and the 2041-2070 model projection at Cold Lake.

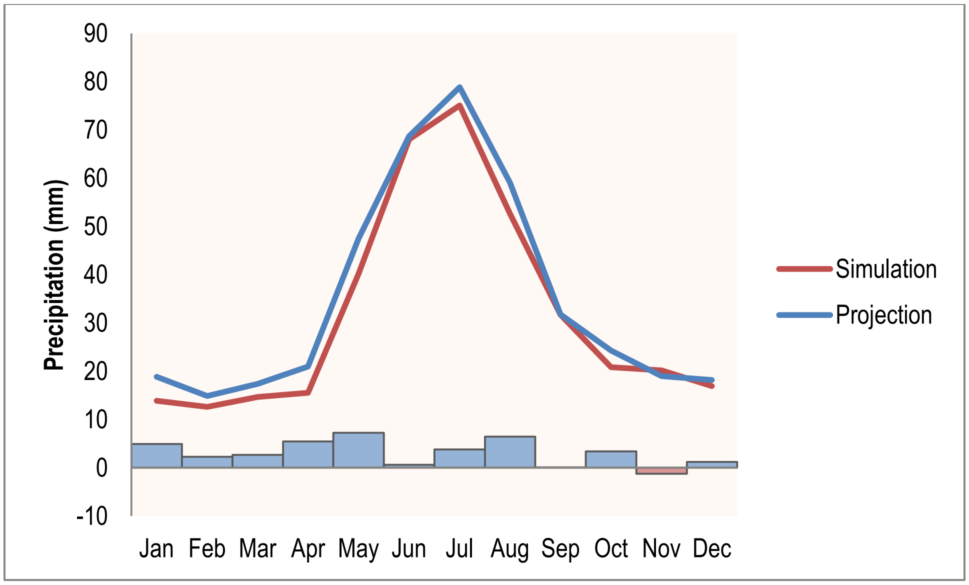

Figure 4.24: Comparison of the 1961-1990 model simulation and the 2041-2070 model projection over the annual cycle at Cold Lake.

4.3.2 Assiniboia

The model projects a decrease in the frequency of small precipitation events of less than 5 mm and in frequency and contribution from 5-10 mm and 10-25 events (Table 4.7). At the same time, an increase in frequency and contribution of 25-50 mm and 50-100 mm precipitation events is seen. The values for the 90th and 99.9th percentile increase while the value for the 99th percentile decreases (Figure 4.25). Annual precipitation increases only very slightly with decreases in monthly averages seen in the warm season from May to September (Figure 4.26). The warm season peak in monthly occurrence of 90th percentile events is somewhat more evenly distributed in the future scenario and the 99th percentile peak is depicted to occur somewhat earlier (Figure 4.9). The accumulated total of wettest months is greater in the future scenario than in the base period (Figure 4.10).

Table 4.7: Comparison of average annual frequency and contribution to total accumulation for classes in daily precipitation between the (a) 1961-1990 model simulation and the (b) 2041-2070 model projection at Assiniboia.

Precipitation (mm)	Annual Occurrence	Contribution (%)	Precipitation (mm)	Annual Occurrence	Contribution (%)
0	128.3	0.0%	0	131.0	0.0%
0.1 - 5	219.1	57.9%	0.1 - 5	217.0	59.4%
5 - 10	13.9	23.6%	5 - 10	13.3	22.3%
10 - 25	4.4	16.0%	10 - 25	4.3	15.2%
25 - 50	0.3	2.5%	25 - 50	0.4	2.7%
50 - 100	0.0	0.0%	50 - 100	0.0	0.4%
100 - 200	0.0	0.0%	100 - 200	0.0	0.0%

(a) (b)

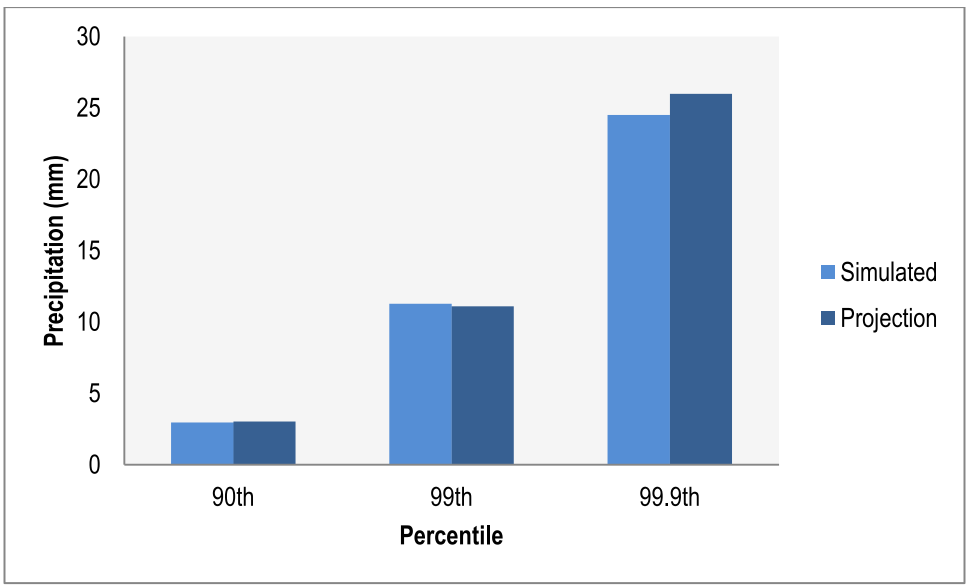

Figure 4.25: Comparison of extreme daily precipitation (90th, 99th, and 99.9th percentile) for the 1961-1990 model simulation and the 2041-2070 model projection at Assiniboia.

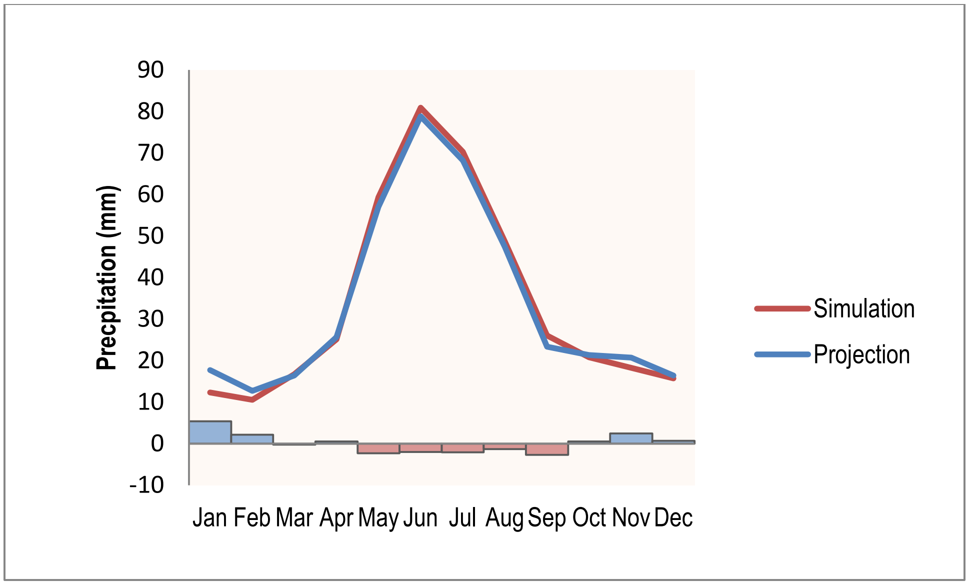

Figure 4.26: Comparison of the 1961-1990 model simulation and the 2041-2070 model projection over the annual cycle at Assiniboia.

4.3.3 High Prairie

From Table 4.8, we see the model projects a decrease in the number of days without precipitation and a decrease in the contribution from small precipitation events with less than 5 mm (although frequency of such events increases). Contribution and frequency of precipitation events in 5-10 mm, 10-25 mm, and 25-50 mm all increase. The values of the 90th and 99th percentile increase while the value of the 99.9th decreases (Figure 4.27). Average annual precipitation increases by over 40 mm with all months seeing increases except July and August (Figure 4.28). The monthly maximum in the frequency of 99th and 99.th percentile events has shifted slightly earlier to June rather than July and August (Figure 4.13). The accumulated total of wettest months is greater in the future scenario than in the base period (Figure 4.14).

Table 4.8: Comparison of average annual frequency and contribution to total accumulation for classes in daily precipitation between the (a) 1961-1990 model simulation and the (b) 2041-2070 model projection at High Prairie.

Precipitation (mm)	Annual Occurrence	Contribution (%)	Precipitation (mm)	Annual Occurrence	Contribution (%)
0	93.5	0.0%	0	88.3	0.0%
0.1 - 5	250.3	64.1%	0.1 - 5	251.4	60.3%
5 - 10	18.2	24.3%	5 - 10	21.5	26.8%
10 - 25	3.8	10.5%	10 - 25	4.6	11.3%
25 - 50	0.2	1.1%	25 - 50	0.3	1.6%
50 - 100	0.0	0.0%	50 - 100	0.0	0.0%
100 - 200	0.0	0.0%	100 - 200	0.0	0.0%

(a) (b)

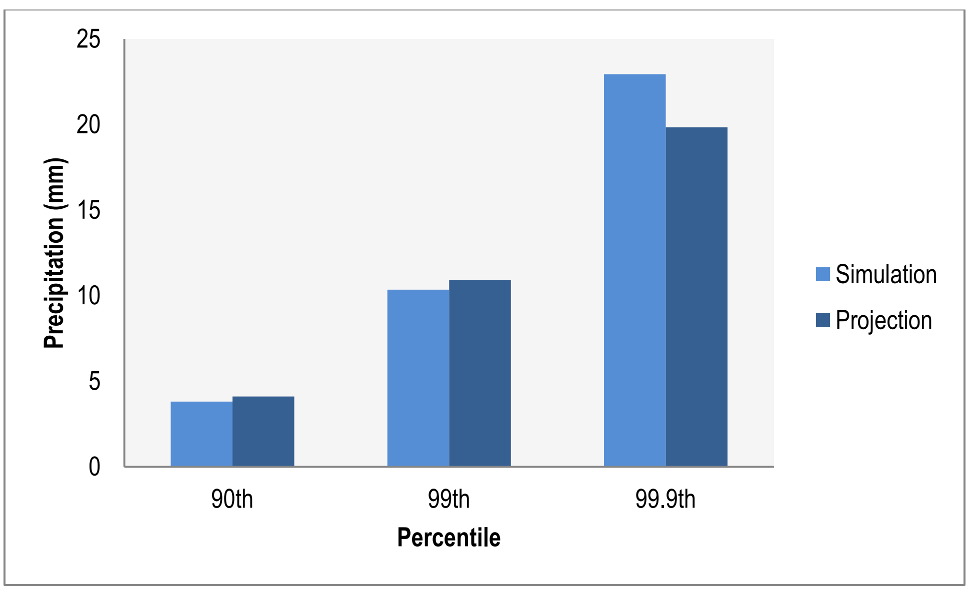

Figure 4.27: Comparison of extreme daily precipitation (90th, 99th, and 99.9th percentile) for the 1961-1990 model simulation and the 2041-2070 model projection at High Prairie.

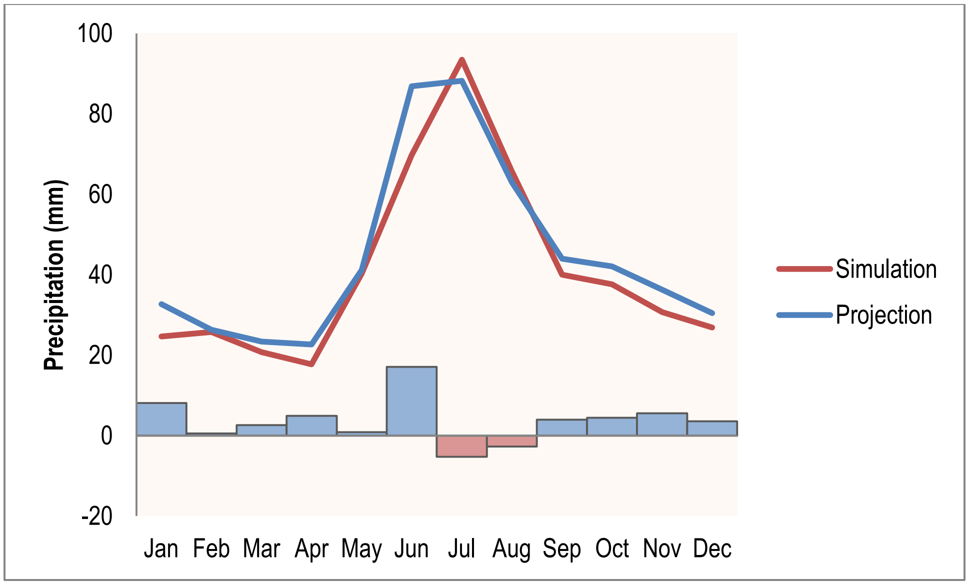

Figure 4.28: Comparison of the 1961-1990 model simulation and the 2041-2070 model projection over the annual cycle at High Prairie.

4.3.4 Guelph

The model projects an increase in the number of days without precipitation and a decrease in the frequency and contribution of events in the < 5 mm, 5-10 mm, and 10-25 mm classes; while there is an increase for the 25-50 mm and 50-100 mm ones (Table 4.9). The values for the 90th, 99th, and 99.9th percentile all increase in the future simulation (Figure 4.29). Average annual precipitation increases by over 70 mm driven by large increases in monthly averages for November and December – while decreases are noted from June to October (Figure 4.30). The first peak in the monthly extreme occurrence has shifted earlier, while the second peak has shifted back and is more prominent in the case of 90th and 99th percentile events (Figure 4.17). The accumulated total of wettest months is greater in the future scenario than in the base period (Figure 4.18).

Table 4.9: Comparison of average annual frequency and contribution to total accumulation for classes in daily precipitation between the (a) 1961-1990 model simulation and the (b) 2041-2070 model projection at Guelph.

Precipitation (mm)	Annual Occurrence	Contribution (%)	Precipitation (mm)	Annual Occurrence	Contribution (%)
0	79.0	0.0%	0	84.4	0.0%
0.1 - 5	234.7	35.6%	0.1 - 5	225.5	31.5%
5 - 10	30.9	24.9%	5 - 10	30.8	22.9%
10 - 25	19.5	32.8%	10 - 25	22.3	35.5%
25 - 50	1.9	6.7%	25 - 50	2.9	9.4%
50 - 100	0.0	0.0%	50 - 100	0.1	0.6%
100 - 200	0.0	0.0%	100 - 200	0.0	0.0%

(a) (b)

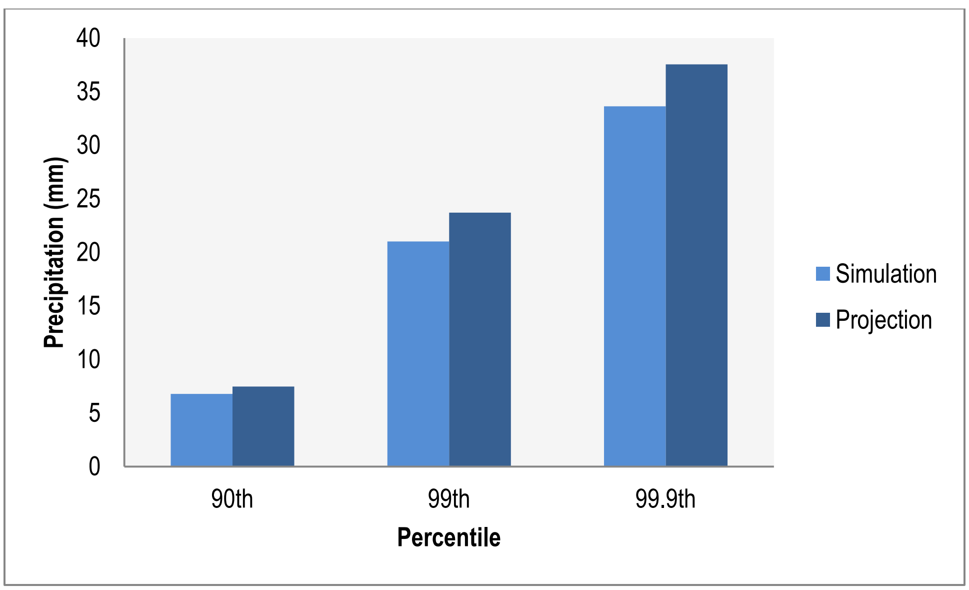

Figure 4.29: Comparison of extreme daily precipitation (90th, 99th, and 99.9th percentile) for the 1961-1990 model simulation and the 2041-2070 model projection at Guelph.

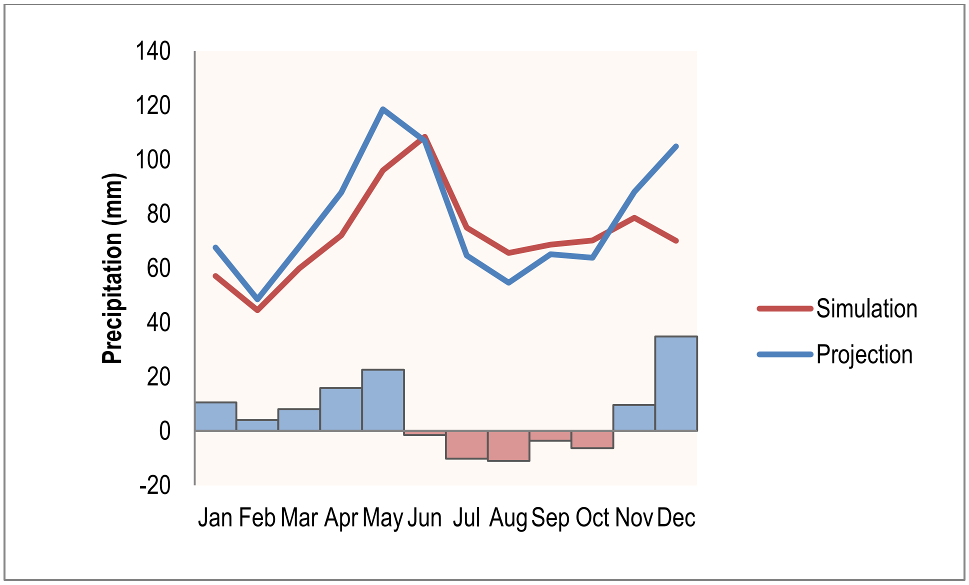

Figure 4.30: Comparison of the 1961-1990 model simulation and the 2041-2070 model projection over the annual cycle at Guelph.

4.3.5 Muskoka

The model projects an increase in the number of days without precipitation and a decrease in the frequency and contribution of events in the < 5 mm, 5-10 mm, and 10-25 mm classes; while there is an increase for the 25-50 mm and 50-100 mm ones (Table 4.10). The values for the 90th and 99th percentiles of daily precipitation increase while the value for the 90th percentile actually decreases (Figure 4.31). Average annual precipitation increases by nearly 100 mm with positive gains seen in all months (particularly November and December) except from August through September and February (Figure 4.32). As in the case of Guelph, the first peak in monthly extreme occurrence has shifted earlier (90th, 99th, and 99,9th percentile) and the second maximum has shifted back later (Figure 4.21). The accumulated total of wettest months is greater in the future scenario than in the base period (Figure 4.22).

Table 4.10: Comparison of average annual frequency and contribution to total accumulation for classes in daily precipitation between the (a) 1961-1990 model simulation and the (b) 2041-2070 model projection at Muskoka.

Precipitation (mm)	Annual Occurrence	Contribution (%)	Precipitation (mm)	Annual Occurrence	Contribution (%)
0	84.3	0.0%	0	87.6	0.0%
0.1 - 5	225.0	32.4%	0.1 - 5	216.6	28.2%
5 - 10	32.4	24.3%	5 - 10	33.4	23.0%
10 - 25	21.9	34.6%	10 - 25	24.2	35.9%
25 - 50	2.4	8.2%	25 - 50	4.1	12.4%
50 - 100	0.1	0.4%	50 - 100	0.1	0.6%
100 - 200	0.0	0.0%	100 - 200	0.0	0.0%

(a) (b)

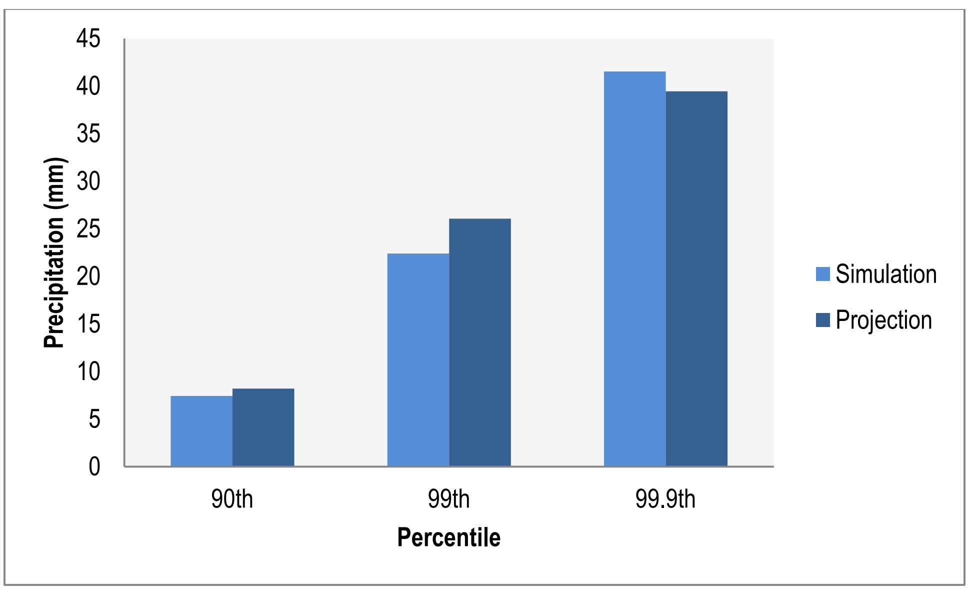

Figure 4.31: Comparison of extreme daily precipitation (90^{th}, 99^{th}, and 99.9th percentile) for the 1961-1990 model simulation and the 2041-2070 model projection at Muskoka.

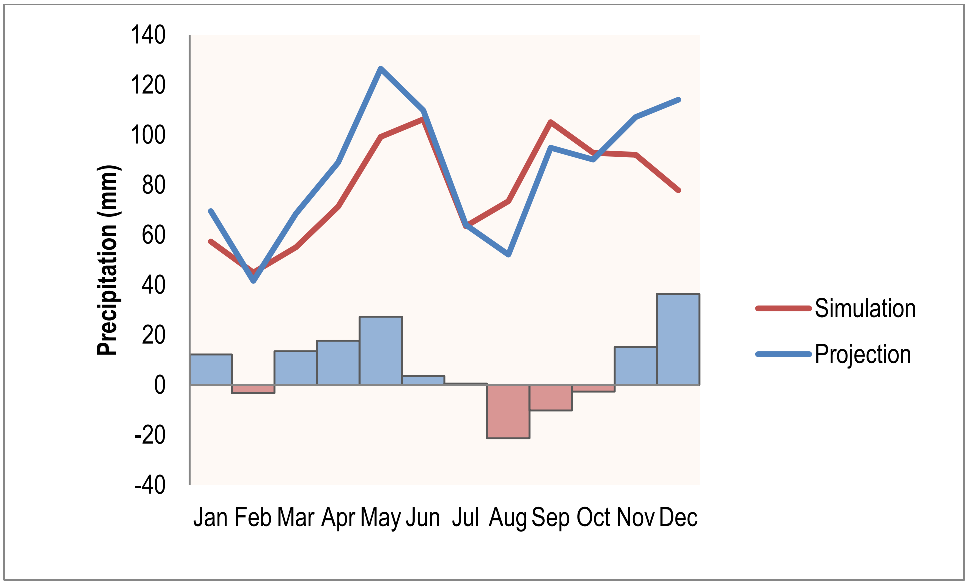

Figure 4.32: Comparison of the 1961-1990 model simulation and the 2041-2070 model projection over the annual cycle at Muskoka.

4.4 Assessment of Characteristics

4.4.1 Top Ten Events

The top ten daily precipitation events were identified in both model datasets (Table 4.11). For all locations except Cold Lake, the highest recorded 24 hour precipitation total was greater in the 2041-2070 scenario than in the base period simulation. The increases were substantial in all cases with most around 10 mm ranging to over 15 mm for Guelph.

Table 4.11: Top 10 precipitation events for the 1961-1990 model simulation and the 2041-2070 model projection at all locations. Cells are colour coded based on the following bins: >60 mm, 50-60 mm, 40-50 mm, 30-40 mm, 25-30 mm, and <25 mm.

Assiniboia		Cold Lake		High Prairie		Guelph		Muskoka	
1961-1990	**Precip. (mm)**	**1961-1990**	**Precip. (mm)**	**1961-1990**	**Precip. (mm)**	**1961-1990**	**Precip. (mm)**	**1961-1990**	**Precip. (mm)**
17-Jul-64	42.4	22-Aug-62	50.2	21-Jun-70	30.7	13-Nov-73	43.8	13-Sep-63	54.4
17-May-88	38.6	25-May-79	36.4	30-Jul-72	29.1	20-Dec-90	41.6	08-Jun-79	51.6
21-Jun-77	38.4	05-Jul-62	33.4	14-Aug-82	28.2	13-Jan-64	40.1	17-Sep-84	47.1
14-Jun-63	36.4	04-Jul-80	33.3	01-Aug-61	27.1	30-Sep-80	39.7	22-May-68	46.3
01-Jul-85	35.4	04-Sep-82	31.2	17-Jul-83	26.8	02-Nov-80	39.0	15-Jun-72	45.4
30-May-78	30.9	16-Jun-66	30.3	22-Jun-81	25.3	06-Dec-76	37.5	13-Nov-77	45.3
11-May-89	28.9	07-Jun-75	25.9	28-Aug-89	24.7	15-Dec-88	37.1	12-Oct-70	44.2
26-Jun-86	28.3	21-Jun-65	25.8	28-Jun-67	23.9	13-Nov-77	36.9	22-Sep-87	43.9
13-Jun-63	27.0	20-Jul-73	25.5	10-Sep-66	23.9	02-May-72	36.7	13-Nov-73	43.0
11-May-88	24.8	02-Jul-90	25.4	06-Aug-86	23.3	27-Nov-74	34.3	16-Aug-65	42.2
03-Jun-89	24.6	24-Jul-61	23.6	25-May-64	23.1	11-Dec-81	34.1	09-Dec-77	42.0
2041-2070	**Precip. (mm)**	**2041-2070**	**Precip. (mm)**	**2041-2070**	**Precip. (mm)**	**2041-2070**	**Precip. (mm)**	**2041-2070**	**Precip. (mm)**
01-Jun-64	51.1	01-Aug-46	36.6	13-Jun-63	41.0	19-Jun-66	60.2	26-May-70	63.9
05-Sep-55	35.8	12-Jul-57	31.4	08-Jun-42	38.0	04-Dec-54	51.0	16-Jun-63	61.6
21-Jun-60	32.0	17-Aug-68	31.3	11-Jun-65	34.0	15-Jan-56	50.3	22-May-51	51.6
23-May-66	31.9	07-Sep-58	30.8	19-Jun-70	34.0	09-May-62	49.9	15-Jun-44	49.5
01-Jul-56	31.9	18-Aug-68	30.0	06-Jun-67	32.0	24-May-70	48.8	31-Aug-46	49.1
30-Sep-57	31.8	27-May-56	28.7	22-Apr-65	27.3	01-Feb-68	43.0	31-May-55	46.8
14-Jun-68	28.8	20-May-62	28.0	22-Aug-53	27.1	30-Oct-43	42.6	18-Sep-63	46.0
27-Jun-56	28.6	17-May-41	27.6	26-Jul-65	25.8	26-Jun-65	42.5	24-Sep-47	43.6
02-Aug-53	28.0	17-Jul-64	26.6	06-Jun-63	23.7	24-Apr-56	42.1	06-Nov-57	42.9
06-Jun-63	26.5	05-Jun-60	25.6	31-Jul-47	22.7	18-Feb-63	40.2	27-May-70	42.6
15-May-47	26.4	06-May-51	25.5	31-May-62	22.0	09-Apr-55	38.0	01-Sep-57	42.4

4.4.2 Characteristics of Most Extreme Events

The most extreme precipitation events over the western locations were associated with cold lows and trowal airstreams. They are generally characterized by a highly meridional or amplified geopotential pattern at 500 hPa with a deep trough or closed low over western Canada and a strong subtropical ridge over the central United States (see Figures 4.33b, 4.34b, 4.35b). There is usually a left exit region of a 500 hPa jet maxima nearby (Figures 4.33e, 4.34e, 4.35e). The 850 hPa flow pattern reveals that the main low level jet and moisture transport are displaced relatively far southeast (Figures 4.33k, 4.34k, 4.35k), suggesting that the western events are more linked with moisture transport that is rooted higher in the atmosphere. The 850 geopotential pattern depicts a strong well defined low (Figures 4.33h 4.34h, 4.35h). Around that low however there is a secondary and easterly low level jet maxima wrapping around the north side of the disturbance.

Eastern locations displayed a less amplified geopotential pattern at 500 hPa during the majority of extreme events for both time sets – with a general ridge over the eastern or Atlantic portions of the United States and a trough to the Northwest (Figures 4.36b and 4.37b). However, there was a very broad, strong flow present at 500 hPa (Figures 4.36e and 4.37e) and they were characterized by warm and moist advection at 850 hPa (Figures 4.36k and 4.37k).

Composites for western sites were generally similar to each other but with differences in the respective position of lows and flow pattern. Variability was also fairly limited between each of the 3 members making the composite (not shown). Eastern composites and their respective members were more variable, with the occurrence of the top three events spread out through the year, and not as concentrated in the warm season as over the west.

4.4.3 Validation of Characteristics

For western locations, the model composites were generally similar to the ones generated from the National Centers for Environmental Prediction reanalysis. However, the flow at 500 hPa and 850 hPa was overestimated by the model (Figures 33d, 33e, 34d, 34e, 35d, 35e) and the corresponding geopotential heights for the disturbances were too low (Figures

33a, 33b, 34a, 34b, 35a, 35b). For eastern locations, flow was grossly overestimated (Figures 36d, 36e, 37d, 37e) and the geopotential pattern depicted a much stronger north to south gradient (Figures 36a, 36b, 37a, 37b). As well, all the top events for Guelph occurred were simulated to have occurred during the winter season while the National Centers for Environmental Prediction reanalysis showed all events occurring during the summer months.

4.4.4 Characteristics of Future Events

The patterns associated with future events (2041 – 2070) as projected by the CRCM are similar to those in the base period simulation except for a slight northward shift in the overall geopotential pattern in most cases at 500 and 850 hPa. This is illustrated by comparing the simulated and projected composites for 500 hPa geopotential height (Figure 33b versus 33c, 34b versus 34c, 35b versus 35c), and for 850 hPa geopotential height (Figure 33h versus 33i, 34h versus 34i, 35h versus 35i). However the general, highly amplified pattern for western locations remains relatively unchanged. In fact, although the geopotential heights have increased, the position of the lows does not actually show much change.

At eastern sites a northwards shift is also depicted in the 500 hPa (Figure 36b versus 36c, Figure 37b versus 37c) and 850 hPa geopotential height contours (Figure 36h versus 36i, Figure 37h versus 37i) by comparing the eastern composites for the model simulation and projection. In the case of Guelph, the shift is quite dramatic. The comparison shows the less amplified yet strong, fast flow continues to characterize future, eastern events as projected by the model.

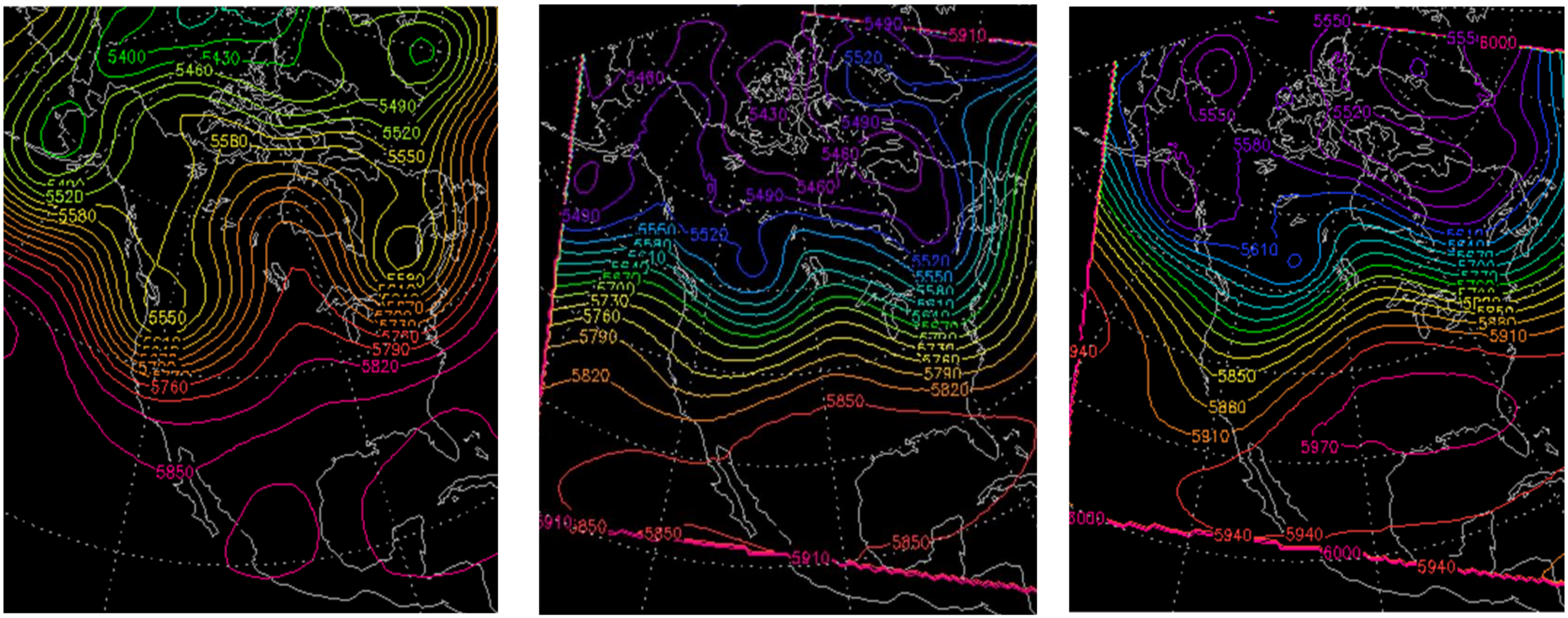

(a) (b) (c)

Figure 4.33: Comparison of 500 hPa geopotential height composites for top 3 daily precipitation events at Cold Lake. (a) 1961-1990 NCEP reanalysis; (b) 1961-1990 model simulation; (c) 2041-2070 model projection.

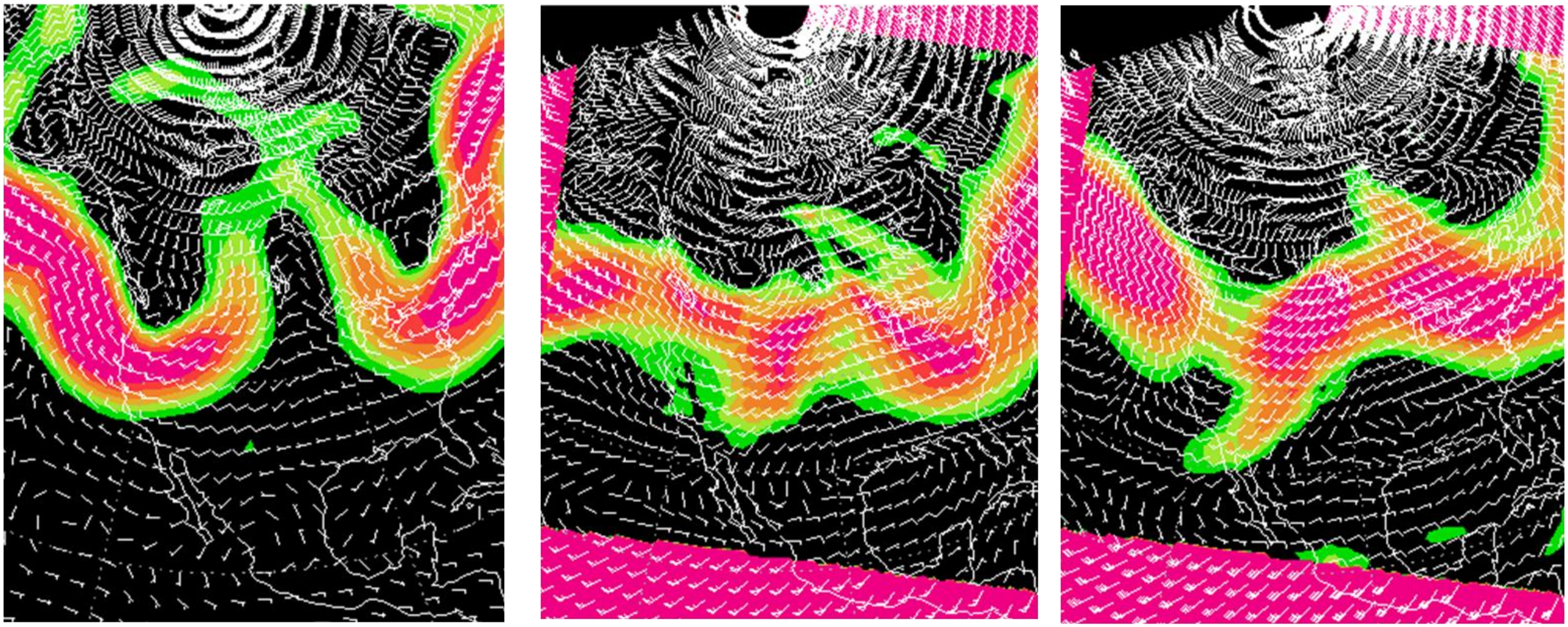

(d) (e) (f)

Figure 4.33: Comparison of 500 hPa vector wind composites for top 3 daily precipitation events at Cold Lake.

(d) 1961-1990 NCEP reanalysis; (e) 1961-1990 model simulation; (f) 2041-2070 model projection.

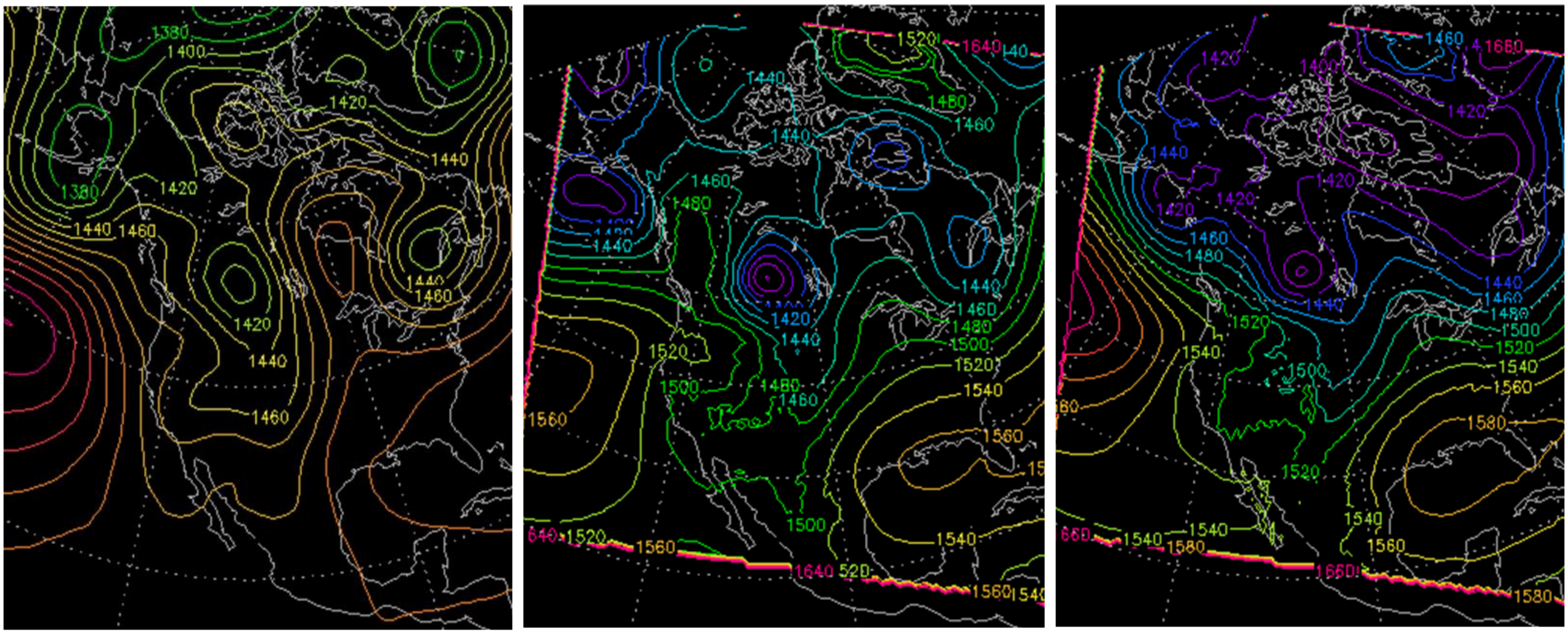

(g) (h) (i)

Figure 4.33: Comparison of 850 hPa geopotential height composites for top 3 daily precipitation events at Cold Lake.

(g) 1961-1990 NCEP reanalysis; (h) 1961-1990 model simulation; (i) 2041-2070 model projection.

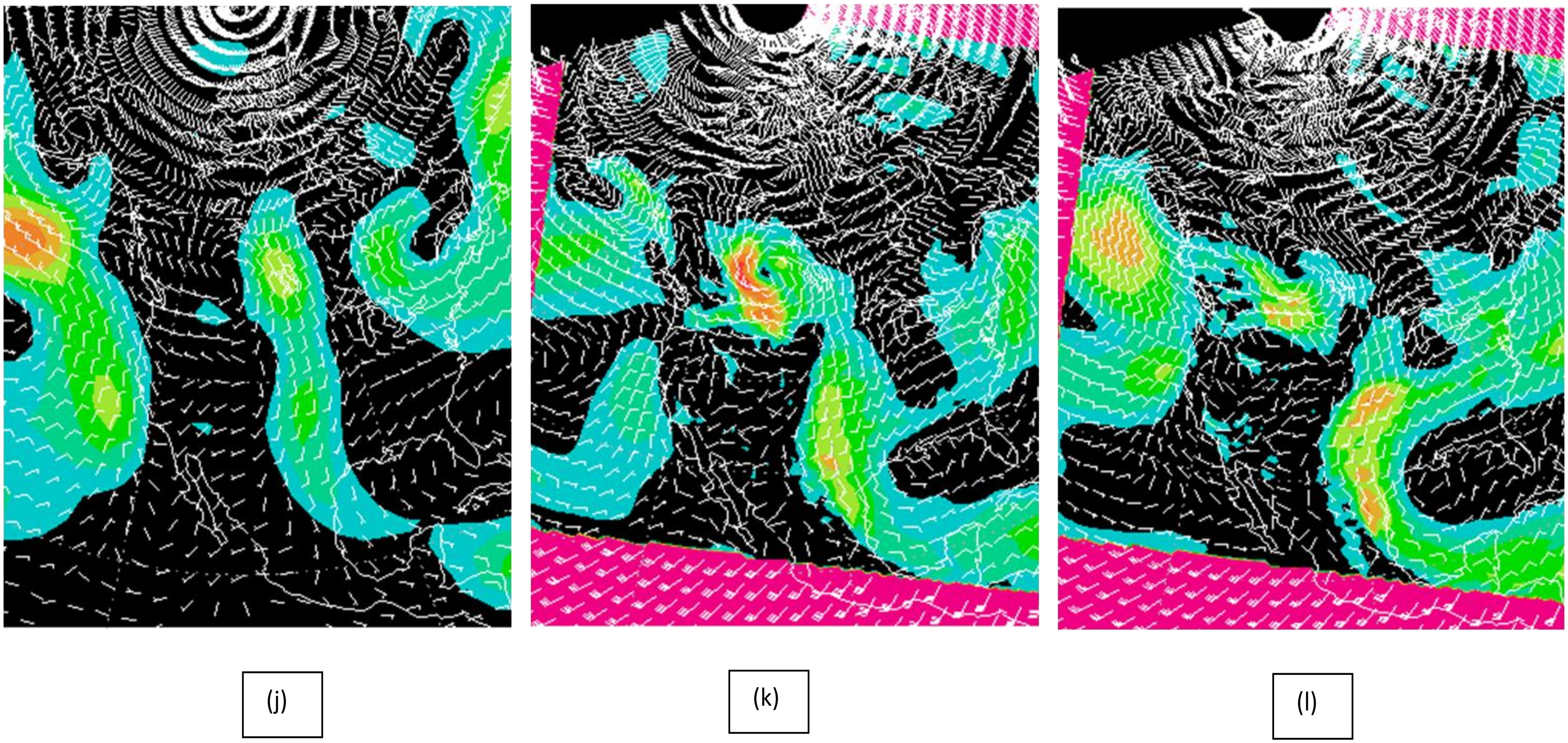

Figure 4.33: Comparison of 850 hPa vector wind composites for top 3 daily precipitation events at Cold Lake.

(j) 1961-1990 NCEP reanalysis; (k) 1961-1990 model simulation; (l) 2041-2070 model projection.

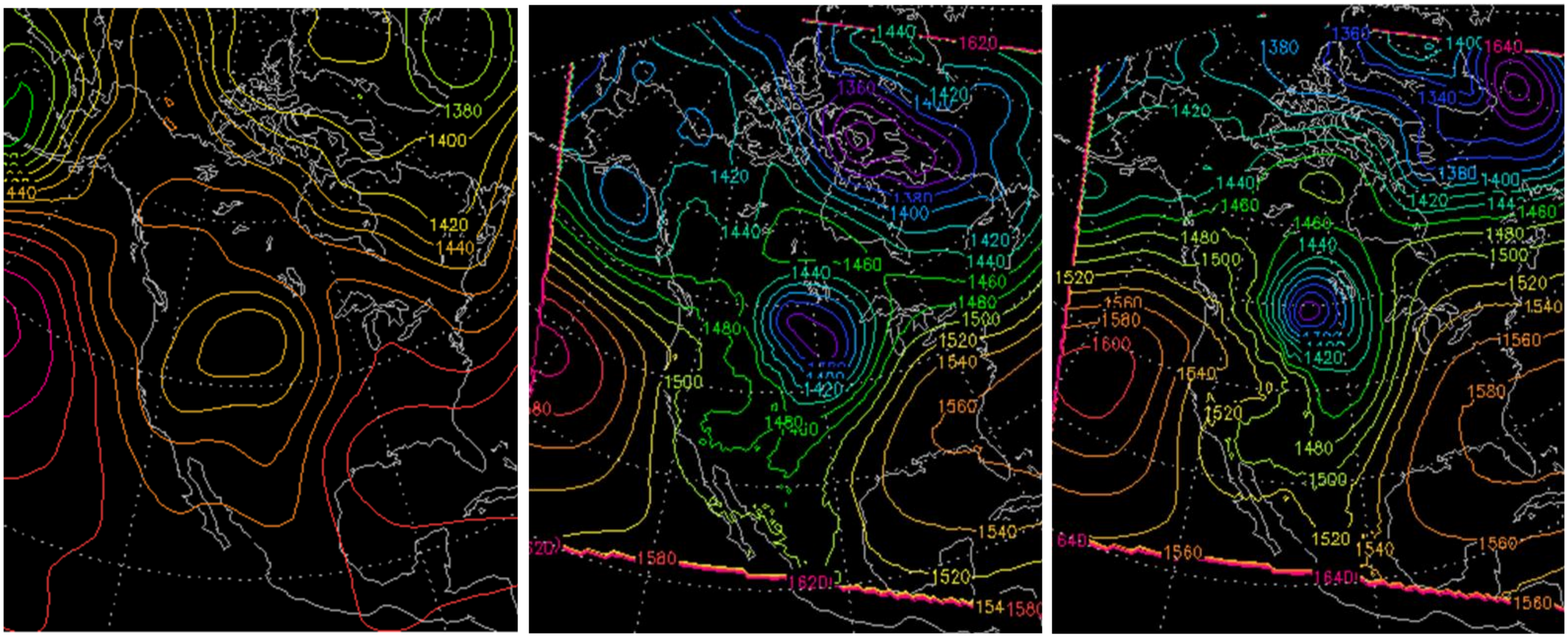

(a) (b) (c)

Figure 4.34: Comparison of 500 hPa geopotential height composites for top 3 daily precipitation events at Assiniboia.

(a) 1961-1990 NCEP reanalysis; (b) 1961-1990 model simulation; (c) 2041-2070 model projection.

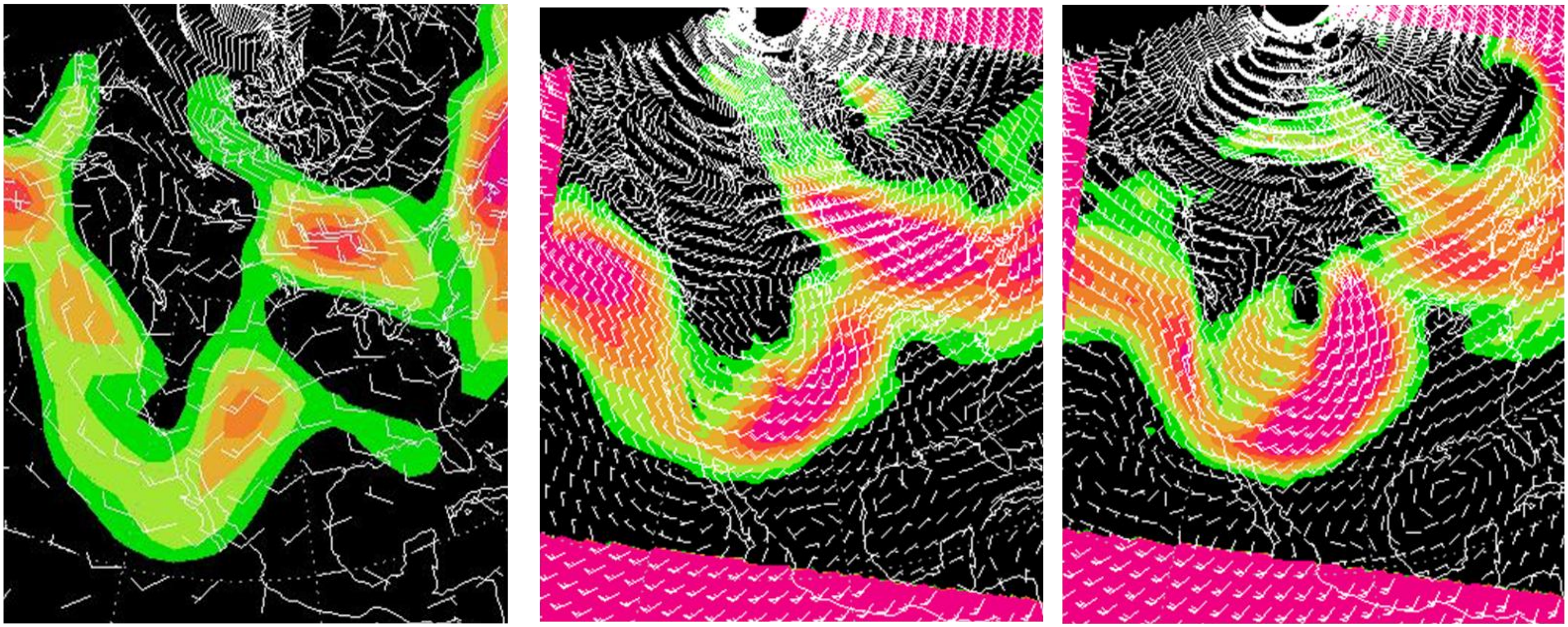

(d) (e) (f)

Figure 4.34: Comparison of 500 hPa vector wind composites for top 3 daily precipitation events at Assiniboia.

(d) 1961-1990 NCEP reanalysis; (e) 1961-1990 model simulation; (f) 2041-2070 model projection.

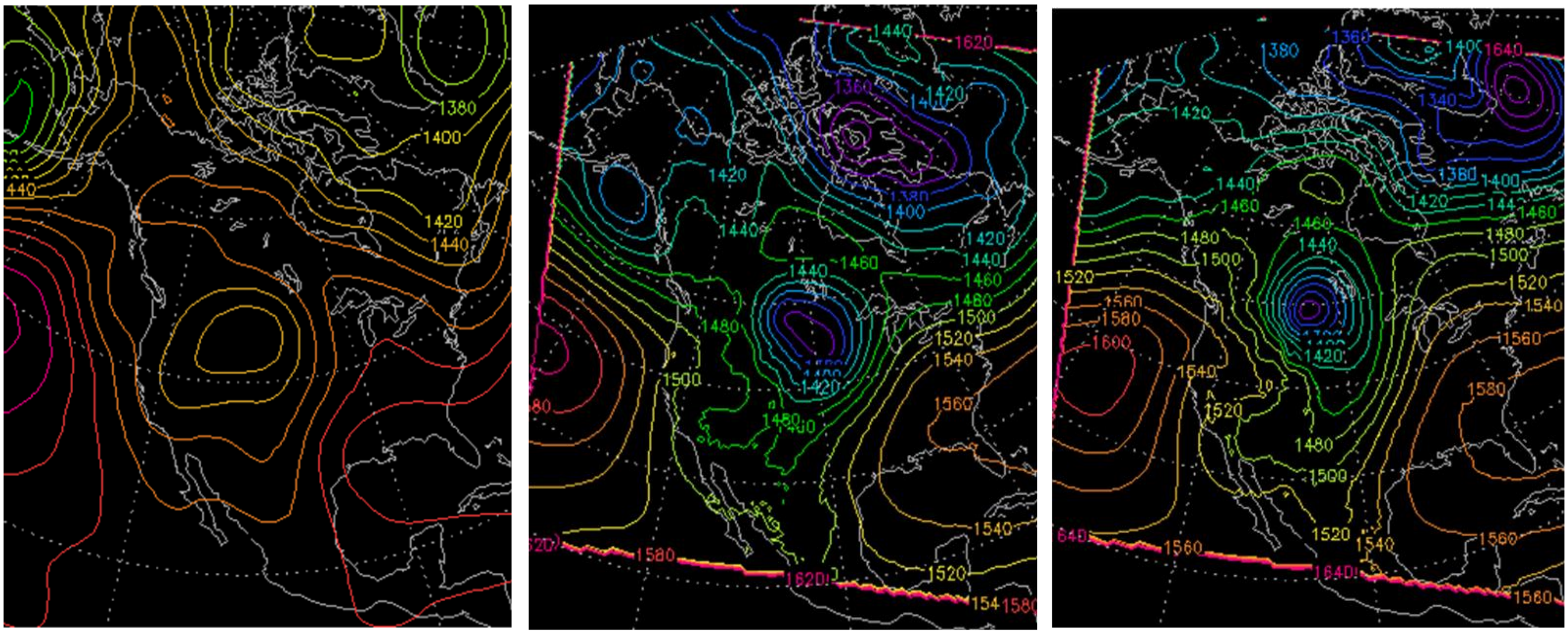

(g) (h) (i)

Figure 4.34: Comparison of 850 hPa geopotential height composites for top 3 daily precipitation events at Assiniboia.

(g) 1961-1990 NCEP reanalysis; (h) 1961-1990 model simulation; (i) 2041-2070 model projection.

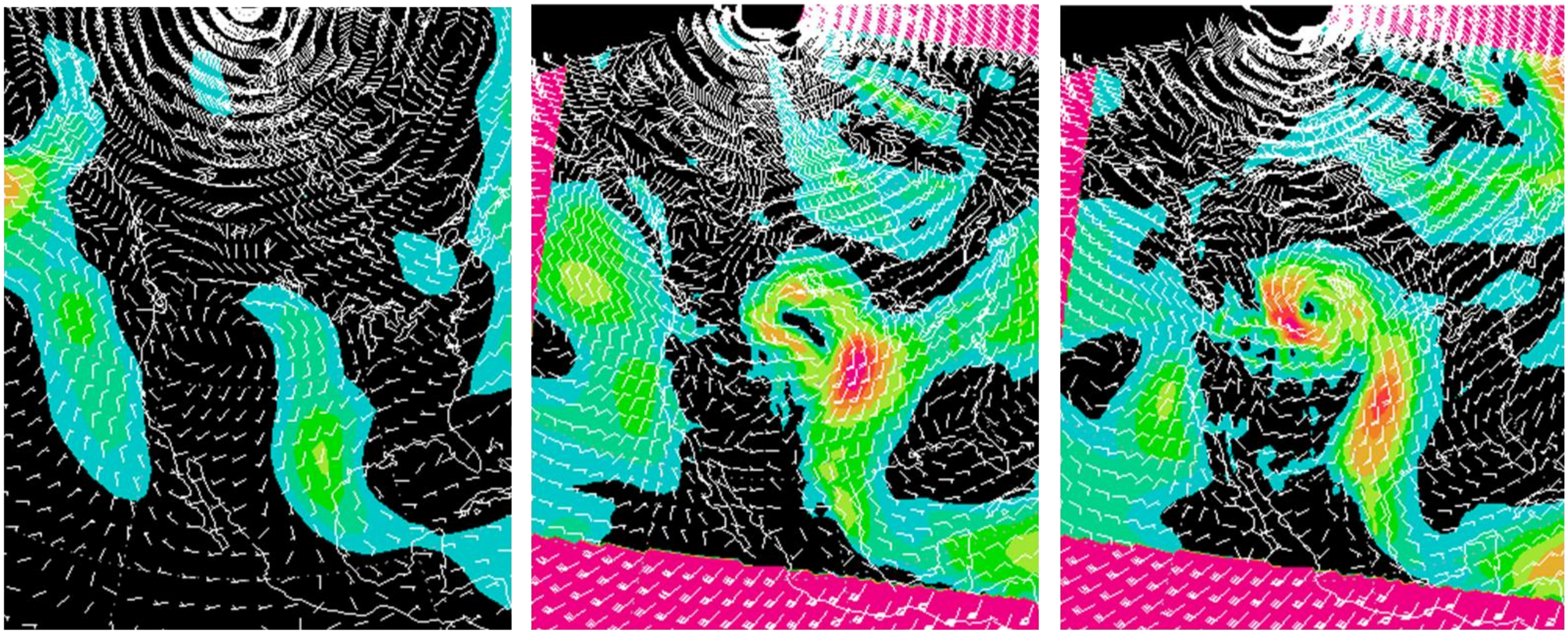

(j)

(k)

(l)

Figure 4.34: Comparison of 850 hPa vector wind composites for top 3 daily precipitation events at Assiniboia.

(j) 1961-1990 NCEP reanalysis; (k) 1961-1990 model simulation; (l) 2041-2070 model projection.

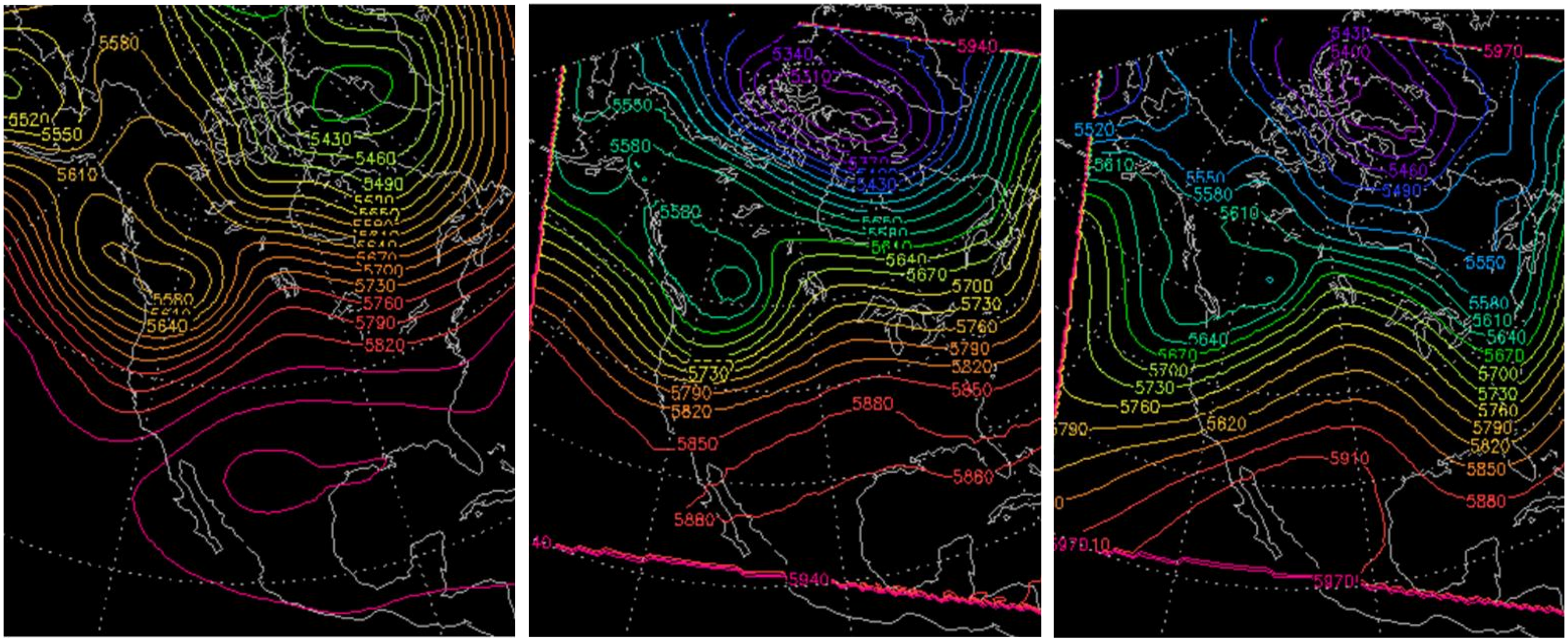

(a)

(b)

(c)

Figure 4.35: Comparison of 500 hPa geopotential height composites for top 3 daily precipitation events at High Prairie.

(a) 1961-1990 NCEP reanalysis; (b) 1961-1990 model simulation; (c) 2041-2070 model projection

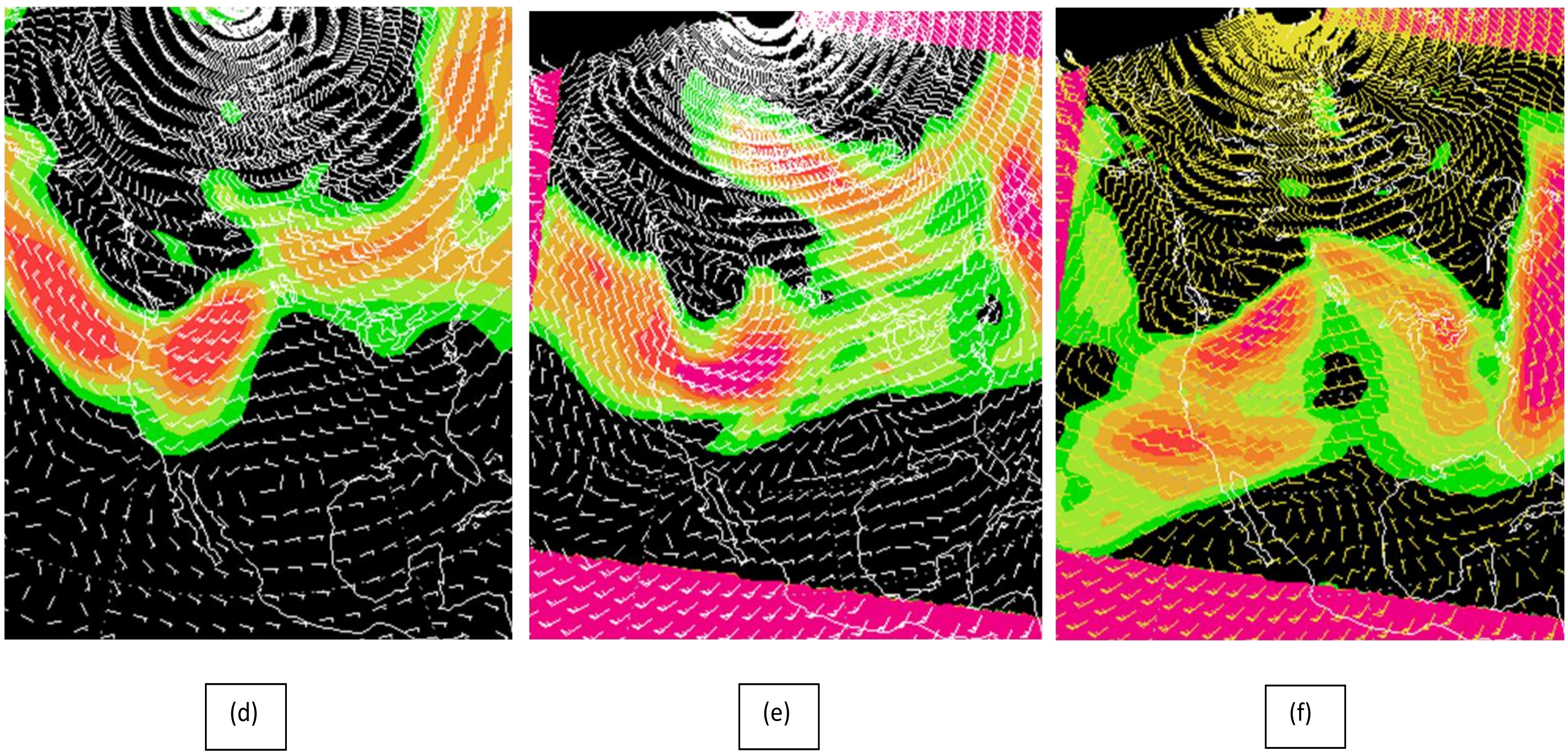

Figure 4.35: Comparison of 500 hPa vector wind composites for top 3 daily precipitation events at High Prairie.

(d) 1961-1990 NCEP reanalysis; (e) 1961-1990 model simulation; (f) 2041-2070 model projection.

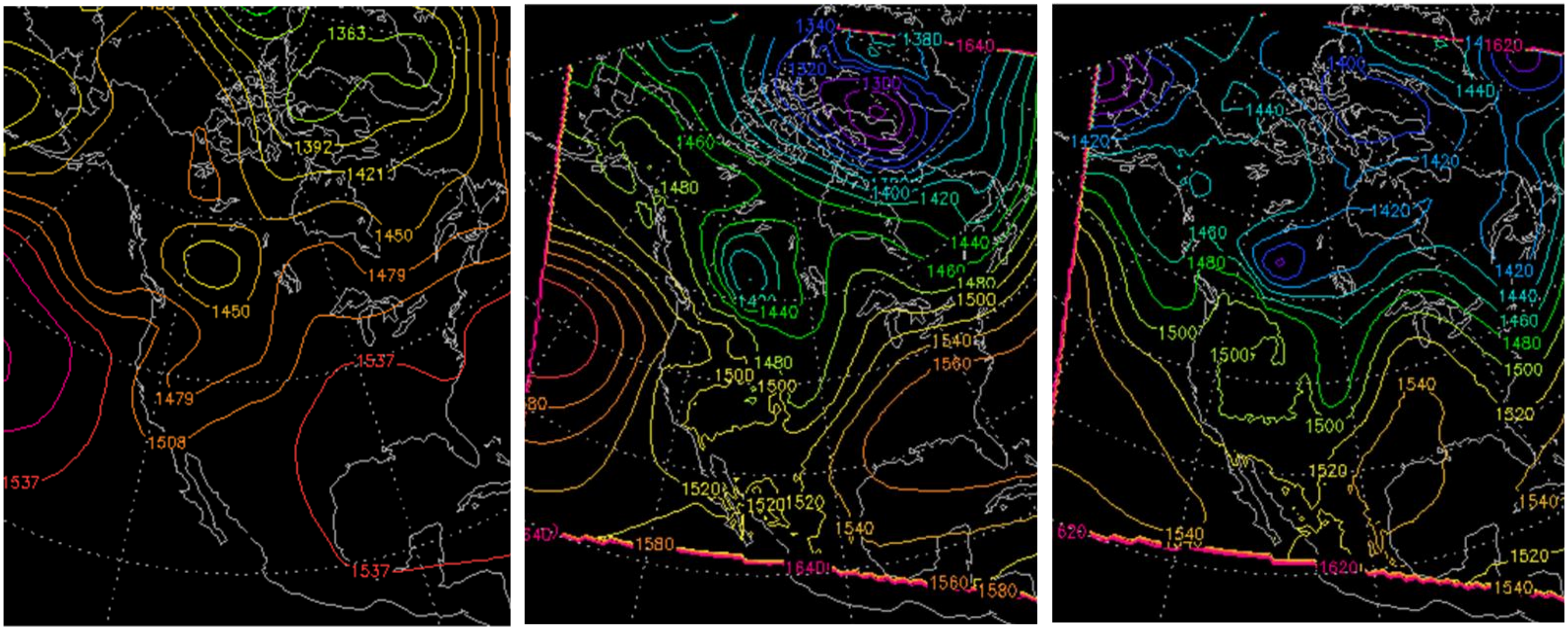

(g) (h) (i)

Figure 4.35: Comparison of 850 hPa geopotential height composites for top 3 daily precipitation events at High Praire.

(g) 1961-1990 NCEP reanalysis; (h) 1961-1990 model simulation; (i) 2041-2070 model projection.

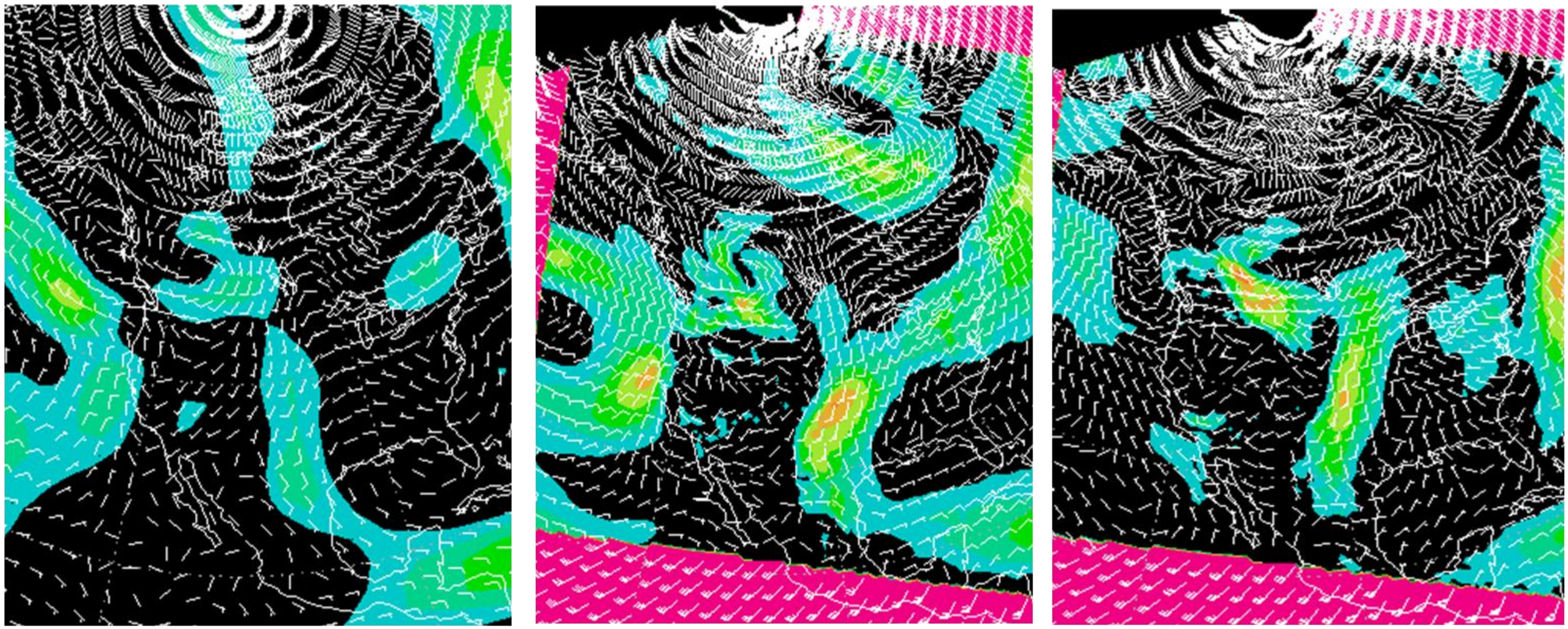

(j) (k) (l)

Figure 4.35: Comparison of 850 hPa vector wind composites for top 3 daily precipitation events at High Prairie.

(j) 1961-1990 NCEP reanalysis; (k) 1961-1990 model simulation; (l) 2041-2070 model projection.

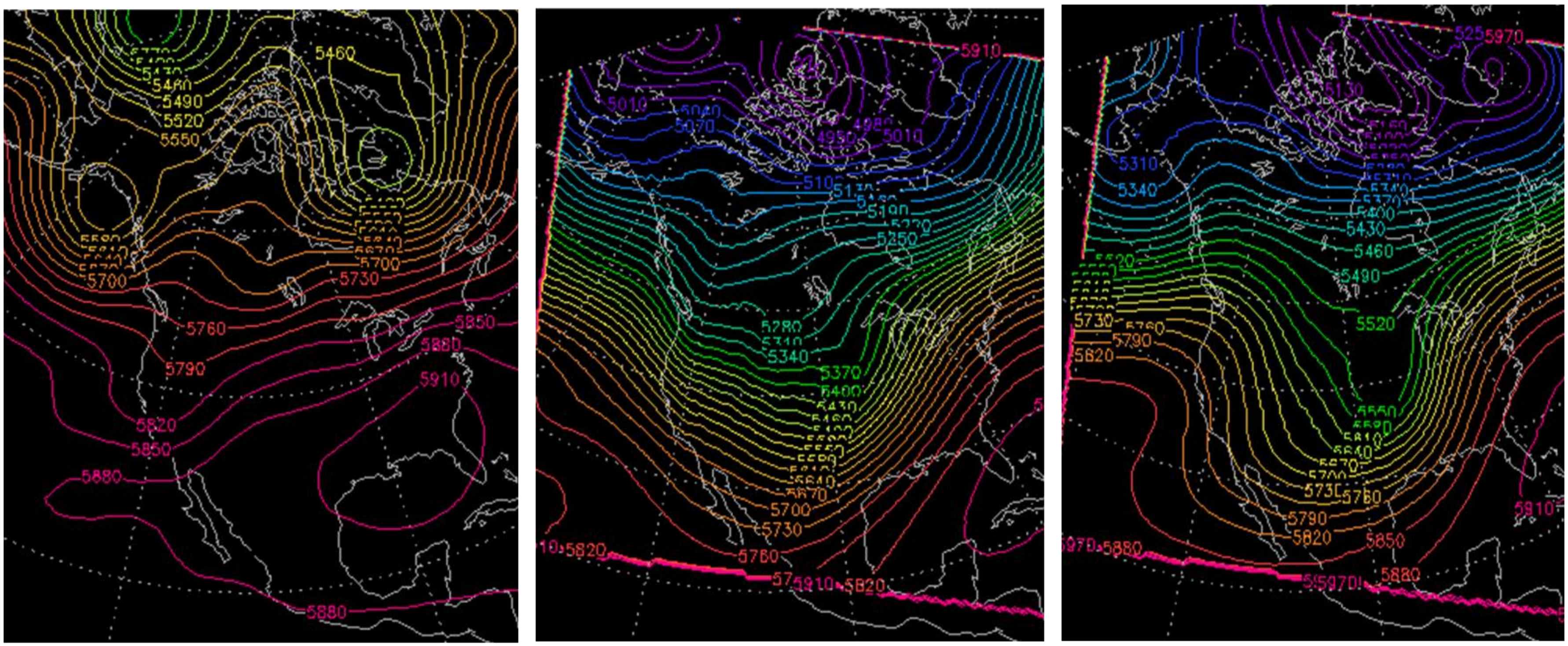

(a)

(b)

(c)

Figure 4.36: Comparison of 500 hPa geopotential height composites for top 3 daily precipitation events at Guelph.

(a) 1961-1990 NCEP reanalysis: (b) 1961-1990 model simulation: (c) 2041-2070 model projection.

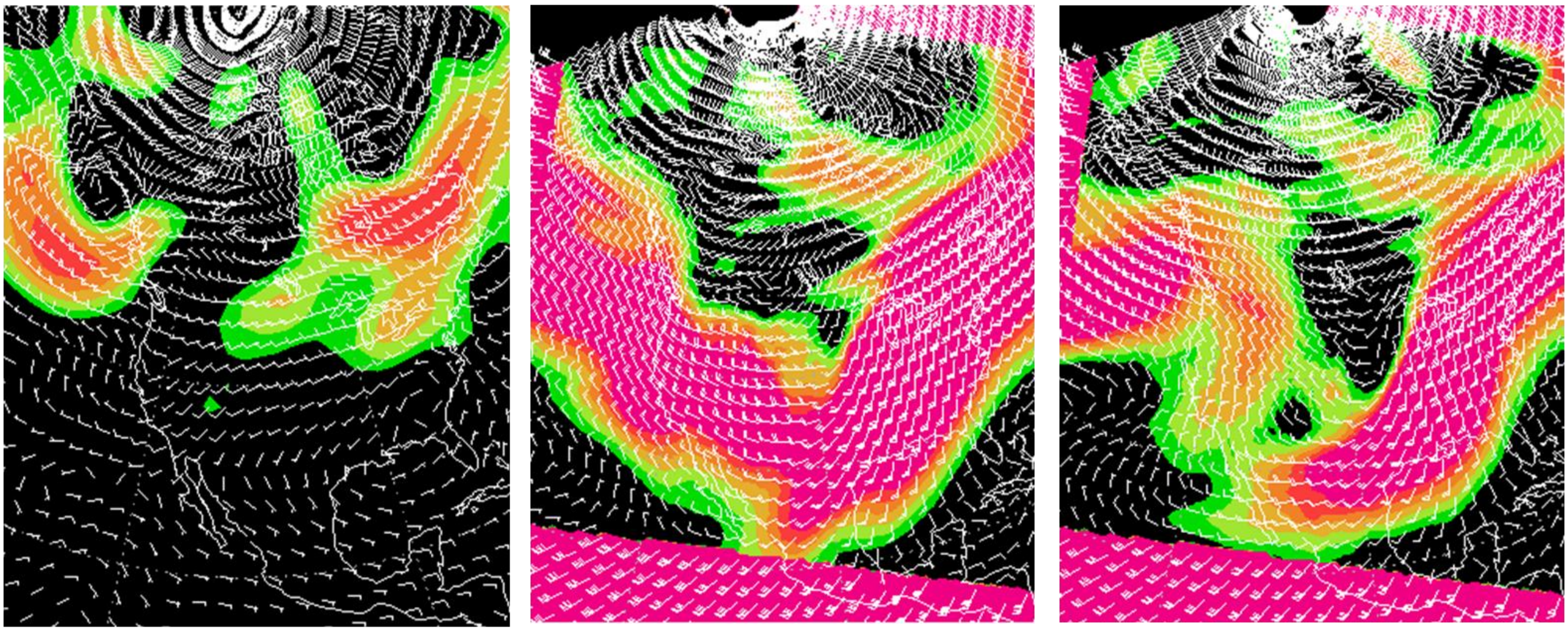

(d) (e) (f)

Figure 4.36: Comparison of 500 hPa vector wind composites for top 3 daily precipitation events at Guelph.

(d) 1961-1990 NCEP reanalysis; (e) 1961-1990 model simulation; (f) 2041-2070 model projection.

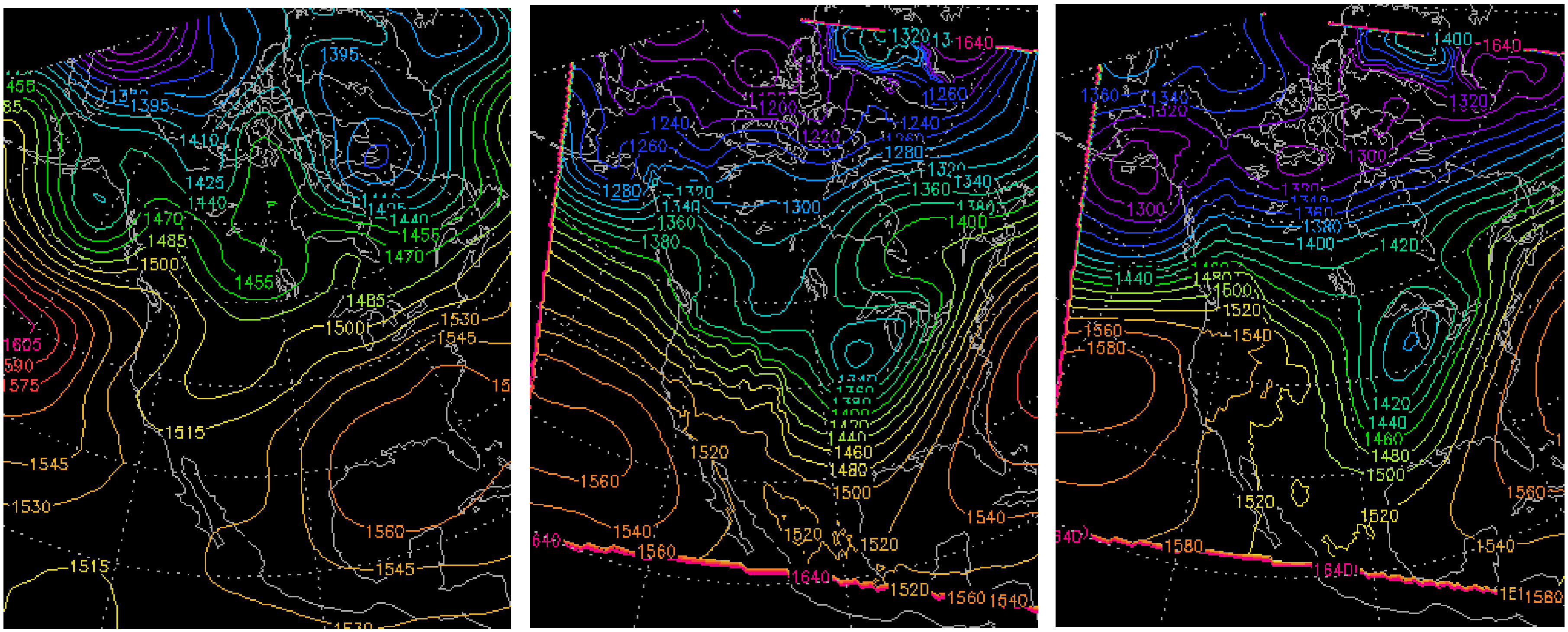

(g) (h) (i)

Figure 4.36: Comparison of 850 hPa geopotential height composites for top 3 daily precipitation events at Guelph.

(g) 1961-1990 NCEP reanalysis; (h) 1961-1990 model simulation; (i) 2041-2070 model projection.

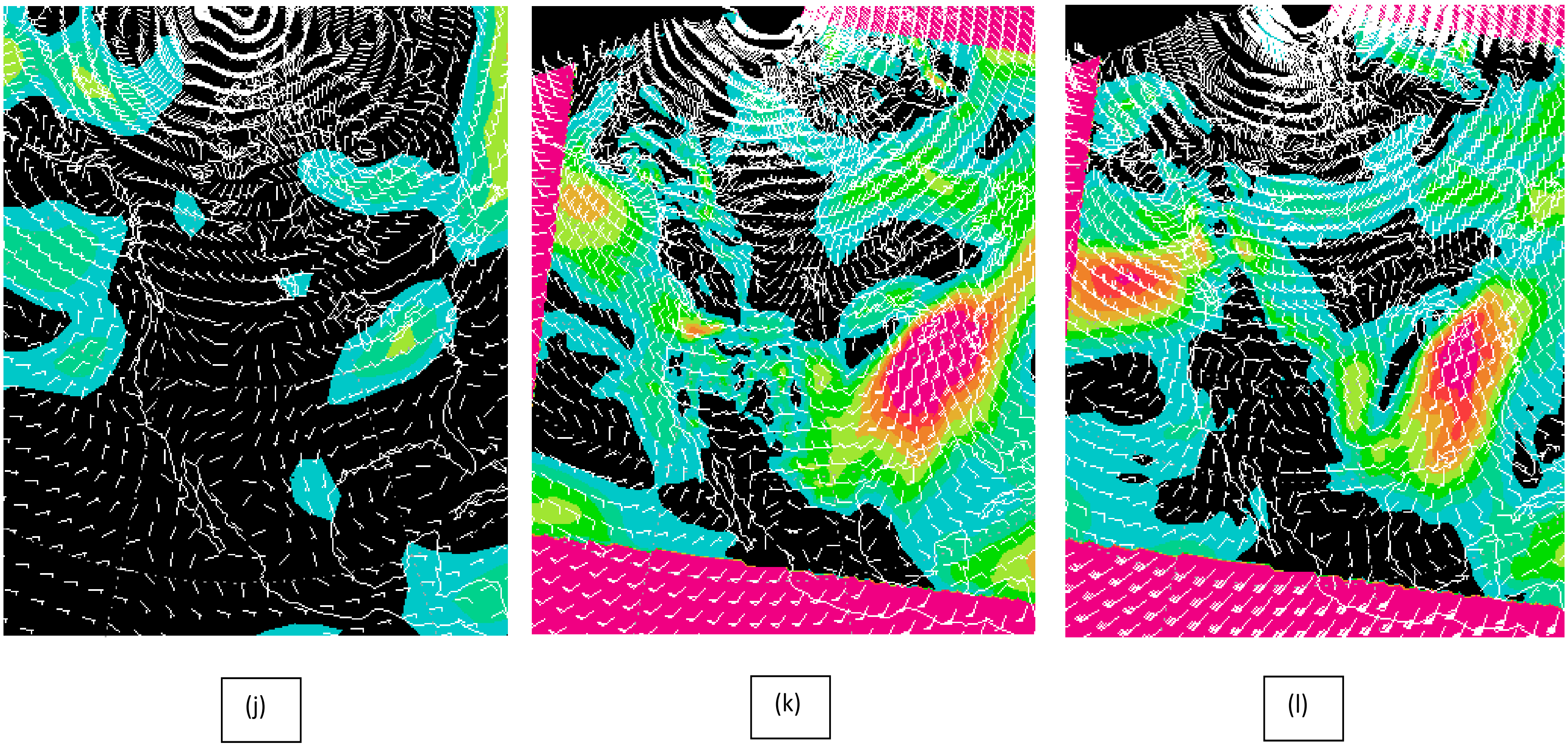

Figure 4.36: Comparison of 850 hPa vector wind composites for top 3 daily precipitation events at Guelph.

(j) 1961-1990 NCEP reanalysis; (k) 1961-1990 model simulation; (l) 2041-2070 model projection.

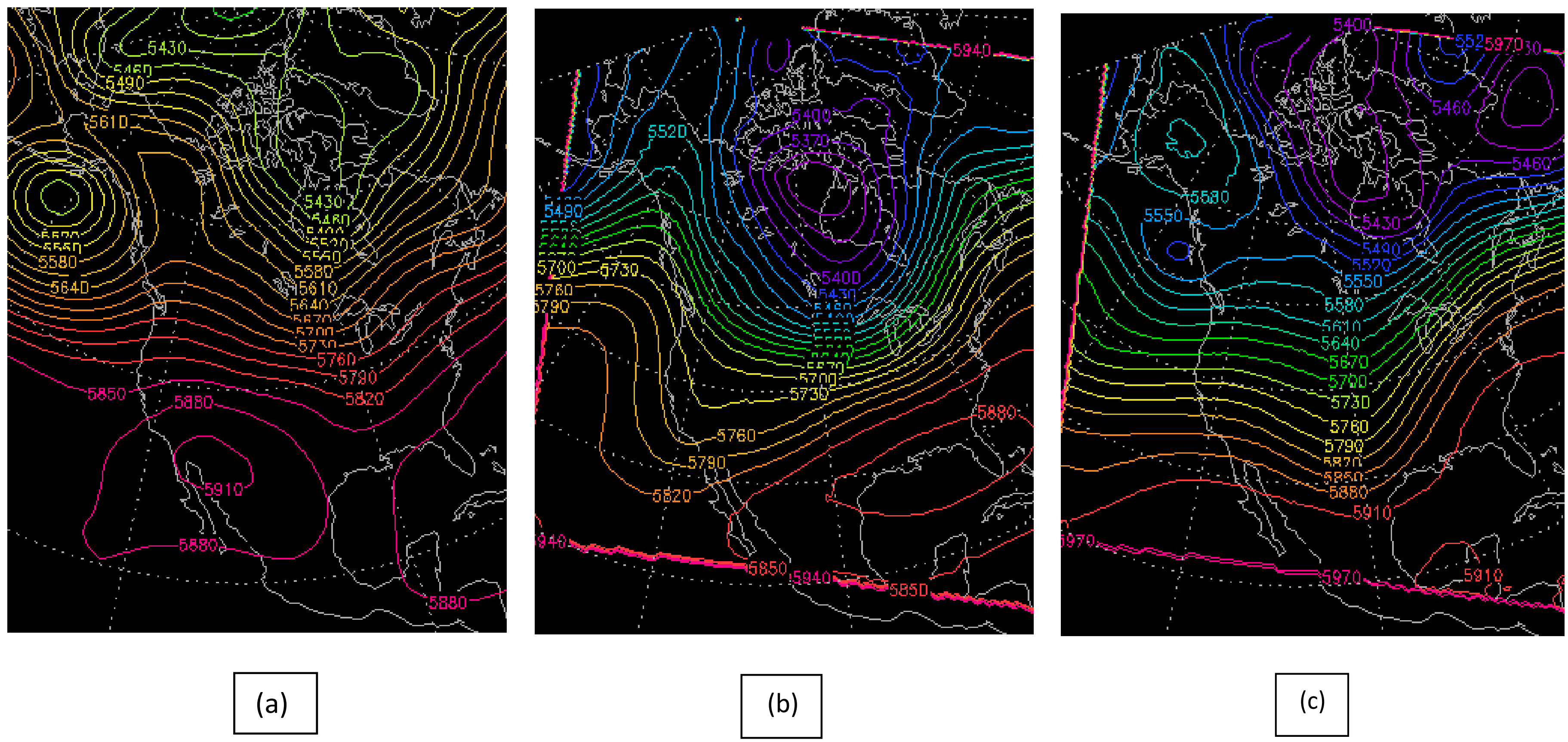

Figure 4.37: Comparison of 500 hPa geopotential height composites for top 3 daily precipitation events at Muskoka.

(a) 1961-1990 NCEP reanalysis; (b) 1961-1990 model simulation; (c) 2041-2070 model projection.

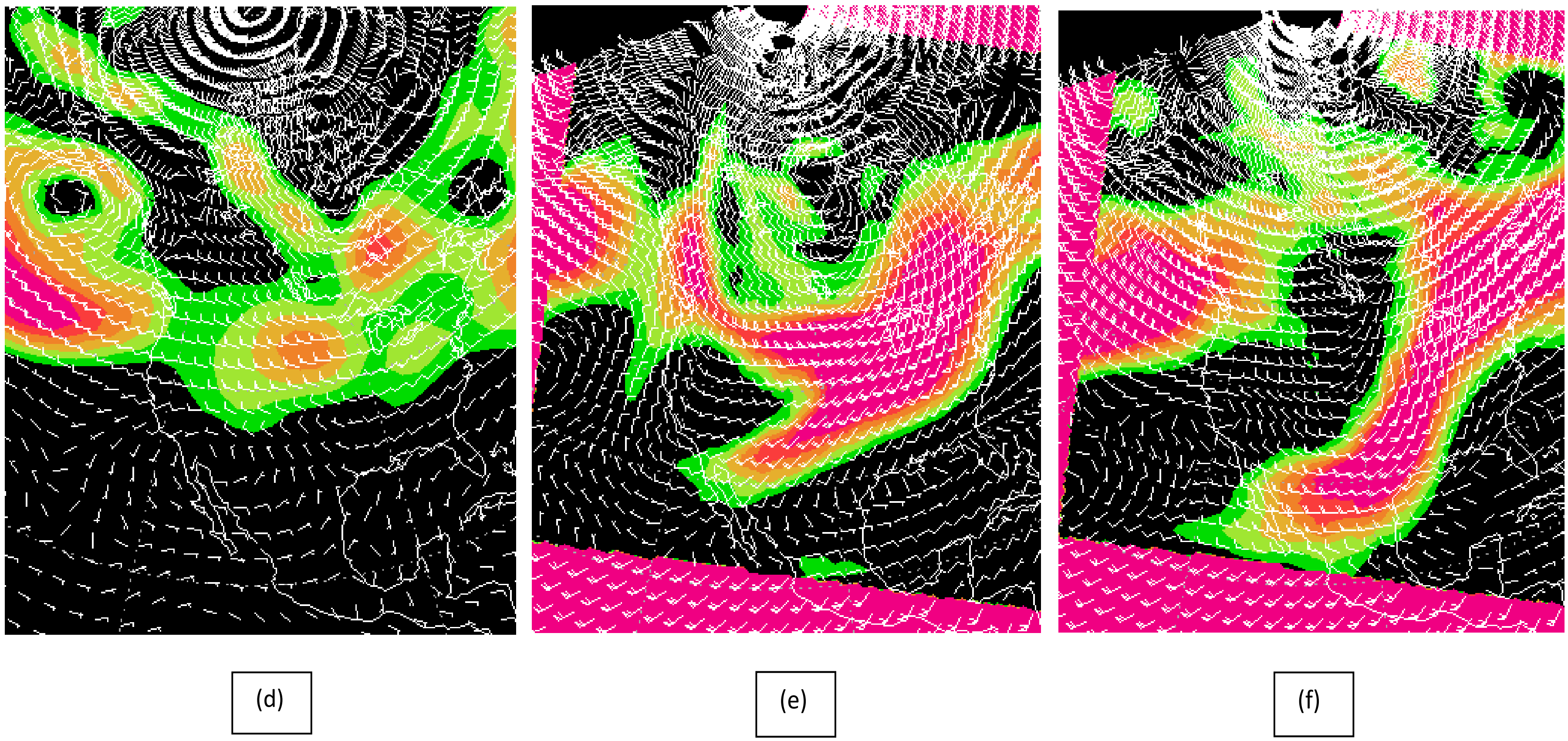

Figure 4.37: Comparison of 500 hPa vector wind composites for top 3 daily precipitation events at Muskoka.

(d) 1961-1990 NCEP reanalysis; (e) 1961-1990 model simulation; (f) 2041-2070 model projection.

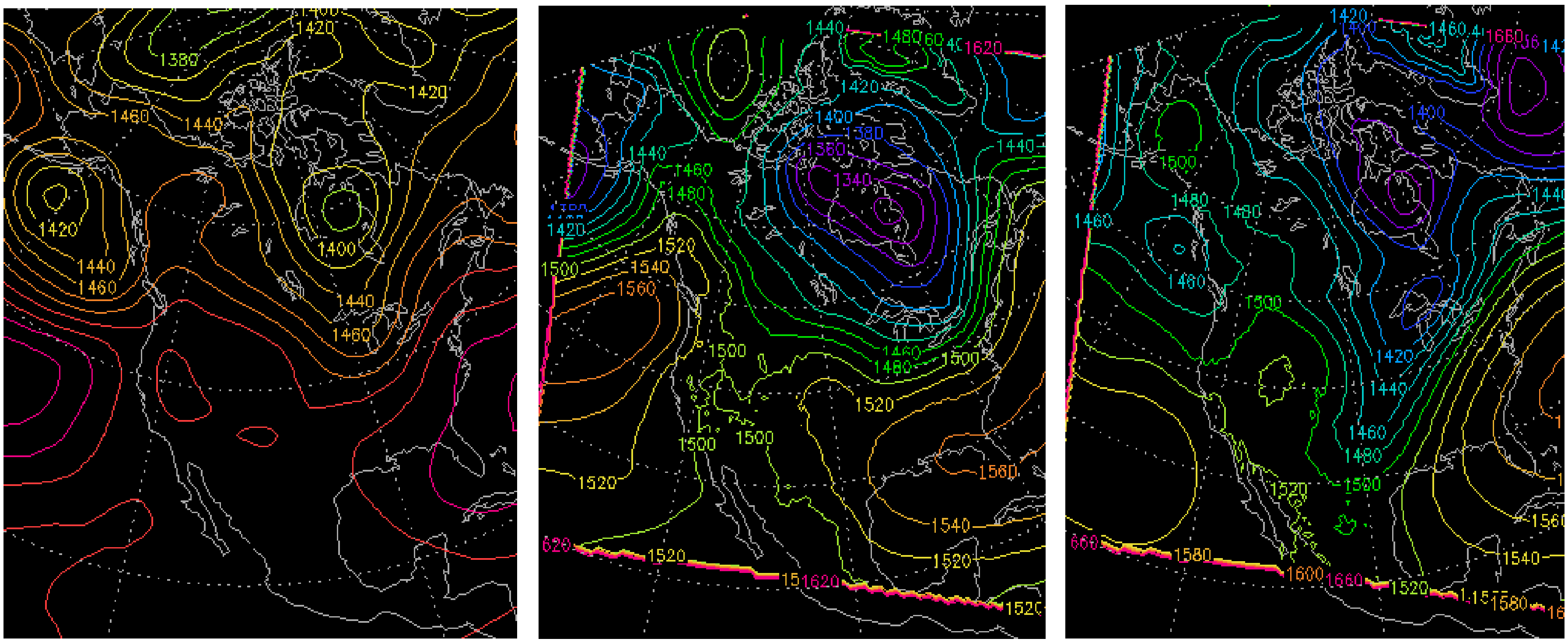

(g) (h) (i)

Figure 4.37: Comparison of 850 hPa geopotential height composites for top 3 daily precipitation events at Muskoka.

(g) 1961-1990 NCEP reanalysis; (h) 1961-1990 model simulation; (i) 2041-2070 model projection.

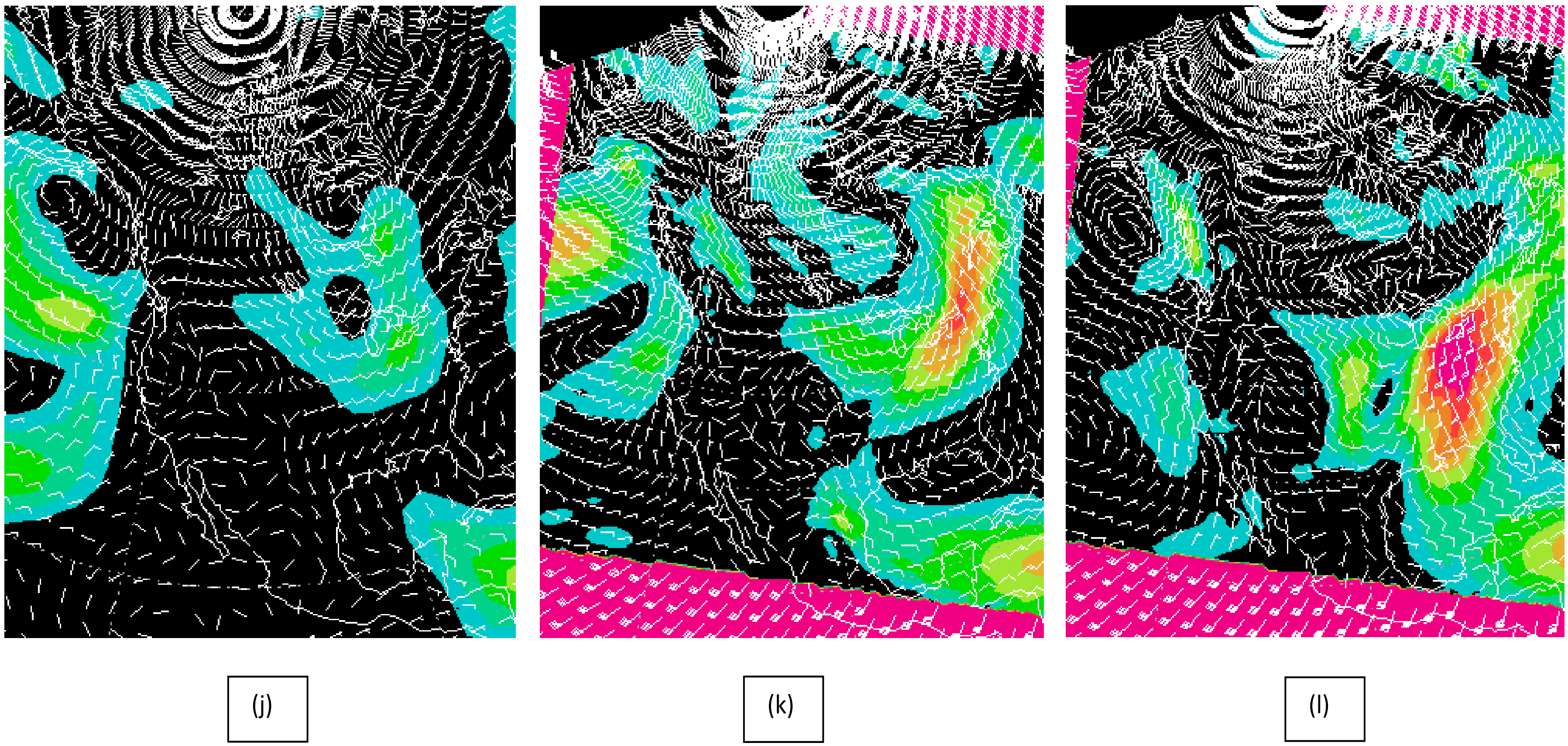

Figure 4.37: Comparison of 850 hPa vector wind composites for top 3 daily precipitation events at Muskoka.

(j) 1961-1990 NCEP reanalysis; (k) 1961-1990 model simulation; (l) 2041-2070 model projection.

CHAPTER 5: DISCUSSION

Given the previous results, a number of key points need to be considered in detail. These include site specific points, comparison of statistical distribution and extremes, an analysis of overall precipitation trends, monthly distribution of extreme events, and an examination of characteristics and phenomena associated with extreme precipitation events. Where applicable, the discussion will be both in term of validation and trends and will be discussed in the following sub-sections.

5.1 Review of Climatologies

The strong summer maximum seen in the monthly precipitation distributions for western sites reflects the high latitude, continental climate of those regions. The more even distribution seen for the Ontario sites reflects a more temperate, maritime influenced environment. The greater annual precipitation averages for eastern locations are achieved due to large monthly precipitation totals during the colder seasons (fall, winter, spring). This is a function of both meso-scale and synoptic influences. Cold air masses passing over the generally warm waters of the Great Lakes during the fall and early winter become moistened and unstable resulting in lake-induced meso-scale precipitation bands – adding extra rain or snow behind synoptic systems. The Ontario sites also lie on the main storm track during the winter season which stretches from the Central Plains through the lower Great Lakes and St Lawrence Valley and are thus exposed to a greater number of synoptic systems.

In contrast, the Prairie locations frequently experience polar and arctic air masses for long periods which suppress the main storm track and jet-stream further south. The associated saturated water vapor pressures are very low with the temperatures of these air masses resulting in little moisture available for precipitation. In addition the low sun angle and snow cover precludes any significant surface based instability and subsequent convection from occurring.

5.2 Site-Specific Points

This sub-section provides an overview of some of the key findings for each specific location

Cold Lake

Model underestimation of precipitation event classes greater than 25 mm, and conversely overestimation of small daily precipitation classes accounts for the low simulated values of the 90th, 99th, and 99.9th percentile compared with climatology. A decrease in the occurrence of small daily precipitation events (less than 5mm), and an increase in larger ones (5 – 50 mm) causes the values of the 90th, 99th, and 99.9th percentile of daily precipitation to increase.

Assiniboia

Model underestimation of daily precipitation events greater than 5 mm and overestimation of events in the 0.1 to 5 mm class accounts for the low simulated values of the 99th and 99.9th percentile compared with climatology. A complicated pattern of changes in the distribution of occurrence for the various daily precipitation classes explains the mixed trend for the percentiles of extreme precipitation (90th, 99th, and 99.9th percentile of daily precipitation). Contribution from the smallest precipitation class increases while it decreases for midrange classes only to again increase for 50 – 100 mm daily events.

High Prairie

Overestimation in the occurrence of the smallest class of daily precipitation by the model, combined with underestimation of classes above 10 mm are responsible for the low simulated values for the 90th , 99th, and 99.9th percentile of daily precipitation. A decrease in the occurrence of small daily precipitation events (less than 5 mm) and an increase in occurrence for all larger ones allow for an increase in the value of the extreme daily precipitation percentiles (90th, 99th). At the same time, the relatively large in increase in the occurrence of daily precipitation events in the 10 – 25 mm class (above the value of the 90th percentile and for the most part the value of the 99th percentile) causes the frequency distribution to skew somewhat left of the 99.9th percentile - thus lowering its value.

Guelph

Model overestimation in the occurrence of daily precipitation classes less than 25 mm, combined with underestimation of those greater than 25 mm accounts for the low simulated values of the 90th, 99th and 99.9th percentile compared with climatology. A decrease in the occurrence of daily precipitation events less than 25 mm, and an increase in those greater than 25 mm cause the values of all the extreme percentiles for daily precipitation (90th,99th, and 99.9th) to increase in the future projection.

Muskoka

Model underestimation of daily precipitation events greater than 25 mm and underestimation of those less than that amount cause the simulated value of the 90^{th}, 99^{th} and 99.9^{th} percentile for daily precipitation to be low compared with climatology. A decrease in the occurrence of daily precipitation events less than 25 mm classes is responsible for the increased value of the 90^{th} and 99^{th} percentiles for daily precipitation. At the same time, a large 4 % increase in the contribution from precipitation events in the 25 – 50 mm class - and likely more specifically in the 25 – 35 mm category (which is less than the value of the 99.9^{th} percentile in the base simulation) - causes a skewing effect and shifts the value of the 99.9^{th} percentile to the left on the distribution. At the same time the frequency of very high daily precipitation events (greater than 50 mm) increases slightly, however it is not enough to offset the skewing effect from the increase in the mid-range classes (25 -35 mm).

5.3 Statistical Distribution and Extremes

At all locations an overestimation in the frequency of days with light precipitation of less than 5 mm (at the expense of days with no measurable precipitation) by the model causes the entire distribution of daily precipitation to be shifted to the left (see Figure 5.1). This has the effect of lowering the value for the 90^{th}, 99^{th} and 99.9^{th} percentile – in other words the intensity of extreme precipitation events. At the same time, the base period simulation underestimates the frequency of events in the 25-50 mm, and 50-100 mm classes further contributing to the skewed distribution. In the future scenario, a general rightwards shift is seen in the entire distribution of daily precipitation. This is fueled mainly by an increase in frequency of events in

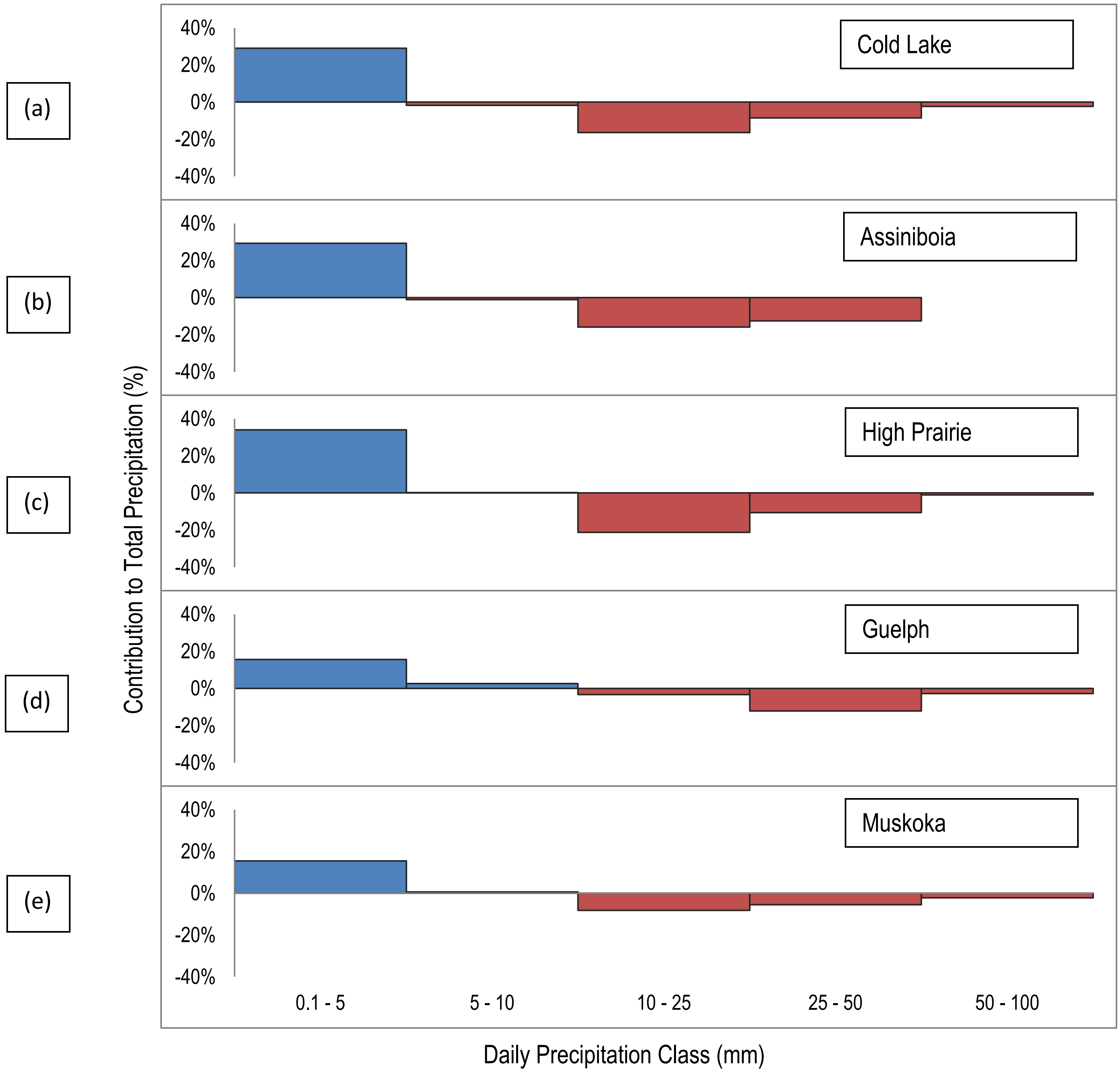

Figure 5.1: Difference in the percent contribution from daily precipitation classes to total accumulation between the 1961-1990 climatology and the 1961-1990 model simulation at all locations. Blue bars represent model overestimation and red bars represent model underestimation. (a) Cold Lake; (b) Assiniboia; (c) High Prairie; (d) Guelph; (e) Muskoka.

the 10 to 25 mm class for western sites and to some extent in the 25 to 50 mm class for eastern locations (Figure 5.2). The result is a higher value for the 90th, 99th, and 99.9th percentile for most locations. In some cases increases in smaller precipitation classes (5-10 mm) have caused the distribution to become skewed to the left but at the same time frequency of events in the 50-100 mm class has increased as with Muskoka.

5.4 Comparison of Annual Precipitation

Precipitation is generally underestimated by the model except for the summer months at most sites perhaps reflecting the simulated presence of the storm track over the respective locations. An interesting pattern is revealed in the future trends with general increases of precipitation at all locations but at the same time decreases noted in summer months. This dichotomy between increased extreme occurrence (which in large part is associated with the summer months) and decreased precipitation during the warmest months would set the stage for extreme oscillations in soil moisture regimes in the future climate.

5.5 Monthly Distribution of Extreme Events

For all western locations, an exaggerated warm season peak is seen in the monthly distribution of extreme events compared with actual observations (Figures 4.5, 4.9, 4.13). This is likely due to model overestimation of synoptic forcing associated with extreme events (see section 5.8) and the simulated and projected presence of the storm track over the Prairies in summer. The eastern locations generally show a bimodal or multimodal peak in the monthly occurrence of extremes which is

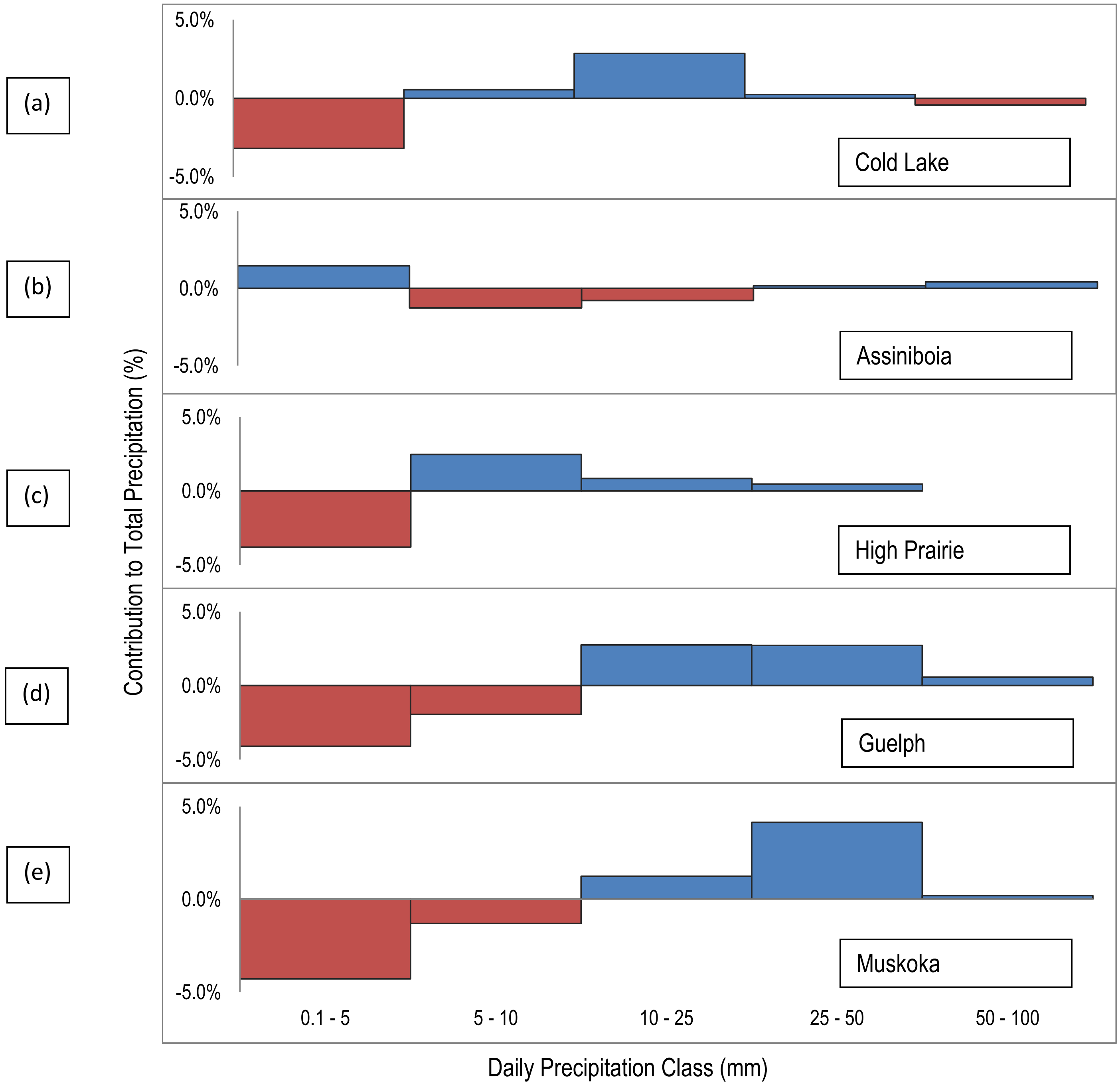

Figure 5.2: Difference in the percent contribution from daily precipitation classes to total accumulation between the 1961-1990 model simulation and the 2041-2070 model projection at all locations. Blue bars represent increases in contribution and red bars represent decreases in contribution. (a) Cold Lake; (b) Assiniboia; (c) High Prairie; (d) Guelph; (e) Muskoka.

not seen in the observed climatology (Figures 4.17 and 4.21). This may possibly be explained by the model's over-aggressive and uniform simulation and projection of storm track migration in response to seasonal changes. That is to say, the model underestimates the variability in storm track position during the entire warmer season (spring, summer, fall) and overestimates the dominance and northwards migration of the sub-tropical Bermuda or Azores ridge.

For western sites, the model projects an earlier spike in monthly extreme occurrence for most cases. This reflects assumptions regarding seasonal changes in storm track and subsequent advection of moist, unstable air into the region. Namely, such moist unstable air masses will affect the regions earlier in the season as a result of the jet stream migrating north earlier. Eastern sites show a larger gap between the first and second maxima of extreme event frequency. This likely suggests a more dominant and northwards displaced sub-tropical heat ridge - suppressing general precipitation along with extremes. It may also suggest increased lake induced activity into the middle part of winter in response to more open water on the great lakes later into the cold season.

In terms of the most extreme events (top 3 daily precipitation events), the pattern of occurrence over the annual cycle for the observed data shows an early to mid-summer maximum for western sites and late summer maxima for eastern locations (Figure 5.3). The model simulation reproduces fairly accurately the distribution of occurrence for western sites, but the simulated occurrence for eastern locations is spread out rather than being concentrated – particularly in the case of Guelph. This demonstrates that the model has difficulty reproducing summer extreme events which are not synoptically driven over the east.

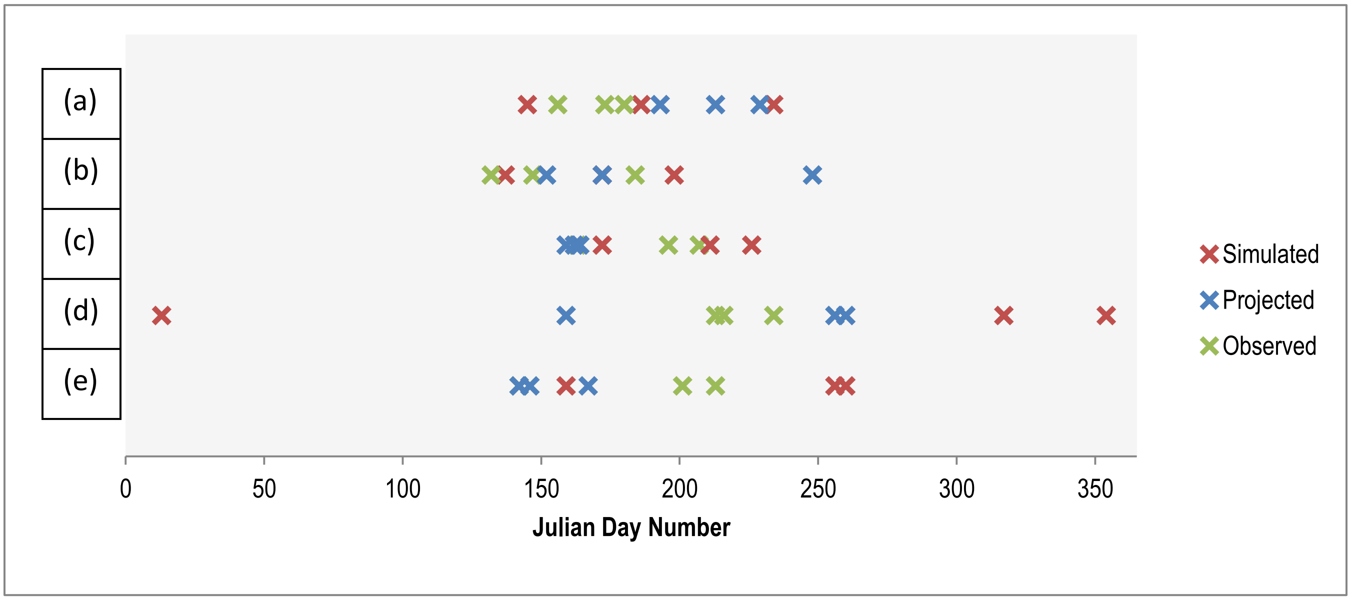

Figure 5.3: Julian day number of the top 3 daily precipitation events for the 1961-1990 climatology, the 1961-1990 model simulation and the 2041-2070 model projection at all locations. (a) Cold Lake; (b) Assiniboia; (c) High Prairie; (d) Guelph; (e) Muskoka.

5.6 Context of Results Within Previous Findings

The general results of this study are consistent with previous model simulations over the Northern Hemisphere as outlined in the introduction and are validated by the increases in extreme precipitation occurrence over regions of North America that have been detected. Specifically, with regards to the particular model used in this study, other investigators have found similar results using this version. Mladjic et al. (2011) found both that the model underestimates extreme events over most of Canada and that the magnitude of 20 year return period events increases over most regions. It is worth mentioning that although underestimation of extremes has been detected, through the incorporation of the new CLASS land surface scheme, validation of extremes (including precipitation) has improved (Roy et al

2011). At the same time, the decreases in summer precipitation seen over several of the locations in this study are in line with the findings of PaiMazumder et al. (2010), who suggest that the occurrence and duration of droughts are expected to increase over the southern prairies after comparing five member ensembles for a base period simulation and a future scenario of the CRCM. The above results add confidence to the inference of increased extremes in moisture regimes and precipitation that this country will be subjected to in the future.

5.7 Characteristics and Phenomena Associated With Extreme Events

Extreme events over western locations tend to be associated with cold lows or easterly trowal airstreams interacting perhaps with upslope terrain. The secondary and easterly, low level jet maxima is key to producing an upslope trajectory. Since they appear to be associated with little low level instability they likely represent mainly stratiform precipitation events. They are often linked with highly meridional 500 hPa geopotential and flow patterns (deep trough over Western Canada and pronounced ridge over the Central United States) because it is those which are capable of transporting moisture from the Gulf of Mexico in at least the middle levels of the atmosphere for great distances. This is validated by studies of actual extreme precipitation events such as Szeto et al. (2011). The importance of an upper blocking pattern situated somewhere over the Hudson Bay region can also be seen. This forces the synoptic system into the western prairies and displaces moisture transport to the southwest.

The most extreme events at the eastern sites show a comparatively less amplified upper flow pattern since they are not as far removed from the ultimate moisture source fueling such events – namely the Gulf of Mexico. They also tend to be associated more with lower-level – that is 850 hPa moisture transport - and convergence from the nose of the low level jet. Some events are also linked to lake effect precipitation characterized by cold advection across the presumably warm waters of the great lakes.

5.8 Validation of Characteristics

The model reproduced fairly accurately the synoptic patterns and conditions associated with extreme events for western locations. Flow and the inferred synoptic forcing were slightly overestimated in the model suggesting that embedded convection plays a larger role in actual extreme events over the west than the model depicts. The flow over eastern sites is overestimated likely due to fact that the simulated events were occurring during the winter season, whereas the actual events occurred during summer. This obscured the fact that eastern events appeared to be linked to summer time mesoscale convective complexes riding along the nose of a discrete low level jet. Extreme occurrences at eastern sites were less synoptically driven than for western locations, but this was not seen in the model.

5.9 Future Characteristics of Extreme Events

In spite of a northwards migration of the storm track and geopotential pattern, the blocking configuration associated with extreme events over western sites appears relatively stable. That is to say it is still responsible for generating conditions which are conducive to extreme precipitation at those specific sites. This is in line with the general consensus of model studies showing a northwards shift in the favored storm track over the Northern Hemisphere.

However it should be noted that more recent studies utilizing extended or better resolution of stratospheric processes actually show that increased wind shear and associated baroclinic instability may shift the storm track further south (Scaife 2011).

The northwards shift seen over the eastern locations – in particular the dramatic shift in Guelph is also explained by the fact that one of the events in the top 3 occur in the summer during the future simulation.

CHAPTER 6: SUMMARY AND CONCLUSIONS

A study has been carried out to examine the occurrence and characteristics of future extreme precipitation events as projected by the Canadian Regional Climate Model 4.2 at five selected locations across Canada. Important findings from the study are summarized below:

i) The observed climatology of the various locations reflects a large dichotomy in the seasonal distribution and totals of precipitation between western and eastern sites. Monthly precipitation shows a strong summer maximum over western locations whereas an even distribution is over eastern ones. The frequency of extreme events (particularly 99th percentile) however does show a warm season maximum for eastern sites.

ii) Cold or cut-off lows in the presence of an amplified, somewhat blocked upper pattern are associated with most of the extreme events over the western locations during the summer months. The top events at eastern sites are associated with a more zonal pattern and strong warm advection ahead of a large synoptic system.

iii) The regional model has been found to underestimate extreme precipitation when compared to the observational data. The values of the 90th, 99th and 99.9th percentile for daily precipitation in the base period simulation are considerably lower than those derived from observational-based climatologies. The model also depicts an exaggerated maximum in the monthly occurrence of extreme events for the western sites and displays a bimodal maximum for the eastern locations.

iv) Annual precipitation regardless of extremes is found to increase at all locations from west to east. However when examining a monthly breakdown, decreases are projected in the summer to early fall months for most of the sites except for Cold Lake.

v) The values for the 90^{th}, 99^{th}, and 99.9^{th} percentiles for daily precipitation increase in the future projection at almost all locations suggesting a rightwards shift in the distribution of daily precipitation and higher extremes. In the case of Muskoka (whose value for the 99.9^{th} percentile decreases) there is still a greater occurrence of precipitation events greater than 50 mm. An increase in mid-range precipitation events may be changing the shape of the distribution resulting in the lower values for the most extreme percentiles. Particular trends are evident in the monthly occurrence of extreme events. For western sites there is an earlier peak for 99th percentile occurrence; for eastern locations, the spring maximum of extreme occurrence has shifted earlier while the late season peak has shifted back.

vi) The model reproduces fairly accurately the basic characteristics and synoptic pattern associated with the most extreme events for western locations increasing confidence in our interpretation of the underlying mechanisms behind such events. However, eastern events were not well replicated, with the importance of summer-time mesoscale convective complexes and elevated instability underestimated.

vii) In spite of a slight northwards shift in the geopotential pattern associated with future extreme events, the blocking pattern observed over western Hudson Bay (for Prairie locations) remains relatively stable in the 2041 to 2070 scenario. This implies the same general mechanism is responsible for future extreme events. There is also some evidence of a more localized, convective pattern of precipitation for western sites.

The findings of this study must be accepted within in the context of its limitations. Namely, models have a difficult time resolving localized, convective precipitation which often has the greatest intensity and is therefore responsible for many extreme events. Furthermore, an ensemble consisting of other members of the CGCM or of different GCMs would provide a more probabilistic approach and reveal the degree of uncertainty associated with the findings. In lieu of using an ensemble, perhaps adjacent grid points from the model could be incorporated, and the results averaged for a more blended approach. Avenues of future study may include selection of more representative sites such as on the eastern Prairies (which are near a sharp gradient in average annual precipitation) and more northern locations.

In summary, it must be realized that future climate change will not have a monolithic effect across our country. With such a diverse array of regional climates and landscapes, the effect of global warming on precipitation extremes will be modulated through local factors. Therefore, we are led to the realization that understanding these regional variances is key to assessing future risk of extreme events and developing coping strategies at particular locations.

REFERENCES

Alpert, P., Ben-Gai, T., Baharad, A., Benjamini, Y., Yektieli, D., Colacino, M., Diodato, L., Homar, V., Manes, A., Michaelides, S., Ramis, C. (2002). The paradoxical increase of Mediterranean extreme daily rainfall in spite of decrease in total values. *Geophys. Res. Lett.*, 29(11), 1536, doi:10.1029/2001GL013554.

Akinremi, O.O., McGinn, S.M., Cutforth, H.W. (1999). Precipitation trends on the Canadian Prairies. *J. Climate*, 12, 2996–3003.

Ashley, S.T. and Ashley, W.S. (2008). Flood Fatalities in the United States. *J. Appl. Meteor. Climatol.*, 47, 805-818.

Beniston, M., Christensen, O.B., Ferro C.A.T., Frei, C., Goyette, S., Halsnacs, K., Jylhä, K., Koffi, B., Semmler, T., Stephenson, D.B., Woth, K. (2007). Future extreme events in European climate: an exploration of regional climate model projections. *Clim Change*, 81, 71–95.

Brunetti, M., Buffoni, L., Maugeri, M., Nanni, T. (2000). Precipitation intensity trends in northern Italy. *International Journal of Climatology,* 20, 1017–1031.

Christensen, J.H., Christensen, O.B. (2002). Severe summertime flooding in Europe. *Nature* 421, 805 - 806.

——, (2004). Intensification of extreme European summer precipitation in a warmer climate. *Glob. Planet. Change*, 44, 107-117.

——, (2007). A summary of the PRUDENCE model projections of changes in European climate by the end of the century. *Clim. Change*, 81, 7–30.

Colman, B. R. (1990a). Thunderstorms above frontal surfaces in environments without positive CAPE. Part I: A climatology. *Mon. Wea. Rev.,* 118**,** 1103–1121.

——, (1990b). Thunderstorms above frontal surfaces in environments without positive CAPE. Part II: Organization and instability mechanisms. *Mon. Wea. Rev.,* 118**,** 1123–1144.

Comfort, L., Wisner, B., Cutter S., Pulwarty, R., Hewitt, K., Oliver-Smith, A., Wiener, J., Fordham, M., Peacock, W., Krimgold, F. (1999). Reframing Disaster Policy: The global evolution of vulnerable communities. *Environmental Hazards*, 1, 39–44.

Curriero, F.C., Patz, J.A., Rose, J.B., Lele, S. (2001). Analysis of the association between extreme precipitation and waterborne disease outbreaks in the United States, 1948–1994. *American Journal of Public Health,* 91, 1194–1199.

Doswell, C.A. III, Brooks, H. E., Maddox, R.A. (1996). Flash flood forecasting: An ingredients-based methodology. *Wea. and Forecasting*, 11, 560-581.

Few, R. (2003). Flooding, vulnerability and coping strategies: local responses to a global threat. *Progress in Development Studies*, 3, 43–58.

Fowler H.J., Ekström, M., Blenkinsop, S., Smith, A.P. (2007). Estimating change in extreme European precipitation using a multi-model ensemble. *Journal of Geophysical Research - Atmospheres,* 112**,** D18104, doi:10.1029/2007JD008619.

Fowler, H.J., Ekström, M. (2009). Multi-model ensemble estimates of climate change impacts on UK seasonal precipitation extremes. *International Journal of Climatology*, 29 (3), 385–416.

French, J., Ing, R., Von Allmen, S., Wood, R. (1983). Mortality from flash floods: a review of national weather service reports, 1969–81. *Public Health Rep*, 98**,** 584–588.

Gordon, H.B., Whetton, P.H., Pittock, A.B., Fowler, A.M., Haylock, M.R. (1992). Simulated changes in daily rainfall intensity due to the enhanced greenhouse effect: implications for extreme rainfall events. *Clim. Dyn*., 8, 83–102.

Groisman, P. Y., Karl, T.R., Easterling, D.R., Knight, R.W., Jamason, P.F., Hennessy, K.J., Ramasamy, S., Page, C.M., Wibig, J., Fortuniak, K., Razuvaev, V.N., Douglas, A., Forland, E., Zhai, P.M. (1999). Changes in the probability of heavy precipitation: Important indicators of climatic change. *Climate Change*, 42, 243–283.

Gutowski, W. J., Jr., Willis, S.S., Patton, J.C., Schwedler, B.R.J., Arritt, R. W., Takle, E. S. (2008). Changes in extreme, cold-season synoptic precipitation events under global warming. *Geophys. Res. Lett.*, 35(20), L20710, doi:10.1029/2008GL035516.

Kimoto, M., Yasutomi, N., Yokoyama, C., Emori, S. (2005). Projected changes in precipitation characteristics around Japan under the global warming. *Scientific Online Letters on the Atmosphere*, 1, 85-88.

Heideman, K. F., and Fritsch, J. M. (1988). Forcing mechanisms and other characteristics of significant summertime precipitation. *Wea. Forecasting,* 3**,** 115–130.

Hennessy, K.J., Gregory, J.M., Mitchell, J.F.B. (1997). Changes in daily precipitation under enhanced greenhouse conditions. *Climate Dyn.*, 13, 667–680.

Houghton, J.T., Callander, B.A., Varney, S. K. (Eds.). (1992). *Climate Change 1992: The Supplementary Report to the IPCC Scientific Assessment.* Cambridge, UK: Cambridge University Press.

Hrudey, S.E., Payment, P., Huck, P.M., Gillham, R.W., and Hrudey, E.J. (2003). A fatal waterborne disease epidemic in Walkerton, Ontario: Comparison with other waterborne outbreaks in the developed world. *Wat. Sci. Tech*., 47, 7–14.

Huntingford, C., Jones, R.G., Prudhomme, C., Lamb, R., Gash, J.H.C., Jones, D.A. (2003). Regional climate-model predictions of extreme rainfall for a changing climate. *Q. J. Roy. Meteorol. Soc*., 129, 607–621.

Iwashima, T., Yamamoto, R. (1993). A statistical analysis of the extreme events: Long-term trend of heavy daily precipitation. *J. Meteor. Soc. Japan,* 71**,** 637–640.

Jones, P.D., Reid, P.A., (2001). Assessing future changes in extreme precipitation over Britain using Regional Climate Model integrations. *International Journal of Climatology*, 21, 1337–1356.

Karl, T.R., Knight, R.W., Easterling, D. R., Quayle, R. G. (1995) Trends in U.S. climate during the twentieth century. *Consequences,* 1**,** 2–12.

Karl, T.R., Knight, R.W. (1998). Secular trends of precipitation amount, frequency, and intensity in the United States. *Bull. Am. Meteorol. Soc.,* 79**,** 231–241.

Katz, R.W., Brown, B.G. (1992). Extreme events in a changing climate: Variability is more important than averages. *Clim. Change*, 21, 289–302.

Knapp, A.K., Beier, C., Briske, D.D., Classen, A.T., Luo, Y., Reichstein, M., Smith, M.D., Smith, S.D., Bell, J.E., Fay, P.A., Heisler, J.L., Leavitt, S.W., Sherry, R., Smith B., Weng, E. (2008). Consequences of more extreme precipitation regimes for terrestrial ecosysytems. *Bioscience*, 58, 811–821.

Kunkel, K.E., Andsager K., Easterling, D.R. (1999). Long-Term Trends in Extreme Precipitation Events over the Conterminous United States and Canada. *J. Climate*, 12(7), 2515–2527.

Lobell, D.B., Torney, A., Field, C.B. (2009). Climate Extremes in California Agriculture. California Climate Change Center.

Maddox, R.A., Chappell, C. F., Hoxit, L. R. (1979). Synoptic and mesoscale aspects of flash flood events. *Bull. Amer. Meteor. Soc.,* 60**,** 115–123.

Meehl, G.A., Arblaster, J.M., Tebaldi, C. (2005). Understanding future patterns of increased precipitation intensity in climate model simulations. *Geophys. Res. Lett.,* 32, L18719, doi:10.1029/2005GL023680.

Mekis, E., and Hogg, W.D. (1999). Rehabilitation and analysis of Canadian daily precipitation time series. *Atmos-Ocean*, 37, 53-85.

Mladjic, B., Sushama, L., Khaliq, M.N., Laprise, R., Caya, D., Roy, R. (2011). Canadian RCM Projected changes to extreme precipitation characteristics over Canada. *J. Climate*, 24, 2565-2584.

Moberg and 38 co-authors. (2006). Indices for daily temperature and precipitation extremes in Europe analyzed for the period 1901–2000. *J. Geophys. Res*., 111, D22106, doi:10.1029/2006JD007103.

Nirupama, N., Simonovic, S.P. (2007). Increase of flood risk due to urbanization: a Canadian example. *Nat Hazards*, 40, 25–41.

Noda A., Tokioka T. (1989). The effect of doubling of CO2 concentration of convective and non-convective precipitation in a general circulation model coupled with a simple mixed layer ocean model. *J. Meteorol. Soc. Jpn*. 67, 1057–1069.

Osborn, T.J., Hulme, M., Jones, P.D., Basnett, T. A. (2000). Observed Trends in the Daily Intensity of United Kingdom Precipitation. *Int. J. Climatol*., 20, 347–264.

PaiMazumder, D., Sushama, L., Laprise, R., Khaliq, N., Sauchyn, D. (2010). Future projections and uncertainties of short and long-term drought characteristics over Canadian Prairies as simulated by the Canadian RCM. *Geophysical Research Abstracts*, 13, EGU2011-164, 2011. EGU General Assembly 2011.

Palmer, T.N., Raisanen, J. (2002). Quantifying the risk of extreme seasonal precipitation events in a changing climate. *Nature*, 415, 512–514.

Patz, J. A., Graczyk, T. K., Geller, N., Vittor, A.Y. (2000). Effects of environmental change on emerging parasitic diseases. *International Journal for Parasitology*, 30, 1395–1405.

Pelling, M. (1997). What determines vulnerability to floods; a case study in Georgetown, Guyana. *Environment and Urbanization*, 9(1), 203–226.

Raddatz, R.L. (2005). Moisture recycling on the Canadian Prairies for summer 16 droughts and pluvials from 1997 to 2003. *Agricultural and Forest Meteorology,* 131, 13-26.

——, and Hanesiak, J.M. (2008). Significant Summer Rainfall in the Canadian Prairie Provinces: Modes and Mechanisms 2000–2004. *Intl J. Climatology*, DOI: 10.1002/joc.1670.

——, and Khandekar, M.L. (1979). Upslope enhanced extreme rainfall events over the Canadian western plains: a numerical simulation. *Mon. Wea. Rev.,* 107, 650-661.

Rosenzweig, C., Tubiello, F.N., Goldberg, R., Mills, E., Bloomfield, J. (2002). Increased crop damage in the US from excess precipitation under climate change. *Global Environ. Change*, 12, 197-202.

Roy, S.S., Balling, R.C. (2004). Trends in extreme daily rainfall indices in India. *Int. J. Climatol*., 24, 457–466.

Roy, P., Gachon, P., Laprise, R. (2011). Assessment of summer extremes and climate variability over the north-east of North America as simulated by the Canadian Regional Climate Model. *International Journal of Climatology*, doi: 10.1002/joc.2382.

Scaife, A.A., Spangehl, T., Fereday, D.R., Cubasch, U., Langematz, U., Akiyoshi, H., Slimane, B., Braesicke, P., Butchart, N., Chipperfield, M.P., Gettelman, A., Hardiman, C., Michou, M., Rozanov, E., Shepherd, T.G. (2011). Climate change projections and stratosphere-troposphere interaction. *Climate Dynamics*, doi:10.1007/s00382-011-1080-7.

Schumacher, R. S., Johnson, R. H. (2006). Characteristics of U.S. Extreme Rain Events During 1999-2003. *Wea. Forecasting,* 21, 69-85.

——, (2005). Organization and environmental properties of extreme-rain-producing mesoscale convective systems. *Mon. Wea. Rev*., 133, 961-976.

Sushama, L., Khaliq, N., Laprise, R. (2010). Dry spell characteristics over Canada in a changing climate as simulated by the Canadian RCM. *Global and Planetary Change*, 74(1), 1-14.

Szeto, K., Henson, W., Stewart, R.E., Gascon, G. (2011). The catastrophic June 2002 Prairie rainstorm: an extreme rain event that occurred during an extreme drought. *Atmos-Ocean*, 49(4), 380-395.

Trenberth, K. (1999). Conceptual framework for changes of extremes of the hydrological cycle with climate change. *Climate Change*, 42, 327–339.

Voss R., May, W., Roeckner, E. (2002). Enhanced resolution modeling study on anthropogenic climate change: changes in extremes of the hydrological cycle. *Int. J. Climatol*. 22, 755-777.

Zhai, P.M., Zhang, X. B., Wan, H., Pan X. H. (2005). Trends in total precipitation and frequency of daily precipitation extremes over China. *J. Clim*., 18, 1096– 1108.

Zhang, X., Vincent, L. A., Hogg, W. D., Niitsoo, A. (2000). Temperature and precipitation trends in Canada during the 20th century. *Atmos.–Ocean,* 38**,** 395–429.

Zhang, X., Hogg, W.D., Mekis, E. (2001). Spatial and temporal characteristics of heavy precipitation events over Canada. *J. Clim*., 14, 1923–1936.

Zwiers, F.W., Kharin, V.V. (1998). Changes in the extremes of the climate simulated by CCC GCM2 under CO2 doubling. *J. Climate,* 11(9), 2200–2222.